ORSAY

Série A

T H È S E

PRESENTEE

A L'UNIVERSITE PARIS SUD

CENTRE D'ORSAY

POUR OBTENIR

LE GRADE DE DOCTEUR ES-SCIENCES PHYSIQUES

PAR

Bernard PIRE

Sujet de la thèse :

CHROMODYNAMIQUE QUANTIQUE ET PHOTOPRODUCTION DE PARTICULES DE GRANDE IMPULSION TRANSVERSE

Soutenue le 27 Janvier 1981 devant la Commission d'Examen

MM. V. ALLESSANDRINI Président
A. KRZYWICKI
M. LE BELLAC
A. MOREL
F. RICHARD
T.N. TRUONG

ORSAY

Série A

T H È S E

PRESENTEE

A L'UNIVERSITE PARIS SUD

CENTRE D'ORSAY

POUR OBTENIR

LE GRADE DE DOCTEUR ES-SCIENCES PHYSIQUES

PAR

Bernard PIRE

Sujet de la thèse :

CHROMODYNAMIQUE QUANTIQUE ET PHOTOPRODUCTION DE PARTICULES DE GRANDE IMPULSION TRANSVERSE

Soutenue le 27 Janvier 1981 devant la Commission d'Examen

MM. V. ALLESSANDRINI Président
A. KRZYWICKI
M. LE BELLAC
A. MOREL
F. RICHARD
T.N. TRUONG

UNIV.
LEIDEN
BIBL.

REMERCIEMENTS

Cette thèse est le résultat de travaux effectués en collaboration avec Dominique Schiff et Michel Fontannaz que je remercie vivement. L'amicale ambiance dans laquelle se sont effectuées nos recherches restera sans doute un moment marquant de ma vie professionnelle.

Je remercie Monsieur le Professeur V. Allessandrini d'avoir bien voulu présider le jury de cette thèse. Je remercie également Monsieur Krzywicki, Monsieur le Professeur M. Le Bellac et Messieurs A. Morel, F. Richard et T.N. Truong d'avoir accepté de faire partie de ce jury.

Je remercie mes collègues du Centre de Physique Théorique de l'Ecole Polytechnique et du Laboratoire de Physique Théorique des Hautes Energies de l'Université d'Orsay pour leur soutien amical et pour les nombreuses et fructueuses discussions que j'ai eues avec eux. Je remercie particulièrement Tran N. Truong avec qui j'ai eu la chance et le plaisir de commencer à faire de la recherche. Je remercie aussi les membres des secrétariats qui ont contribué à la préparation matérielle de cette thèse et des articles qu'elle contient.

Digitized by the Internet Archive
in 2026

https://archive.org/details/IA41547321_0034

S O M M A I R E

Chapitre 1 Introduction et discussion des résultats obtenus

Introduction à la chromodynamique quantique
Les conséquences des équations du groupe de renormalisation
Etude de la diffusion inélastique profonde
Le modèle des partons
L'approche diagrammatique
La fonction de structure du photon
Discussion des résultats obtenus

Chapitre 2 Tests de QCD dans la hadroproduction de paire de leptons de grande impulsion transverse.

- Hadronic Jets with a large Q_T lepton pair trigger (publié dans Physics Letters 78 B).

Chapitre 3 Photoproduction de hadrons de grande impulsion transverse et tests de QCD

- A clear test of perturbative QCD in large p_T photoproduction (publié dans Physics Letters 89 B)
- Large p_T photoproduction and tests of QCD (publié dans Zeitschrift für Physik C 6)

Chapitre 4 La Physique du Gluon et la photoproduction de hadrons de grande impulsion transverse.

- How to extract the gluon fragmentation function from large p_T photoproduction (publié dans Physics Letters 94 B).
- Gluon Physics in large p_T photoproduction (publié dans Zeitschrift für Physik C6)

Chapitre 5 La photoproduction de hadrons de grande impulsion transverse avec des photons polarisés.

- Photoproduction with polarized photons as a source of polarized gluon jets (publié dans physics letters 95 B)
- Asymmetries in polarized large p_T photoproduction (sous presse dans Zeitschrift für Physik C).

PREMIERE PARTIE

INTRODUCTION ET DISCUSSION DES RESULTATS OBTENUS

Introduction à la chromodynamique quantique

La description des hadrons en termes de quarks, classés dans un triplet du groupe SU(3), s'est révélée très fructueuse. La symétrie SU(3) introduite par Gell Mann [1] permet de classifier les particules observées selon certaines représentation de ce groupe d'invariance ; elle amène de plus à des prédictions théoriques bien vérifiées expérimentalement. La découverte d'autres parfums (charme, beauté, ...) est incorporée par une généralisation immédiate des idées originales, le groupe de symétrie considéré étant élargi de SU(3) à SU(4), SU(5).... Ce schéma présentait cependant quelques problèmes sérieux et pour les surmonter Gell Mann [2] proposa que les quarks portent un nombre quantique supplémentaire appelé couleur, les interactions fortes étant invariantes par rapport aux rotations dans l'espace des couleurs. Le groupe de symétrie était supposé être $SU(3)_c$. Cette idée résout plusieurs problèmes :

- la liaison entre spin et statistique ne semblait pas réalisée dans le modèle des quarks. En effet on ne pouvait pas construire le Δ^{++} dans un état de spin $J_z = 3/2$ et dans un état S donc symétrique par rapport aux permutations des coordonnées spatiales. Si la fonction d'onde est antisymétrique par rapport à la couleur

$$|uuu> \to \frac{1}{\sqrt{6}} \varepsilon^{\alpha\beta\gamma} | u_\alpha u_\beta u_\gamma >$$

le problème est résolu.

- le taux de désintégration du pion neutre en deux photons est exactement calculable, à la limite chirale, à partir du diagramme

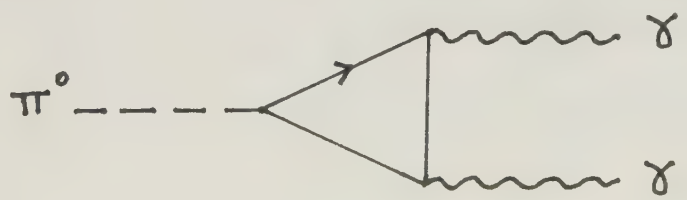

On voit que l'amplitude est proportionnelle au nombre de couleurs. Le résultat, dans le cas de quarks habituels (de charges fractionnaires) est [3]

$$\Gamma(\pi^o \to \gamma\gamma) = 7.87\ (N_c/3)^2\ \text{eV}$$

où N_c est le nombre de couleurs, alors que la valeur expérimentale est

$$\Gamma(\pi^o \to \gamma\gamma) = 7.95 \pm 0.05\ \text{eV}$$

- Si on suppose que la section efficace totale d'annihilation electron-positron en hadrons est décrite par le diagramme

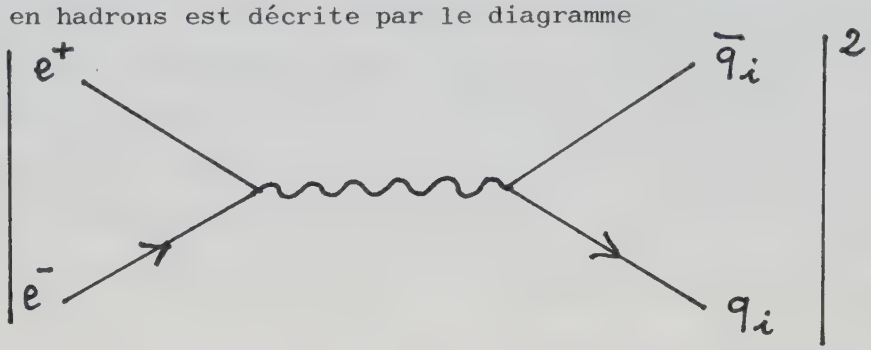

cette quantité est proportionnelle au nombre N_c de couleurs et les données indiquent que N_c est de l'ordre de 3.

Les succés de l'électrodynamique quantique, théorie de jauge des interactions électromagnétiques, amènent à essayer de construire à partir de la notion de couleur une théorie ayant une structure semblable, c'est-à-dire invariante par rapport à une transformation de jauge locale. Le fait d'imposer que la symétrie par rapport aux rotations dans l'espace de la couleur soit locale conduit alors à une théorie des interactions fortes décrites par le lagrangien de Yang et Mills [4]

$$\mathcal{L} = -\frac{1}{4} F^a_{\mu\nu} F^{a\mu\nu} + i\, \bar{\psi}_{qi}(x)\, \gamma_\mu\, D^\mu_{ij}\, \psi_{qj}(x) \qquad (1)$$

où les $F^a_{\mu\nu}$ sont définis à partir du potentiel vecteur A^a_μ par

$$F^a_{\mu\nu} = \partial_\mu A^a_\nu - \partial\ \ A^a_\mu + g\, f_{abc}\ \ A^b_\mu\, A^c_\nu \qquad (2)$$

et où les D^μ_{ij} représentent les dérivées covariantes

$$D^\mu_{ij} = \partial^\mu\, \delta_{ij} - ig\, A^\mu_a\, \lambda^a_{ij}/2 \qquad (3)$$

On a noté f_{abc} les constantes de structure du groupe de jauge, le groupe de couleur $SU(3)_c$. g est la constante de couplage (sans dimension) fondamentale

de la théorie. Les matrices λ^a sont les huit matrices de Gell Mann [1] qui vérifient les relations

$$[\lambda^a, \lambda^b] = 2 i f_{abc} \lambda^c \tag{4}$$

On peut ajouter un terme de masse $[-m_i \bar{\psi}_{qi}(x) \psi_{qi}(x)]$ au Lagrangien écrit ci-dessus. Dans ce travail, nous considérerons uniquement le cas de quarks légers (dont on peut négliger la masse devant l'échelle de la théorie) et nous n'aurons donc pas besoin de considérer un tel terme supplémentaire.

Les conséquences des équations du groupe de renormalisation [5]

La théorie ainsi définie, la chromodynamique quantique, est renormalisable [6]. L'étude de la renormalisation amène à d'intéressantes conclusions. Les équations du groupe de renormalisation [7] expriment le fait que les quantités physiques ne dépendent pas du choix du point de renormalisation μ. Considérons une fonction de Green $\Gamma(p_i, \alpha_s, a, \mu)$ qu'on peut écrire sous la forme du produit

$$\Gamma(p_i, \alpha_s, a, \mu) = Z_\Gamma(\mu, \varepsilon) \Gamma^o(p_i, \alpha_s^o, a^o, \varepsilon) \tag{5}$$

où a est un paramètre de jauge et ε le paramètre introduit par la régularisation dimensionnelle. Le facteur Z_Γ représente le produit des facteurs de renormalisation des fonctions d'ondes qui apparaissent dans Γ. Dire que Γ^o ne dépend pas de μ peut s'écrire sous la forme

$$\left[\mu \frac{\partial}{\partial \mu} + \beta \alpha_s \frac{\partial}{\partial \alpha_s} + \beta_a \frac{\partial}{\partial_a} + \gamma_\Gamma\right] \Gamma(p_i, \alpha_s, a, \mu) = 0 \tag{6}$$

où on a défini les fonctions universelles suivantes.

$$\beta(\alpha_s, a, \varepsilon) = \frac{\mu}{\alpha_s} \frac{d\alpha_s}{d\mu}$$

$$\beta_a(\alpha_s, a, \varepsilon) = \mu \frac{da}{d\mu} \tag{7}$$

et où γ_Γ est, dans le cas d'une fonction de Green à n_G gluons et n_F fermions externes

$$\gamma_\Gamma(\alpha_s, a, \varepsilon) = -\frac{1}{2}\left[n_G \frac{\mu}{Z_{3G}} \frac{dZ_{3G}}{d\mu} + n_F \frac{\mu}{Z_{2F}} \frac{dZ_{2F}}{d\mu}\right]$$

La théorie étant renormalisable, les fonctions β, β_a et γ_Γ sont régulières lorsque $\varepsilon \to 0$. Si on se place dans la jauge de Landau, la fonction β_a est identiquement nulle. Nous utiliserons cette simplification pour la suite de l'exposé. Montrons brièvement comment on calcule la fonction β en perturbation. On évalue le vertex $q\bar{q}$ au premier ordre non trivial, c'est-à-dire par les diagrammes

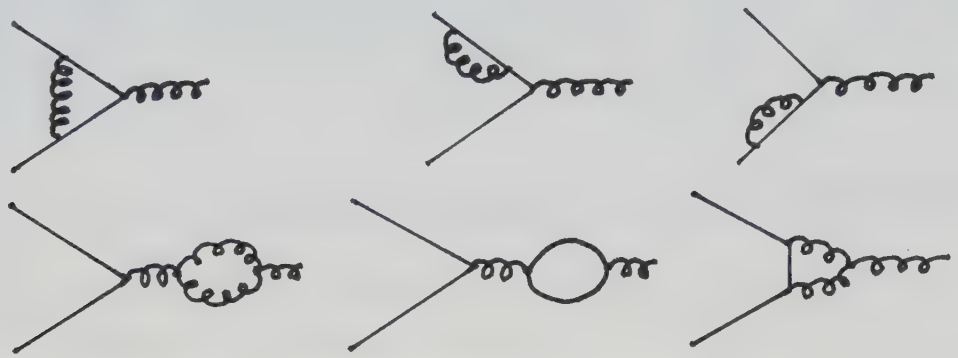

et on substitue l'expression obtenue dans l'équation (6). On obtient de cette façon [8]

$$\beta(\alpha_s) = \frac{\alpha_s}{\pi} \beta_1 + O(\alpha_s^2) \tag{8}$$

$$\beta_1 = -\frac{11}{2} + \frac{n_f}{3} \tag{9}$$

n_f étant le nombre de parfums de la théorie. Le fait que β_1 soit négatif (pourvu qu'il existe moins de 16 parfums) est primordial. Nous montrerons bientôt pourquoi.

L'équation du groupe de renormalisation (6) peut être combinée à une analyse dimensionnelle de la fonction de Green comme suit. Considérons l'effet d'une dilatation des impulsions p_i par un facteur λ. Si D est la dimension de Γ (en unités de masses) on peut écrire que $\Gamma(\lambda p_i, \alpha_s, \mu)/\mu^D$ est sans dimension, ce qui implique,par le théorème d'Euler sur les fonctions homogènes, que

$$\left[\lambda \frac{\partial}{\partial \lambda} + \mu \frac{\partial}{\partial \mu} - D\right] \Gamma(\lambda p_i, \alpha_s, \mu) = 0 \tag{10}$$

Combinant les équations (6) et (10) et notant

$$t = \log \lambda$$

on obtient

$$\left[-\frac{\partial}{\partial t} + \beta(\alpha_s)\ \alpha_s \frac{\partial}{\partial \alpha_s} + D - \gamma_\Gamma(\alpha_s)\right] \Gamma(e^t p_i, \alpha_s, \mu) = 0 \qquad (11)$$

La solution de cette équation exprime la dépendance par rapport aux dilatations de la fonction de Green considérée :

$$\Gamma(e^t p_i, \alpha_s, \mu) = \lambda^D \exp\{-\int_0^t dt'\ \gamma_\Gamma[\bar{\alpha}_s(t', \alpha_s)]\}\ \Gamma(p_i, \bar{\alpha}_s, \mu) \qquad (12\,a)$$

qu'on peut réécrire sous la forme

$$\Gamma(e^t p_i, \alpha_s, \mu) = \lambda^D\ \Gamma(p_i, \bar{\alpha}_s, \mu)\ \exp - \int_{\alpha_s}^{\bar{\alpha}_s(t\ ,\alpha_s)} \frac{\gamma_\Gamma(\alpha'_s)}{\alpha'_s \beta(\alpha'_s)}\, d\alpha'_s \qquad (12\,b)$$

où la constante de couplage courante $\bar{\alpha}_s$ est la solution de l'équation différentielle suivante

$$\frac{d\bar{\alpha}_s(t,\alpha_s)}{dt} = \bar{\alpha}_s \beta(\bar{\alpha}_s)$$
$$\bar{\alpha}_s(0,\alpha_s) = \alpha_s \qquad (13)$$

Il est facile de montrer, en utilisant l'équation (8) qu'on a, à l'ordre d'une boucle :

$$\bar{\alpha}_s(t,\alpha_s) = \frac{\alpha_s}{1 - \beta_1 \frac{\alpha_s}{\pi} t} \qquad (14)$$

Si β_1 est négatif, $\bar{\alpha}_s(t,\alpha_s)$ décroît lorsque t croît. Ceci implique que $\Gamma(e^t p_i, \alpha_s, \mu)$ s'exprime en fonction d'une quantité $\Gamma(p_i, \bar{\alpha}_s, \mu)$ dans laquelle la constante de couplage est petite et qu'on peut donc calculer en perturbation. On dit qu'une théorie dans laquelle les fonctions de Green ont un tel comportement est asymptotiquement libre : les fonctions de Green sont, à part un facteur de dimension anormale, asymptotiquement égales aux fonctions correspondantes d'une théorie libre. On peut en fait exprimer la constante de couplage effective $\bar{\alpha}_s$ en fonction d'une échelle fondamentale

de la théorie. On montre aisément à partir de l'équation (13) définissant $\bar{\alpha}_s$ que la quantité

$$\frac{1}{2}\log \mu^2 + \frac{\pi}{\beta_1 \alpha_s(\mu)} \equiv \frac{1}{2}\log \Lambda^2 \qquad (15)$$

est invariante par rapport au groupe de renormalisation. C'est ce paramètre Λ qu'on prendra pour échelle fondamentale de la théorie. Les résultats expérimentaux montreront qu'il est de l'ordre de 500 MeV. On écrira souvent

$$\bar{\alpha}_s(Q^2) \simeq \frac{12\pi}{(33 - 2n_f)\log Q^2/\Lambda^2} \qquad (16)$$

Etude de la diffusion inélastique profonde [9]

Dans cette section nous allons brièvement montrer comment l'application des idées exposées ci-dessus permet d'obtenir des informations sur les fonctions de structure de la diffusion inélastique profonde d'un lepton sur un hadron. Nous verrons en particulier que les équations du groupe de renormalisation amènent à prédire une violation logarithmique de l'invariance d'échelle ; il se trouve que ce comportement a effectivement été observé expérimentalement, ce qui justifie l'intérêt porté à la chromodynamique quantique.

Considérons donc la diffusion profondément inélastique d'un électron sur un proton, les notations étant explicitées par le diagramme ci-dessous

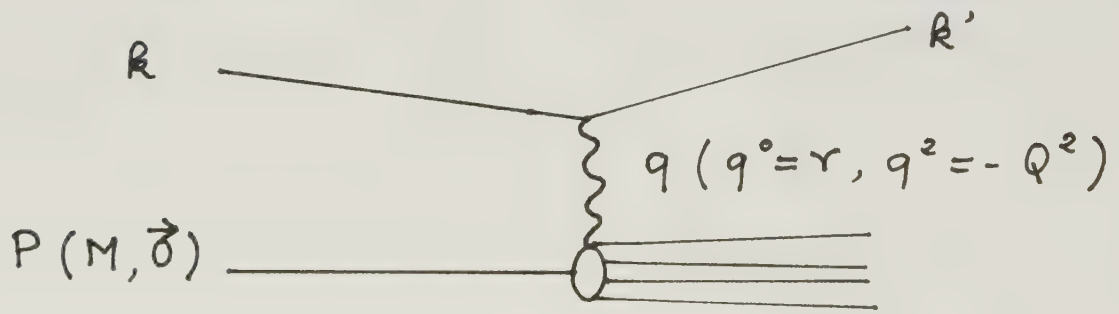

Nous nous intéressons à la limite de Bjorken de ce processus, limite définie par

$$Q^2 \to \infty \; ; \; P.q \to \infty \; ; \quad x \equiv Q^2/2P.q \text{ fixe} \qquad (17)$$

la section efficace différentielle peut s'écrire sous la forme

$$\frac{d\sigma}{dQ^2 d\nu} = \frac{\pi \alpha^2}{k^{o2}} \frac{1}{Q^4} L^{\mu\nu} W_{\mu\nu} \tag{18}$$

dans l'approximation de l'échange d'un seul photon, les quantités étant exprimées dans le référentiel lié au laboratoire (proton initialement au repos). Le tenseur leptonique $L^{\mu\nu}$ est calculé dans le cadre de l'électrodynamique quantique

$$L^{\mu\nu} = 2[k^{\mu} k'^{\nu} + k^{\nu} k'^{\mu} - g^{\mu\nu} k.k'] \tag{19}$$

si la masse de l'électron est négligée. Le tenseur hadronique peut, quant à lui, se décomposer sous la forme

$$W^{\mu\nu} = - (g^{\mu\nu} - \frac{q^{\mu} q^{\nu}}{q^2}) W_1(Q^2, \nu) + (P^{\mu} - q^{\mu} \frac{P.q}{q^2})(P^{\nu} - q^{\nu} \frac{P.q}{q^2}) W_2(Q^2,\nu)/M^2 \tag{20}$$

qui définit les fonctions de structure $W_1(Q^2, \nu)$ et $W_2(Q^2,\nu)$. On peut exprimer ce tenseur hadronique à partir de l'amplitude Compton élastique vers l'avant

$$W_{\mu\nu}(P,q) = \frac{1}{2\pi} \text{Im } T_{\mu\nu}(P,q) \tag{21}$$

$T^{\mu\nu}$ étant elle-même définie par

$$T_{\mu\nu}(P,q) = i \int d^4 y \, e^{iq.y} < P | T(J_{\mu}^{+}(y) \, J_{\nu}(0)) | P > \tag{22}$$

Dans la limite euclidienne profonde ($q^o \to i\infty$) la région $y \to 0$ domine l'intégrale du membre de droite. En utilisant dans cette limite (où $|x| \to \infty$) le développement de Wilson [10] d'un produit d'opérateurs, on peut écrire $T_{\mu\nu}$ comme une série de termes

$$T_{\mu\nu}(P,q) = \sum_{N,i} \{-(g_{\mu\mu_1} g_{\nu\mu_2} q^2 - g_{\mu\mu_1} q_{\nu} q_{\mu_2} - g_{\nu\mu_2} q_{\mu} q_{\mu_1} + g_{\mu\nu} q_{\mu_1} q_{\mu_2}$$
$$\overline{F}_{2i}^{N}(q^2,\mu^2,\alpha_s) + (g_{\mu\nu} - \frac{q_{\mu} q_{\nu}}{q^2}) q_{\mu_1} q_{\mu_2} \overline{F}_{Li}^{N}(q^2,\mu^2,\alpha_s)\}$$
$$q_{\mu_3} \ldots q_{\mu_N} \left(\frac{2}{-q^2}\right)^N < P | O_i^{\mu_1 \ldots \mu_N}(0) | P > \tag{23}$$

Définissant l'élément de matrice de l'opérateur local $O_i^{\mu_1 \cdots \mu_N}(0)$ comme

$$< P \,|O_i^{\mu_1 \cdots \mu_N}(0)|\, P > \equiv P^{\mu_1} .. P^{\mu_N} < P|O_i^N|P >$$

l'équation (23) se réécrit sous la forme

$$T_{\mu\nu}(q^2,x) = \sum_{i,N} (\frac{1}{x})^N \{(g_{\mu\nu} - \frac{q_\mu q_\nu}{q^2}) \overline{F}^N_{L,i}(q^2,\mu^2,\alpha_s) +$$

$$+ (g_{\mu\nu} - \frac{P_\mu q_\nu + P_\nu q_\mu}{P.q} + \frac{P_\mu P_\nu}{(P.q)^2} q^2) \overline{F}^N_{2i}(q^2,\mu^2,\alpha_s)\} \; < P|O_i^N|\, P > \qquad (24)$$

où les fonctions $\overline{F}$ ne dépendent pas de la cible. Les termes dominants d'une telle série lorsque $q^2 \to \infty$ sont ceux qui correspondent à des $< P|O_i^N|\, P >$ de dimension minimale (en termes de masses), c'est-à-dire à des opérateurs $O_i^{\mu_1 \cdots \mu_N}$ de twist (dimension - spin) minimum. Pour tout N, il existe trois opérateurs de twist 2. Si on s'intéresse à des quantités << non-singulet>> par rapport aux transformation de parfums, il n'en existe même qu'un

$$\overline{\psi} \gamma^{\mu_1} D^{\mu_2} \ldots D^{\mu_N} \tau^K \psi - \text{traces}$$

où τ^K est une matrice agissant sur les parfums et la dérivée covariante D^μ a été définie plus haut.

La série (24) ne converge pas dans la région physique $|x| < 1$ mais elle définit T comme fonction analytique en x avec une coupure sur le segment réel $[-1, +1]$. Si on se restreint par exemple à la partie non-singulet de $\overline{F}_2$, on peut isoler le coefficient de $(1/x)^N$ dans l'expression (24) en prenant le $(N+1)^e$ moment (c'est-à-dire en multipliant par x^{N-1}) et en intégrant sur un contour qui entoure la coupure

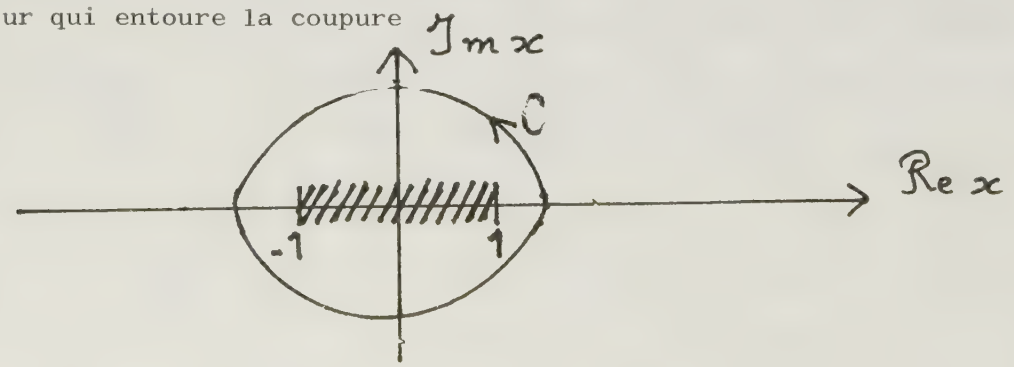

$$\frac{1}{2i\pi} \int_C dx\, x^{N-1}\, T(q^2,x) = \overline{F}^N_{2,ns}(q^2, \mu^2, \alpha_s) < P \,|O^N_{ns}|\, P > \qquad (25)$$

Ceci peut s'écrire, puisque $W_{\mu\nu}$ est relié à la partie imaginaire de $T_{\mu\nu}$ par l'équation (21), comme

$$4 \int_0^1 dx\, x^{N-1}\, W_{2,ns}(q^2,x) = \overline{F}^N_{2,ns}(q^2,\, \mu^2,\, \alpha_s) \,\langle P|O^N_{ns}|\, P\rangle \qquad (26)$$

On vérifie que les fonctions $\overline{F}^N$ obéissent à une équation du groupe de renormalisation semblable à l'équation (11) où γ_Γ est remplacée par la dimension anormale de l'opérateur O^N. On applique donc la formule (12 b) à la fonction $\overline{F}^N_{2,ns}$ pour obtenir l'évolution des moments M^N de la fonction de structure $\nu W_{2,ns}(q^2,x)$ définis par

$$M^N_2(q^2) = \int dx\, x^{N-2}\, \nu W_{2,ns}(q^2,x) \qquad (27)$$

On obtient :

$$M^N_2(q^2) = M^N_2(q_o^2) \left(\frac{\overline{\alpha}_s(q^2)}{\overline{\alpha}_s(q_o^2)} \right)^{-\gamma^N_o/4\beta_1} \qquad (28)$$

où γ^N_o est le premier coefficient non nul dans le développement en α_s de la dimension anormale de l'opérateur O^N_{ns} définie par

$$\gamma^N = \mu \frac{d}{d\mu} \ln \left(\frac{O^N_{ns}}{O^{N,u}_{ns}} \right) \qquad (29)$$

où $O^{N,u}$ est l'opérateur O^N non renormalisé, et

$$\gamma^N = \gamma^N_o \frac{\alpha_s}{4\pi} + O(\alpha_s^2) \qquad (30)$$

On voit donc que cette approche nous a permis de prédire l'évolution en Q^2 des moments des fonctions de structure. En inversant la définition des moments, on peut donc prédire la dépendance en Q^2 des fonctions de structure de la diffusion inélastique profonde, qui sont directement liées dans le langage du modèle des partons que nous allons maintenant présenter, au contenu en partons des hadrons.

Il se trouve que malheureusement on ne peut pas appliquer une analyse semblable aux processus durs pour lesquels Q^2 est du genre temps. L'approche diagrammatique de ces processus que nous exposerons brièvement

plus loin est au contraire très féconde et permet de justifier le modèle des partons. Dans le cas de la diffusion inélastique profonde, les deux approches sont parfaitement équivalentes.

Le modèle des partons [11]

Avant que ne soit développée l'approche qui vient d'être exposée, les propriétés d'invariance d'échelle des fonctions de structure qu'on avait observées à SLAC avaient été expliquées dans le cadre du modèle des partons [11]. Ce modèle, qualifié depuis de naïf, permet d'avoir une image très physique des processus durs. Nous verrons dans la section suivante comment la chromodynamique quantique et l'approche diagrammatique des processus durs justifient et donnent une base théorique solide à ce modèle.
Rappelons brièvement quelles sont les hypothèses du modèle des partons appliqué par exemple au problème de la diffusion inélastique profonde d'un électron sur un proton. Dans le système de référence P_∞ (où le proton est très rapide), le proton est supposé être équivalent à une collection de partons ponctuels libres se déplaçant presque parallèlement au nucléon et se partageant son impulsion. La section efficace de diffusion inélastique à grand Q^2 est la somme incohérente des sections efficaces de diffusion sur chacun des partons du proton. Dans le cadre de ce modèle, on calcule aisément les fonctions de structure à la limite de Bjorken (17). Si on note $G_{i/p}(x)$ le nombre de partons de type i et de charge e_i qui emportent la fraction d'impulsion longitudinale x du proton, on obtient

$$\begin{aligned} MW_1(x,Q^2) &\longrightarrow \frac{1}{2} \sum_i e_i^2 \, G_{i/p}(x) \\ \nu W_2(x,Q^2) &\longrightarrow x \sum_i e_i^2 \, G_{i/p}(x) \end{aligned} \qquad (31)$$

Remarquons que le modèle des partons est strictement invariant d'échelle. Les résultats expérimentaux sont en première approximation bien expliqués par ce modèle. Sans entrer dans une énumération des tests expérimentaux, notons que ce modèle conduit à la notion de jets hadroniques dans toute situation expérimentale où un processus dur est à l'oeuvre. Plus précisément lorsqu'un parton est produit dans une collision violente, il donne naissance à une gerbe de particules dont la distribution en impulsion ne dépend que de la nature du parton et non de la façon dont il a été produit. On définit ainsi une fonction de fragmentation du parton en hadrons $D_i^h(z)$ invariante

d'échelle et qu'on peut mesurer soit dans les réactions de diffusion inélastique $ep \to ehX$ soit dans les réactions d'annihilation $e^+e^- \to hX$. z est la fraction longitudinale de l'impulsion du parton emportée par le hadron.

On peut appliquer le modèle des partons à d'autres processus durs, la production hadronique d'une paire de leptons de grande masse invariante [12] (Processus de Drell Yan) ou la hadroproduction de particules possédant une grande impulsion transverse au faisceau incident, entre autres exemples. Explicitons, pour l'exemple, le cas de la réaction.

$$\gamma p \to \pi X$$

où le pion est produit avec une grande impulsion transverse. La section efficace différentielle de ce processus s'écrit comme [13]

$$\frac{E_\pi \, d\sigma}{d\vec{p}_\pi} = \sum_{\substack{ab \\ cd}} \int_0^1 dx_a \int_0^1 dx_b \int_0^1 \frac{dz}{z^2} \; G_{a/\gamma}(x_a) \; G_{b/p}(x_b) \; D_{\pi/c}(z) \; \delta(\hat{s} + \hat{t} + \hat{u}) \; \frac{\hat{s}}{\pi} \; \frac{d\hat{\sigma}}{d\hat{t}} (ab \to cd) \tag{32}$$

où les fonctions $G_{a/A}(x_a)$ sont les fonctions de distribution du parton a dans la particule A, la fonction $D_{\pi/c}(z)$ la fonction de fragmentation du parton c en un pion emportant une fraction z de son impulsion et $\hat{\sigma}$ est la section efficace du sous processus partonique dont les invariants de Mandelstam, notés $\hat{s}$, $\hat{t}$ et $\hat{u}$ sont reliés aux invariants de la réaction globale par les relations

$$\hat{s} = x_a \; x_b \; s$$

$$\hat{t} = x_a \; t/z$$

$$\hat{u} = x_b \; u/z$$

Dans une telle approche on néglige les mouvements de Fermi des constituants dans les hadrons et des hadrons dans les jets. Les fonctions de structure sont tirées des expériences de diffusion inélastique profonde et les fonctions de fragmentation des expériences d'annihilation électron-positron. La section efficace du sous-processus peut quant elle être calculée dans le

cadre d'un modèle donné.

L'approche diagrammatique [14]

L'étude de la diffusion profondément inélastique que nous avons présentée plus haut a montré que la description de cette réaction par le modèle des partons devait être modifiée, l'invariance d'échelle des fonctions de structure étant violée logarithmiquement. Le problème majeur de cette approche est qu'on ne peut pas l'appliquer aux autres réactions que le modèle des partons permettait d'analyser. La propriété de liberté asymptotique permet d'autre part d'espérer analyser directement en termes de diagrammes les réactions de collision dure. La réalisation de ce programme dont nous allons indiquer les grandes lignes permet de justifier l'emploi du modèle des partons, qui devient en quelque sorte l'ordre zéro d'un développement . Elle permet de plus de calculer les modifications ("logarithmiques") qu'on doit apporter à la formulation originale. On peut montrer qu'elle amène aux même résultats, dans le cas de la diffusion inélastique profonde, que l'approche présentée plus haut.

Une analyse en jauge physique (c'est-à-dire où seuls se propagent les gluons ayant une polarisation physique) des graphes les plus généraux permet de montrer [15] que toute section efficace de processus dur peut s'écrire comme une convolution du type

$$\sigma = \sum_i f_i(x,Q^2) \otimes \sigma_i(x, \alpha_s(Q^2)) \qquad (33)$$

où les σ_i sont des section efficaces partoniques finies calculées perturbativement dans le cadre de QCD ; les fonctions f_i sont des fonctions de distribution ou de fragmentation dont on ne peut prédire que l'évolution en Q^2 . Pour être plus précis, lorsqu'on calcule perturbativement une section efficace, on voit apparaitre des divergences de masse (les divergences infrarouges s'annulent en général) dues à l'émission de partons collinéaires. La démonstration de la factorisation exprimée par l'équation (33) revient en fait à démontrer qu'on peut regrouper ces facteurs divergents dans la quantité $f_i(x,Q^2)$. La section efficace restante σ_i est alors parfaitement finie mais contient des $\log Q^2/\mu^2$ qu'on resomme à tous les ordres. Il apparait alors que la constante de couplage devient courante: $\alpha_s(Q^2)$. Par exemple la section efficace de production d'un pion à grand p_T peut s'écrire

$$E\frac{d\sigma}{d\vec{p}}(AB\to\pi X)=\sum_{abc}\int dx_a\,dx_b\,\frac{dz}{z^2}\,G_{a/A}(x_a,Q^2)\,G_{b/B}(x_b,Q^2)\,D_{\pi/c}(z,Q^2)\,\frac{E_c\,d\hat{\sigma}}{d\vec{p}_c}(ab\to cX) \tag{34}$$

où les quantités $G_{a/A}(x,Q^2)$ sont les mêmes que celles qui apparaissent dans la diffusion inélastique profonde et les facteurs $E_c\,d\hat{\sigma}/d\vec{p}_c$ dépendent de la réaction envisagée et sont calculés avec une constante de couplage courante $\alpha_s(Q^2)$.

L'exploitation de ce résultat se fait en plusieurs étapes. On considère d'abord la contribution des logarithmes dominants, c'est-à-dire celle où $d\hat{\sigma}$ ne tient compte que des termes de Born (améliorés par l'utilisation du groupe de renormalisation) de type $ab\to cd$, et où les violations d'invariance d'échelle des $G_{a/A}$ et $D_{\pi/c}$ sont calculées à l'ordre d'une boucle (c'est-à-dire comme nous les avons présentés dans l'étude de la diffusion inélastique profonde) et où $\alpha_s(Q^2)$ est donné par l'expression 14. La formule (34) se réécrit donc dans ce cas sous la forme

$$E\frac{d\sigma}{d\vec{p}}(AB\to\pi X)=\sum_{abc}\int dx_a\,dx_b\,\frac{dz}{z^2}\,G_{a/A}(x_a,Q^2)\,G_{b/B}(x_b,Q^2)\,D_{\pi/c}(z,Q^2)\,\delta(\hat{s}+\hat{t}+\hat{u})\,\frac{\hat{s}}{\pi}\frac{d\hat{\sigma}}{d\hat{t}}(\hat{s},\hat{t},\hat{u},\alpha_s(Q^2)) \tag{34'}$$

On peut ensuite considérer les termes suivants dans le développement en $\log Q^2/\Lambda^2$. Nous nous restreindrons dans ce travail à la première étape de ce programme. Précisons de plus que dans un processus de production d'une particule de grande impulsion transverse, la définition précise de Q^2 n'est pas sans ambiguité. Nous choisirons pour notre part la définition proposée par Feynman et collaborateurs [16]

$$Q^2=\frac{2\hat{s}\hat{t}\hat{u}}{\hat{s}^2+\hat{t}^2+\hat{u}^2} \tag{35}$$

qui a la propriété suivante

$$Q^2\longrightarrow -t \qquad \text{lorsque} \qquad |t|\ll s,\ |u|$$

La verification expérimentale de la formule 34 se révèle être assez complexe dans le cas des collisions hadron-hadron ; la situation est en particulier compliquée par les deux circonstances suivantes :

- les sous processus qu'on doit prendre en compte au niveau du terme de Born sont $qq \to qq$, $qg \to qg$ et $gg \to gg$. La méconnaissance des fonctions $G_{g/p}$ et $D_{h/g}$ qui ne sont pas accessibles directement dans les processus de diffusion inélastique et dans les réaction d'annihilation e^+e^-, respectivement, rend toute prédiction très dépendante du modèle choisi pour ces fonctions.

- Il apparait que les partons ont probablement un mouvement transverse intrinsèque (qu'on ne peut pas prédire par QCD) non négligeable dans le proton. Il a été démontré [17] que la section efficace différentielle inclusive dépendait beaucoup de la façon dont on traitait ce mouvement à moins de se placer à très grande impulsion transverse ; les données sont malheureusement peu précises dans cette région là, les sections efficaces étant faibles.

Il se trouve que ces obstacles sont levés dans le cas de la photoproduction de particules de grande impulsion transverse. Comme nous l'expliciterons en détail au chapitre 3, on peut isoler les différents sous processus qui contribuent à cette réaction. L'idée fondamentale est de tirer profit de la nature ponctuelle du photon et de son couplage au quark proportionnel à la charge électrique. On voit alors que parmi les graphes de couplage direct

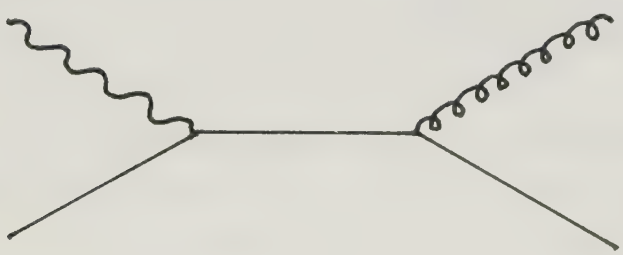

graphe Compton

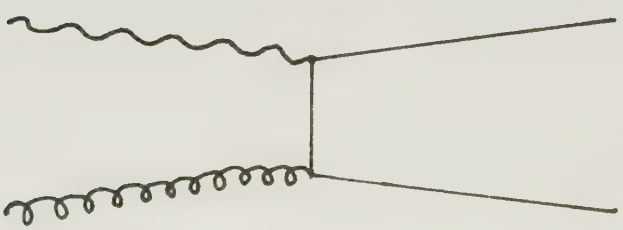

graphe de Fusion

seul le graphe Compton contribue à une différence de sections efficaces du

type $d\sigma(\gamma p \to h^+ X) - d\sigma(\gamma p \to h^- X)$. En fait, seule la partie valence de la fonction de structure et seule la fonction de fragmentation du quark intervient dans ce calcul (cf. la formule (34')). Il est de plus évident que les effets de mouvement de Fermi intrinsèque seront moins importants ici que dans la hadroproduction. Nous avons montré plus précisément qu'ils étaient négligeables.

Dans une analyse en logarithmes dominants, certains des graphes de couplage non direct sont du même ordre que les graphes de couplage direct. Il s'agit des contributions où le photon intervient par l'intermédiaire de sa fonction de structure anormale. En effet cette fonction de structure à laquelle nous consacrerons la prochaine section, est proportionnelle à $\log Q^2/\Lambda^2$, ce qui compense la constante de couplage supplémentaire $\alpha_s(Q^2)$. Ces graphes sont du type schématisé ci-dessous

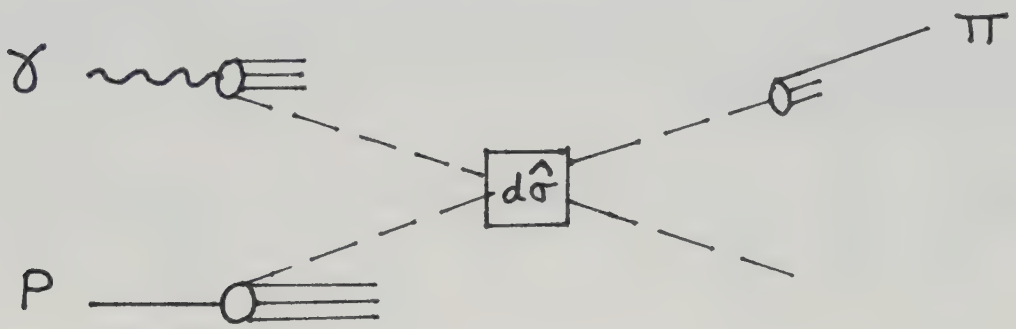

où les lignes discontinues symbolisent des partons (quarks ou gluons). On peut de plus estimer une partie des corrections à l'approximation des logarithmes dominants en considérant (voir section suivante) la partie hadronique de la fonction de structure du photon. Il ressort de ces calculs que la photoproduction est une réaction très adéquate à l'application de la chromodynamique quantique pourvu qu'on considère des différences de sections efficaces du type $d\sigma(\gamma p \to h^+ X) - d\sigma(\gamma p \to h^- X)$.

Il resterait bien sûr à calculer complètement l'ordre suivant dans le développement en logarithmes dominants. Certains termes ont été calculés [18] dans le cas de la hadroproduction de mésons ainsi que dans celui de la hadroproduction de photons de grandes impulsions transverses. Le résultat en est que, alors que dans le premier cas ces corrections sont très importantes ce qui met en doute l'intérêt du calcul à l'ordre dominant, elles sont petites dans le second cas.

Quelle que soit l'importance de ces corrections dans le cas de la photoproduction, l'analyse que nous allons développer dans les chapitres 3, 4 et 5 garde son intérêt. En effet, elle indique la méthode permettant de séparer les diverses contributions à la photoproduction et elle calcule les ordres de grandeur des quantités liées à ces contributions isolées, ce qui démontre que ces quantités sont bien observables.

Comme nous l'avons mentionné plus haut, l'étude de la photoproduction de particules de grande impulsion transverse fait intervenir la fonction de structure du photon. Cet objet très intéressant peut se calculer dans le cadre du traitement perturbatif de QCD et à l'approximation des logarithmes dominants. Nous allons maintenant rappeler brièvement les résultats le concernant.

La fonction de structure du photon

Avant la collision dure, le photon peut émettre des fermions selon une distribution reliée à sa fonction de structure. Dans cette section, nous rappelons brièvement les résultats liés à cette fonction. La référence fondamentale est le travail de E. Witten [19] qui utilise le développement d'un produit d'opérateurs et les techniques liées au groupe de renormalisation. Nous exposerons plutôt ici les grandes lignes du calcul dans la méthode diagrammatique [20].

Considérons la partie imaginaire de l'amplitude Compton vers l'avant sur une cible de photon réel, au premier ordre par rapport à la constante de couplage électromagnétique. Si les interactions fortes (c'est-à-dire les gluons) n'existaient pas, elle pourrait simplement s'écrire comme :

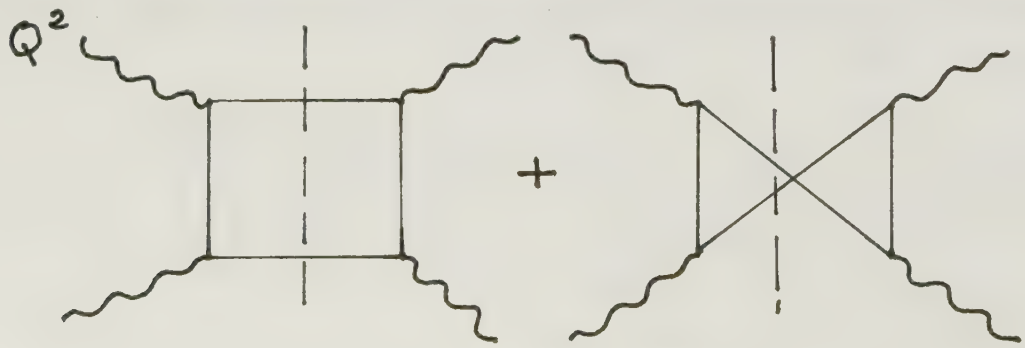

Un tel calcul est simple mais le résultat en est très intéressant. On remarque

d'abord que, si on choisit une jauge physique pour le photon cible, le diagramme carré est dominant (par un facteur Log Q^2 dû à la région de l'espace de phase où les deux fermions émis par le photon sont colinéaires)

$$\nu W_2^o(x,Q^2) = \frac{3}{2}\frac{e_i^4}{\pi}\,\alpha\, x\,[(1-x)^2 + x^2]\,\text{Log}\,Q^2/m_i^2 + \ldots \qquad (36)$$

La fonction de distribution d'un quark dans un photon est donc, à cette approximation, proportionnelle à Log Q^2

$$G^o_{q_i/\gamma}(x,Q^2) = \frac{3\alpha}{2\pi}\, e_i^2\,[x^2+(1-x)^2]\,\text{Log}\,Q^2/m_i^2 \qquad (37)$$

où e_i est la charge du quark. La prise en considération des interactions fortes modifie sensiblement ce résultat. Si on se place dans une jauge physique (aussi bien pour les gluons que pour le photon cible), on est amené à considérer deux types principaux de diagrammes représentés ci-dessous

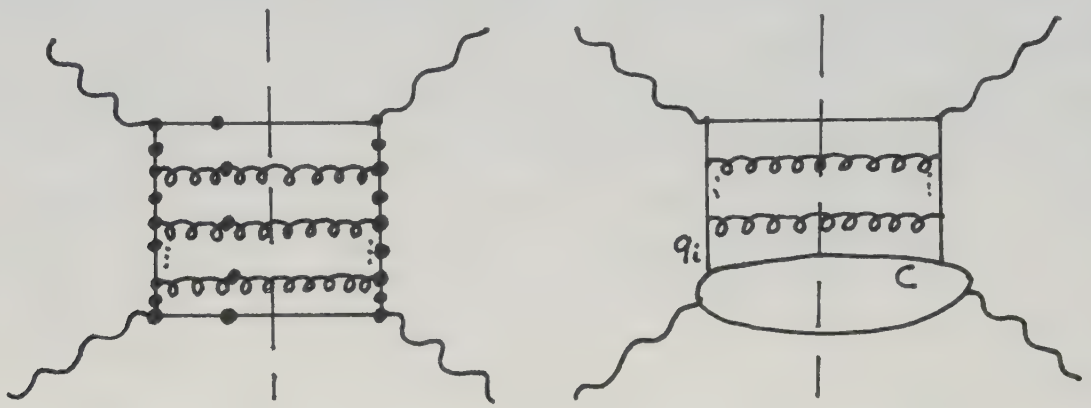

où les points signifient qu'on a renormalisé les vertex et les propagateurs. C représente ici une amplitude 2 particules irréductible telle que le photon n'interagit pas ponctuellement avec le quark q_i. On peut se représenter C sous la forme suivante

le photon cible a alors un comportement hadronique et sa fonction de

structure aura un comportement en Q^2 semblable au cas hadronique. La contribution du graphe en échelle (qu'on appelle contribution anormale) peut quant à elle être calculée à l'approximation des logarithmes dominants pourvu que tous les transferts soient grands pour qu'un calcul en perturbation soit justifié. On obtient, en terme de contenu en quark et en gluons du photon,

$$G_{q_i/\gamma}(x,Q^2) = \mathrm{Log}(Q^2/\Lambda^2)\ q_i(x) \qquad i = 2/3,\ 1/3$$
$$G_{g/\gamma}(x,Q^2) = \mathrm{Log}(Q^2/\Lambda^2)\ g(x) \qquad (38)$$

où $q_i(x)$ et $g(x)$ sont des fonction calculables dont plusieurs paramétrisations ont été proposées.

La contribution hadronique ne peut pas être calculée perturbativement et on l'estime habituellement dans un modèle de dominance vectorielle. Son ordre de grandeur est en général inférieur à celui de la contribution anormale pour des Q^2 moyens.
Soulignons en conclusion l'intérêt de la détermination expérimentale d'un objet tel que $G_{q/\gamma}(x,Q^2)$ dont le comportement en x et Q^2 est complètement spécifié, à l'ordre dominant, par la théorie, le résultat étant nettement différent du comportement prédit par un simple modèle des partons. Les expériences de diffusion inélastique profonde sur un photon sont malheureusement difficiles. Elles se font dans les études des collisions photon-photon auprès des anneaux de collision e^+e^- selon le diagramme ci-dessous.

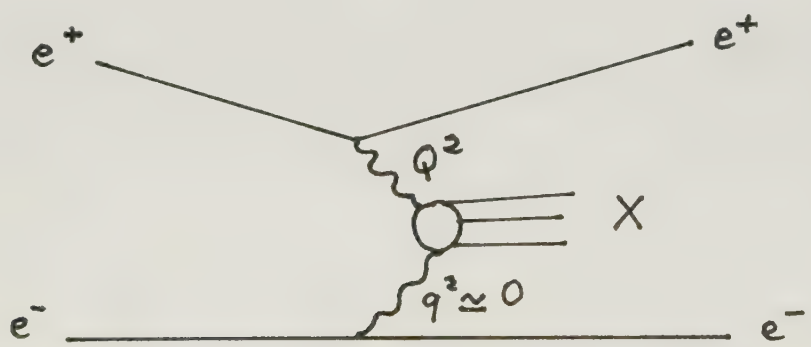

Des premiers résultats ont été obtenus à PETRA mais leur précision est encore insuffisante. Terminons cette section en montrant l'allure des fonctions de distribution des quarks et des gluons dans le photon. Leur comportement à x assez grand est particulièrement remarquable.

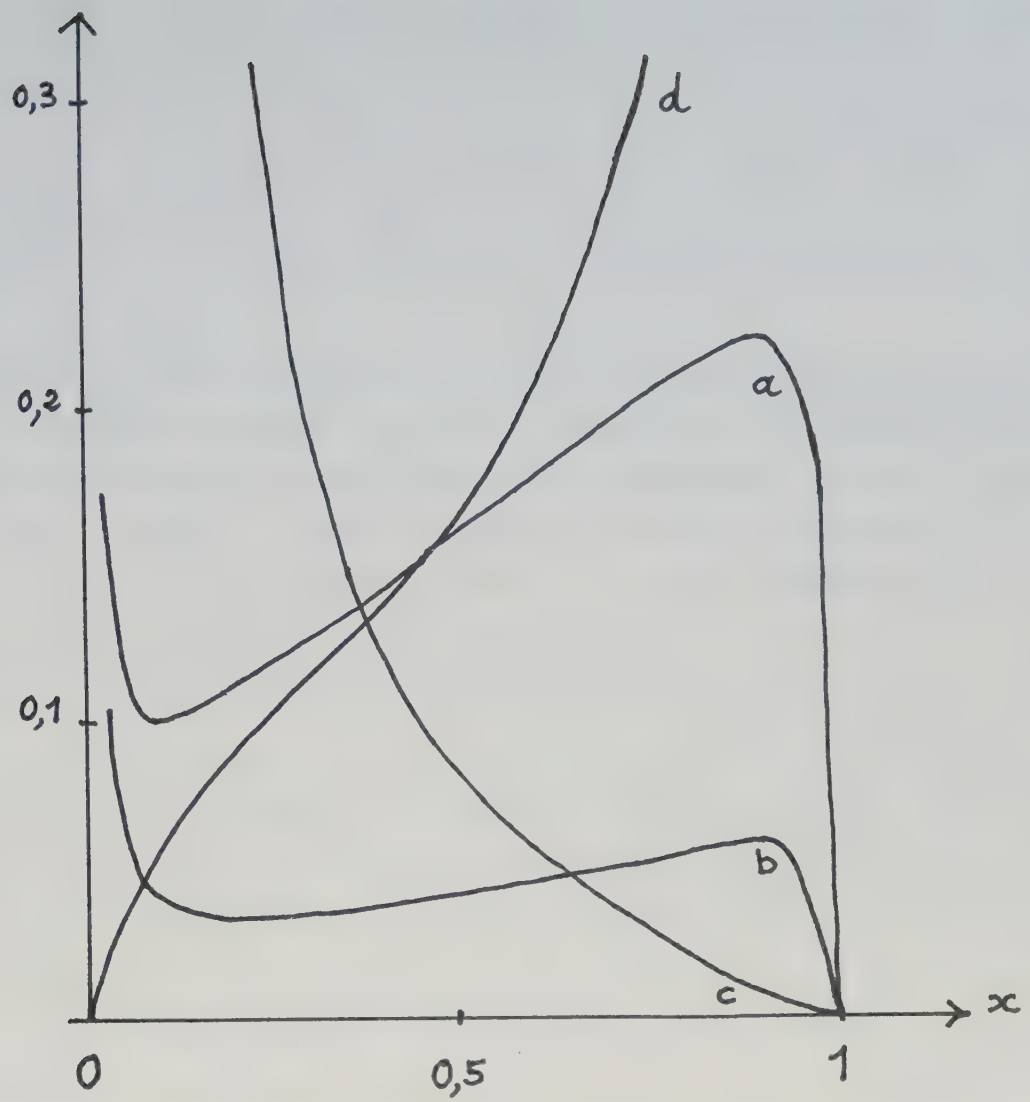

Les fonctions de distribution $xG_{q/\gamma}(x,Q^2)$ et $xG_{g/\gamma}(x,Q^2)$ en unités $\alpha\ \ell n(Q^2/\Lambda^2)/\pi$

a) pour un quark de charge 2/3

b) pour un quark de charge 1/3

c) pour un gluon

d) pour un quark de charge 2/3 lorsqu'on oublie l'interaction forte.

Discussion des résultats obtenus

Dans cette section nous discutons brièvement les résultats exposés dans les chapitres suivants. Ils ont fait l'objet d'articles publiés ou en cours de publication dans diverses revues ainsi que dans les compte rendus de plusieurs conférences internationales.

Chapitre 2 La production de paires de leptons de grande masse invariante

et d'impulsion transverse de l'ordre de plusieurs GeV/c dans les collisions hadroniques peut être expliquée dans le cadre de la chromodynamique quantique par les sous-processus

$$q + \bar{q} \longrightarrow \gamma^* + g$$
$$q + g \longrightarrow \gamma^* + q \qquad (39)$$

La distribution en moment transverse de la paire de leptons est bien expliquée [21] mais des propositions alternatives l'expliquent aussi bien [22]. Nous avons proposé d'observer le jet hadronique produit dans l'hémisphère opposé à la paire de leptons. La multiplicité des hadrons de ce jet ainsi que son contenu en nombre quantique (le rapport K^+/K^- par exemple)est très caractéristique du sous processus à l'oeuvre et permet par conséquent de vérifier si les réactions (39) sont bien responsables de la production de paire de grande impulsion transverse.

Chapitre 3 On présente ici une étude complète des conséquences de l'application de la chromodynamique quantique perturbative à la photoproduction de particules de grande impulsion transverse. On montre en particulier comment on peut isoler les contributions des différents sous processus à l'oeuvre : couplage direct du photon par les mécanismes Compton ou de Fusion, couplage indirect par l'intermédiaire du contenu en partons du photon tant sous la forme de la composante anormale que de la composante hadronique de sa fonction de structure. Les résultats expérimentaux préliminaires de la collaboration WA4 au CERN sont analysés. Ils indiquent une intéressante convergence entre théorie et expérience vers des impulsions transverses de 2,5 GeV/c. La production de jets est également étudiée. On montre qu'on peut isoler les jets gluoniques. Des estimations à très haute énergie, correspondant aux projets HERA ou TRISTAN d'anneaux de collision ep, sont données.

Chapitre 4 Ce chapitre aborde l'étude spécifique de la physique des gluons qu'on peut effectuer dans les réactions de photoproduction à grande impulsion transverse. En effet, une fois que les tests proposés dans la partie précédente ont été confrontés aux résultats expérimentaux (et à condition que cette comparaison se révèle favorable), on est en mesure d'obtenir à partir de ces données des résultats très fiables et très intéressants concernant les gluons. On peut d'abord mesurer la fonction de fragmentation du gluon en hadrons, y compris sa variation en Q^2 telle qu'elle est prédite par la chromodynamique quantique. Ceci est une situation exceptionnellement

favorable ; si les réaction d'annihilation e^+e^- permettent l'observation d'événements à 3 jets, la séparation des propriétés du gluon se révèle être extrèmement délicate dans ces expériences. On peut ensuite mesurer le contenu en gluons du proton, en isolant la contribution du sous processus de fusion $\gamma g \to q\bar{q}$; les ordres de grandeur obtenus sont amplement suffisants à une bonne détermination de cette fonction dont diverses formes ont été proposées dans la littérature.

Chapitre 5 Toutes les sections efficaces calculées dans les chapitres précédents étaient moyennées sur les états de polarisation possibles des particules initiales. Dans ce nouveau chapitre, on étudie l'effet de polarisations initiales données. On montre d'abord que, lorsque la cible n'est pas polarisée et que le processus Compton $\gamma q \to qg$ est isolé (par des moyens exposés au chapitre 3 par exemple), la polarisation du photon incident est fortement corrélée à la polarisation du gluon produit. En étudiant la variation avec la polarisation initiale de certaines quantités caractérisant le jet gluonique (l'impulsion transverse moyenne en dehors du plan de diffusion par exemple) on peut par conséquent observer des manifestations du spin du gluon. On calcule ensuite les asymétries liées à des états de polarisations des deux particules incidentes ; il se trouve que ces quantités prennent en général des valeurs caractéristiques de la théorie sous jacente et que leur mesure constitue par conséquent un test fin de la chromodynamique quantique. On montre de plus que l'étude de telles réactions permettrait d'isoler la fonction de distribution polarisée des gluons dans le proton, une quantité qu'il parait très difficile d'isoler d'une autre façon. Les expériences nécessaires sont évidemment des expériences de "seconde génération" mais leur intérêt est évident.

REFERENCES

[1] M. Gell Mann and Y. Neeman, The Eightfold Way, Benjamin (1964)

[2] M. Gell Mann, Acta Physica Austriaca,Suppl IX (1972) 733.

[3] S. Adler et W. Bardeen, Phys. Rev. 182 (1969) 1517.

[4] C.N. Yang et R. Mills, Phys. Rev. 96 (1954) 191.

[5] Parmi les nombreuses revues traitant ce sujet, je réfère en particulier au cours d'E. de Rafael à l'Ecole de Gif 1978 et X GIFT International Seminar on Theoretical Physics, Jaca (1979), Lecture Notes in Physics 118, Springer Verlag.

[6] G.t'Hooft, Nucl. Phys. B 61 (1973) 455

[7] E. Stueckelberg et A. Peterman, Helv. Phys. Acta 26 (1953) 499
M. Gell Mann et F. Low, Phys. Rev. 95 (1954) 1300.

[8] H. Politzer, Phys. Rev. Lett. 30 (1973) 1346.
D. Gross et F. Wilczek, Phys. Rev. Lett. 30 (1973) 1343.

[9] H. Politzer, Phys. Reports 14C (1974) 129
C.H. LLewellyn Smith , Acta Physica Austriaca, Suppl. XIX (1978) 331

[10] K. Wilson, Phys. Rev. D3, (1971) 1818.

[11] R. Feynman, Photon Hadron Interactions, Benjamin (1972).
F. Close, An Introduction to quarks and partons, Academic Press (1979).

[12] S. Drell et T. Yan, Annals of Physics 66 (1971) 578.

[13] D. Sivers et al., Physics Reports 23C (1976) 1.

[14] C. Sachrajda, X GIFT International Seminar on Theoretical Physics,Jaca (1979), Lecture Notes in Physics 118, Springer Verlag.

[15] R. Ellis et al, Phys. Lett. 78B (1978) 281 ; Nucl. Phys. B152 (1979) 285

[16] R. Feynman et al, Phys. Rev. D18 (1978) 3320

[17] M. Fontannaz et D. Schiff, Nucl. Phys. B132, 457 (1978)

[18] R. Ellis et al, LBL preprint 10304 (1979)
A. Contorougis et al, M Gill preprint 80-0352 et 80-0355 (1980)
P. Aurenche et J. Lindfors, Nucl. Phys. B168(1980) 296

[19] E. Witten, Nucl. Phys. B120 (1977) 189

[20] C.H. Llewellyn Smith, Phys. Lett. 79B (1978) 83
R. De Witt et al, Phys. Rev. D19 (1979) 2046
W. Frazer et J. Gunion, Phys. Rev. D19 (1978) 2 447 et D20 (1979) 147.

[21] G. Altarelli, G. Parisi et R. Petronzio, Phys. Rev. Lett. 76B (1978) 351 et 356

[22] M. Duong Van, K. Vasavada et R. Blankenbecler,Phys. Rev. D16 (1977) 1389.

D E U X I E M E P A R T I E

TESTS DE Q.C.D. DANS LA HADROPRODUCTION DE PAIRE DE LEPTONS DE GRANDE IMPULSION TRANSVERSE

HADRONIC JETS WITH A LARGE $Q_\perp$ LEPTON PAIR TRIGGER

J.M. BRUCKER and J. HUSSER
Laboratoire de Physique Théorique, CRN, B.P. 20 CRO, 67037 Strasbourg Cedex, France

M. FONTANNAZ and D. SCHIFF
Laboratoire de Physique Théorique et Hautes Energies, Orsay, France[1]

B. PIRE
Centre de Physique Théorique, Ecole Polytechnique, Palaiseau 91128, France[2]

Received 8 June 1978

We propose to observe hadron jets in correlation with large $Q_\perp$ transverse momentum lepton pairs. This would allow to test the theoretical idea that the large transverse momentum of the pair is mainly produced through a scattering subprocess $a + b \to c + \gamma^*$. The quantum number content of these jets is a specific signature of the subprocess, especially of those involved in perturbative QCD.

It is now commonly believed that the massive lepton pairs observed in high energy hadronic collisions are produced through the Drell–Yan mechanism [1] (fig. 1a). In this picture, the pair transverse momentum $Q_\perp$ is due to the quark transverse momentum $K_\perp$ within the incident hadrons. The mean value $\langle Q_\perp^2 \rangle = 1.9\ (\mathrm{GeV}/c)^2$ measured at FNAL [2] leads to $\langle K_\perp^2 \rangle \approx 0.95\ (\mathrm{GeV}/c)^2$.

This rather large value of $\langle K_\perp^2 \rangle$ led many theorists to assume that, for large $Q_\perp$, another mechanism was winning over the Drell–Yan process (hereafter called (a)). The idea being that the virtual photon recoil is taken by a single parton (as illustrated in fig. 1b) and the massive pair is now created through a $2 \to 2$ hard scattering subprocess. In the QCD approach [3,4], the partons entering in the subprocess of fig. 1b, hereafter called subprocess (b), are quarks, antiquarks and gluons. Within the CIM model [5], the partons may be quarks, antiquarks, diquarks (qq) or mesonic ($q\bar{q}$) states. Both pictures lead to a satisfactory fit of $d\sigma/dQ_\perp$, but are not free from ambiguities, an important problem being possible double counting between mechanism (a) and (b) when $Q_\perp$ is not large [4]; thus, a fit of $d\sigma/dQ_\perp$ is not a sufficient proof that mechanism (b) is really at work [6] nor a way to distinguish QCD from CIM predictions.

In this letter, we want to show that the observation of hadrons in correlation with a large $Q_\perp$ lepton pair is a way to clearly determine the presence of mechanism (b). One expects, within this picture, to see a jet of hadrons recoiling against the lepton pair, with

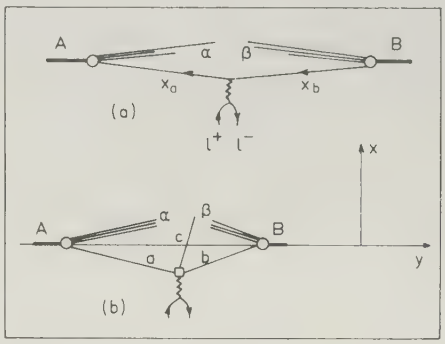

Fig. 1. The production mechanism of a large $Q_\perp$ pair (a) Drell–Yan mechanism; the recoil is taken by the spectators α and β. (b) $2 \to 2$ hard scattering; the recoil is essentially taken by a single parton c.

[1] Laboratoire associé au Centre National de la Recherche Scientifique, Postal address: Bât. 211, Université de Paris-Sud 91405 Orsay, France.

[2] Equipe de Recherche associée au Centre National de la Recherche Scientifique.

quantum numbers specific of either approach: QCD or CIM. For clarity, we present here the detailed results within QCD and sum up the results of CIM (more details may be found in ref. [7]).

Let us begin by a qualitative discussion of hadronic production associated with a large $Q_\perp$ massive lepton pair. In mechanism (a), the pair transverse momentum is balanced by the spectators α and β which travel coherently in the forward and backward direction. In the case of a π^- initiated reaction, for instance, the secondaries are fragments of the spectator quark and diquark which recoil against the trigger, each with a transverse momentum of the order $Q_\perp/2$. We thus expect to observe a recoil of the hadronic background mainly in the forward and backward fragmentation regions (large $|x_F|$). On the contrary, in mechanism (b) recoiling hadrons are fragments of a jet at small $|x_F|$, which leads to a net increase of the multiplicity in this region, analogous to what is observed in large $p_\perp$ hadronic reactions [9].

Let us now describe quantitatively mechanism (b). It is straightforward to write down the expression of the double inclusive cross section for observing a massive lepton pair with four-momentum Q, rapidity $y = \frac{1}{2}\ln[(Q_0 + Q_\parallel)/(Q_0 - Q_\parallel)]$ and a hadron of momentum p and rapidity Y, coming from the away jet:

$$\frac{d\sigma^{(2)}}{dQ^2\,dQ_\perp\,dy\,dY\,dz} = \frac{4}{3}\left(\frac{\alpha}{2\pi}\right)^2 \frac{1}{s^2}\,\frac{1}{Q^2}\left(-T^\mu_\mu\right) \times \frac{G_{a/A}(x_a)G_{b/B}(x_b)}{x_a x_b}\, D^h_c(z), \tag{1}$$

$G_{a/A}(x_a)$ is the probability to find parton a in hadron A with longitudinal momentum fraction x_a, $D^h_c(z)$ describes the fragmentation of parton c into hadron h which takes the fraction z of the parton momentum: $z = -p_x/Q_x$ (see fig. 1 for axis definition) and $T^\mu_\mu = \Sigma_\mu \mathcal{M}^\mu \mathcal{M}^*_\mu, \mathcal{M}_\mu$ being the matrix element of the subprocess $a + b \to \gamma^* + c$. p_z (component of p perpendicular to scattering plane) has been summed over and we have

$$x_{\substack{a\\b}} = (Q^{(\pm)} + Q_\perp e^{\pm y})s^{-1/2}/\sqrt{s} \tag{2}$$

with $s = (p_A + p_B)^2$, $Q^{(\pm)} = Q_0 \pm Q_\parallel = (Q^2 + Q_\perp^2)^{1/2} \times e^{\pm y}$. The pair inclusive cross section is simply given by:

$$\frac{d\sigma^{(1)}}{dQ^2\,dQ_\perp\,dy} = \int dY\,\frac{4}{3}\left(\frac{\alpha}{2\pi}\right)^2 \frac{1}{s^2}\,\frac{1}{Q^2}\left(-T^\mu_\mu\right) \times \frac{G_{a/A}(x_a)G_{b/B}(x_b)}{x_a x_b}. \tag{3}$$

In what follows we shall calculate the hadronic multiplicity:

$$\frac{dN^h}{dY\,dz} = \frac{d\sigma^{(2)}}{dQ^2\,dQ_\perp\,dy\,dY\,dz} \Big/ \frac{d\sigma^{(1)}}{dQ^2\,dQ_\perp\,dy} \tag{4}$$

which is normalized to

$$\int dY\,\frac{dN^h}{dY\,dz} = D^h_c(z).$$

We choose typical values for kinematics $s = 20$ GeV^2, $y = 0$, $Q^2 = 16$ GeV^2, it will turn out that our results are little dependent on Q^2. We take $Q_\perp = 2$ GeV/c for which we may expect a large enough counting rate and that mechanism (b) dominates over mechanism (a) [4]; moreover, the recoiling jet should be clearly visible. In eqs. (1) and (3), we do not take the parton Fermi motion into account. A detailed discussion of this effect in the large $p_\perp$ hadronic reactions has been given in ref. [8] from which we infer that introducing the parton transverse momentum in our treatment would affect essentially the single particle inclusive cross section. With parton transverse momenta of the order of 600 MeV/c, Altarelli et al., find a 50% enhancement of the pair inclusive distribution when $Q_\perp = 2$ GeV/c. The way to include the parton transverse momenta being rather arbitrary, we shall not give a detailed treatment but refer the interested reader to ref. [8].

We shall mainly discuss the reaction $\pi^- p \to \ell^+\ell^- + h + X$. Let us first consider subprocess $g + q \to \gamma^* + q$($g + \bar{q} \to \gamma^* + \bar{q}$); its contribution to the lepton pair distribution has already been written down by many authors [3,4]. Description of this subprocess requires the knowledge of the gluon structure function. We take, in agreement with dimensional counting rules [10]

$$G_{g/h}(x) = \tfrac{1}{2}(k+1)(1-x)^k/x, \tag{5}$$

with $k = 3(6)$ for the pion (proton). In eq. (5), the gluons carry half the hadron momentum. For $G_{q/p}(x)$,

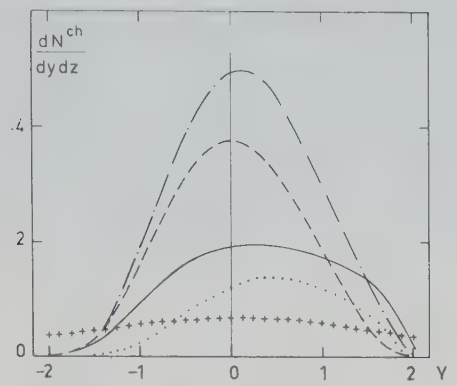

Fig. 2. The charged hadron multiplicity ($z = 1/2$). –.–.– $q + g \to q + \gamma^*$ (. . . . the gluon comes from π^-; - - - - the gluon comes from p). ——— $q + \bar{q} \to g + \gamma^*$ (+ + + estimated contribution from the Drell–Yan mechanism (see text)).

we use a fit due to Gunion [11] and for $G_{q/\pi}(x)$, a form which has been motivated and used in a previous work [12] on large $p_\perp$ hadronic inclusive distributions with pion beams [‡1]:

$$G_{q/\pi}(x) = 2x(1-x) + 0.72(1-x)^3/x^{1/2} + 0.15(1-x)^5/x.$$

Finally, we describe the fragmentation of a quark (or antiquark) into charged hadrons by:

$$D_q^{ch}(z) = (1-z)/z \qquad (6)$$

assuming that charged hadrons take half the quark momentum. The charged hadron multiplicities are shown in fig. 2 for $p_x = 1$ GeV/c ($z = 1/2$); we have separated the two contributions where the gluon comes from the pion or from the proton. The asymmetry of the curve in the latter case, reflects the fast decrease of $G_{g/p}(x)$ compared to $G_{q/\pi}(x)$ when $x \to 1$ whereas the difference in the heights of the two contributions may be traced back to squared charge factors.

Let us now turn to $q + \bar{q} \to \gamma + g$. We describe the gluon fragmentation into charged hadrons by:

$$D_g^{ch}(z) = 2(1-z)^3/z, \qquad (7)$$

[‡1] This form allows a good fit to the data for the ratio of π^0 inclusive distributions with pion and proton beams. The calculation of ref. [12] is done with a specific hard scattering subprocess, but the result, however, is more generally valid for any subprocess with two quarks in the initial state.

assuming, as above, that charged hadrons take half the gluon momentum. Let us point out that this form is somewhat tentative. In fact, a very different form has been proposed leading to multiplicities which grow like powers of the energy [13]. Our hypothesis, here, is that gluon jets are not very different from quark jets, and experiment should soon test it. Within this hypothesis, we obtain the result shown in fig. 2 for $dN^{ch}/dYdz$. Up to now we have considered separately the two subprocesses but their relative weight is determined within QCD. We find that the double inclusive cross sections for charged secondaries are equal within 30% for $z = 1/2$ and $Y = 0$. Of course, such a prediction depends strongly on the assumptions done in eqs. (5), (6) and (7) and, as we shall discuss, an experimental study of the quantum number content of the away jet could say what is the dominant process. Let us emphasize that the relative weight of these two subprocesses depends crucially on the nature of the initial beam. In $\bar{p}p$ collisions, the $q + \bar{q} \to \gamma^* + g$ contribution would be enhanced due to the fact that two $\bar{u}$ quarks may annihilate two u-quarks, so that it is the *best place to study gluon jets.* On the contrary, in pp collisions, this contribution is suppressed and the dominant subprocess would be $g + q \to \gamma^* + q$.

In order to compare our predictions with the multiplicity expected in mechanism (a), we draw $dN^{(a)}/dYdz$ which we have estimated as follows. A rough fit for the charged particle inclusive cross section in πp collisions [14] at 200 GeV/c is

$$dN/dY \approx 2\,e^{-0.15\,Y^2},$$

excluding the diffractive component. We assume the transverse momentum distribution to be given by:

$$dN/dYdp_x = 2\sqrt{A/\pi}\,e^{-0.15\,Y^2}\,e^{-Ap_x^2} \qquad (8)$$

with $A \approx 6(\text{GeV}/c)^2$ corresponding to $\langle p_\perp \rangle = 360$ MeV/c. Neglecting kinematical correlations, we then derive

$$dN^{(a)}/dYdz = |Q_x|\,dN^{(a)}/dYdp_x$$

by performing a shift in p_x in eq. (8): $p_x \to p_x^- - \langle p_x \rangle$, where $\langle p_x \rangle \approx \frac{1}{2}|Q_x|/\langle n_c \rangle$: the idea being that half the recoil ($\frac{1}{2}|Q_x|$) is taken by hadrons in the central region ($Y < 1.5$) with mean multiplicity $\langle n_c \rangle \approx 8$ and the other half is taken by the fast hadrons in the forward and backward fragmentation regions (such a descrip-

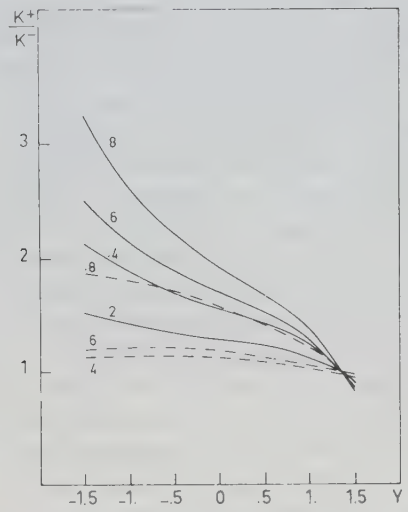

Fig. 3. The ratio of the K^+ and K^- multiplicities calculated at fixed z. ——— $q + g \to q + \gamma^*$. - - - - - summed contributions of $q + g \to q + \gamma^*$ and $q + \bar{q} \to \gamma^* + g$. Each curve is labelled by the corresponding value of z.

tion is in reasonable agreement with data on the background recoil in large $p_\perp$ hadronic reactions [8]). The resulting multiplicity is drawn in fig. 2 which shows the large multiplicity increase due to the away jet in mechanism (b) compared to the background associated with mechanism (a).

Let us now study the quantum number content of the away jet, which we shall describe in terms of the ratio of multiplicities of produced hadrons A and B. For *the subprocess* $g + q \to \gamma^* + q$ we have:

$$A/B(Y,z) = \{\sigma^{(2)}_{g/\pi}(Y)[8\,D^A_u(z) + D^A_d(z)]/9 + \sigma^{(2)}_{g/p}(Y)[4\,D^A_u(z) + D^A_d(z)]/5\}^{-1} \times \{\sigma^{(2)}_{g/\pi}(Y)[8\,D^B_u(z) + D^B_d(z)]/9 + \sigma^{(2)}_{g/p}(Y)[4\,D^A_u(z) + D^A_d(z)]/5\}^{-1}, \quad (9)$$

where $\sigma^{(2)}$ is given by the two particle inclusive distribution [eq. (1)] for charged hadrons with $D^{ch}_q(z)$ divided out. As an example we draw in fig. 3 the ratio $K^+/K^-(Y,z)$ calculated with fragmentation functions taken from Feynman and Field [15]. The shape of the curves $K^+/K^-(Y,z)$ is a clear signature of the subprocess $g + q \to \gamma^* + q$ although the detailed behavior depends on our specific choice of structure functions. It should be contrasted with $K^+/K^-(Y,z)$ for the subprocess $q + \bar{q} \to \gamma + g$ which is equal to 1 independently of Y and z due to the neutral nature of the gluon. Moreover, from large $p_\perp$ hadronic reactions we may infer the ratio $K/\pi \approx 0.5$ in a gluon jet at large z (probability to create an $s\bar{s}$ pair is smaller than probabilities for $u\bar{u}$ or $d\bar{d}$ by about a factor 2). All these features are, in turn, clear signatures of a gluon jet. Finally, we present in fig. 3 the results for $K^+/K^-(Y,z)$ when summing on both subprocesses. We have assumed that $D^K_g(z) = \frac{1}{2}D^\pi_g(z)$ in agreement with above. $K^+/K^-(Y,z)$ is now closer to 1, due to the gluon jet. This tendency increases with Q^2, $q + \bar{q} \to \gamma + g$ becoming more and more dominant.

Let us now compare the results of the above discussion in the framework of QCD with the situation within CIM and exhibit the distinctive features. We shall consider first the subprocess $M(q\bar{q}) + q \to \gamma^* + q$, where M is essentially π^- and thus it is the valence d quark which takes the recoil. Since it also has a large longitudinal momentum, the distribution $dN^{ch}/dYdz$ of its fragments (essentially π^- at large enough z) is strongly peaked at $Y = 2$ and negligeable around $Y = 0$. For the subprocess $D(qq) + \bar{q} \to \gamma^* + q$, on the other hand, where the diquark D comes from the proton, multiplicity is similar to the dashed line in fig. 2. The recoiling jet is essentially either a u or a d quark. The ratio h^+/h^- depends little on Y and the ratio K^-/K^+ should be very small at large enough z. These features are very different from QCD, which should allow to decide in favour of either picture. More detailed calculations and comparisons with QCD may be found in ref. [7].

Finally, let us emphasize that all the above considerations are equally valid for large $Q_\perp$ real photons. Indeed, experiment indicates that the Drell–Yan mechanism sets in for $\sqrt{Q^2} > 3$–4 GeV, but mechanism (b) may already be at work at a much smaller value of $\sqrt{Q^2}$ if $Q_\perp$ is large enough, including real photons. In this case eqs. (1)–(4) are still valid (with modifications since $Q^2 = 0$) and we have calculated that $dN^{ch}/dYdz$ increases by less than 30% when going from $Q^2 = 16\ \mathrm{GeV}^2$ to 0.

As a last point we should mention the interest of observing the backward and forward fragments α and β (fig. 1) in correlation with a massive lepton pair trigger. For small $Q_\perp$ where mechanism (a) is at work, one should observe the background associated with a

Drell–Yan trigger [17], whereas for large $Q_\perp$ the nature of the observed fragments should change according to which subprocess is dominant. Supposing, for instance, that $q + g \to \gamma^* + q$ is at work, one should observe specific fragments coming from a colored octet mesonic or baryonic state, for which it would be very interesting to measure the x_F distribution.

References

[1] S.D. Drell and T.M. Yan, Phys. Rev. Lett. 24 (1970) 855.

[2] D.M. Kaplan et al., Phys. Rev. Lett. 40 (1978) 435.

[3] J. Kogut, Phys. Lett. 65B (1977) 377;
D. Soper, Phys. Rev. Lett. 38 (1977) 461;
I. Hinchliffe and C.H.Llewellyn-Smith, Phys. Lett. 66B (1977) 281;
A.V. Radyushkin, Phys. Lett. 69B (1977) 245;
C.S. Lam and T.M. Yan, Phys. Lett. 71B (1977) 173;
H. Fritzsch and P. Minkowski, Phys. Lett. 73B (1978) 80;
D. Politzer, Nucl. Phys. B129 (1977) 301;
K. Kajantie, J. Lindfors and R. Raitio, Helsinki preprint HU/TFT/78-5.

[4] G. Altarelli, G. Parisi and R. Petronzio, CERN preprints TH-2413 and TH-2450.

[5] G. Chu and J.F. Gunion, Phys. Rev. D10 (1974) 3672;
M. Fontannaz, Phys. Rev. D14 (1976) 3127;
K. Kinoshita, Y. Kinoshita, J. Cleymans and B. Petersson, Phys. Lett. 68B (1977) 355;
M. Duong Van and R. Blankenbecler, preprint SLAC-PUB 2017.

[6] F. Halzen and D.M. Scott, Phys. Rev. Lett. 40 (1978) 1117; UW-Madison preprints COO-881-21.

[7] J.M. Brucker and J. Husser, Ph.D. Thesis, Strasbourg University, France (1978).

[8] M. Fontannaz and D. Schiff, Nucl. Phys. B132 (1978) 457;
M. Fontannaz, Bielefeld Workshop on Large transverse momentum phenomena, BI-TP 77/39 (November 1977).

[9] P. Darriulat et al., Nucl. Phys. B110 (1976) 365;
CCHK collaboration M. Della Negra et al., Nucl. Phys. B127 (1977) 1.

[10] S.J. Brodsky and R. Blankenbecler, Phys. Rev. D10 (1974) 2973.

[11] J.F. Gunion, Phys. Rev. D10 (1974) 242.

[12] M. Fontannaz and D. Schiff, Phys. Lett. 64B (1976) 314.

[13] Y.P. Yao, in: Proceedings of the 12th Rencontre de Moriond, ed. J. Tran Thanh Van.

[14] J. Whitmore, Phys. Rep. 27C (1976) 189.

[15] R.P. Feynman and R.D. Field, Phys. Rev. D15 (1977) 2590.

[16] H. Fritzsch and P. Minkowski, Phys. Lett. 69B (1977) 316.

[17] S.J. Brodsky, in: Proc. of the 12th Rencontre de Moriond, ed. J. Tran Thanh Van;
T.A. Degrand and H.I. Miettinen, Phys. Rev. Lett. 40 (1978) 612;
M. Fonannaz, B. Pire and D. Schiff, Phys. Lett., to be published.

T R O I S I E M E P A R T I E

PHOTOPRODUCTION DE HADRONS DE GRANDE IMPULSION TRANSVERSE ET TESTS DE Q.C.D.

A CLEAR TEST OF PERTURBATIVE QCD IN LARGE-p_T PHOTOPRODUCTION

M. FONTANNAZ [a], A. MANTRACH [a,1], B. PIRE [b] and D. SCHIFF [a]
[a] *LPTHE[2], Université Paris Sud, 91405 Orsay, France*
[b] *CPT[3], Ecole Polytechnique, 91128 Palaiseau Cédex, France*

Received 29 October 1979

It is shown that measurement of the cross-section differences $E\,d\sigma/d^3p\,(\gamma p \to h^+X) - E\,d\sigma/d^3p\,(\gamma p \to h^-X)$ at large transverse momentum provides a good test of perturbative QCD. Such differences are insensitive to the parton Fermi motion and to the poorly known sea-quark and gluon distribution functions. Moreover the hadronized photon component is shown to contribute little compared to the point-like one. Presently available photon beams at the CERN-SPS and FNAL are sufficient to test QCD in large-p_T photoproduction.

Introduction. The phenomenology of Quantum Chromodynamics [1] has achieved tremendous progress in the understanding of leptoproduction, e^+e^- annihilation and lepton-pair hadro-production. However, in these reactions QCD manifests itself as a higher-order correction to the Born terms involving only quarks. As pointed out by Fritzsch and Minkowski [2], the case of large-p_T photoproduction [3] is different since gluons appear already at the Born term level.

The purpose of this letter is to show that the study of the quantity Δ^h defined as:

$$\Delta^h(\boldsymbol{p}) = \frac{E\,d\sigma}{d\boldsymbol{p}}(\gamma p \to h^+X) - \frac{E\,d\sigma}{d\boldsymbol{p}}(\gamma p \to h^-X)\,, \qquad (1)$$

is a very clear way of isolating the QCD Compton effect: $\gamma q \to gq$. We shall find indeed that subtracting cross sections as in eq. (1) allows to get rid of most of the hadronized photon contribution which is not well under control. Let us notice that this component is completely negligible in the case of an isoscalar target. Moreover, we shall show that the theoretical predictions for $\Delta^h(\boldsymbol{p})$ are not obscured by the uncertainties encountered in large-p_T hadronic collisions, namely those due to the treatment of the internal Fermi motion of the partons inside hadrons and those implied by the current ignorance of the gluon structure and fragmentation functions. If experiment confirms the presence of the QCD Compton effect, further studies of two-particle correlations will provide direct information on the gluon fragmentation function [4]. Indeed, in the only graph contributing to $\Delta^h(\boldsymbol{p})$ (fig. 1a) a gluon jet recoils in the hemisphere opposite to the trigger.

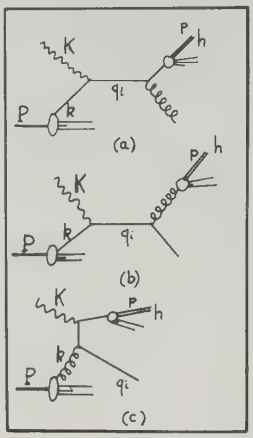

Fig. 1. The Born graphs for photoproduction at large p_T.

The Born term. The graphs of fig. 1 (and their crossed versions) represent the Born approximation to the photoproduction of a large-p_T pion. The differential cross section may be written as

[1] On leave from LPT, Faculté des Sciences de Rabat, Maroc.
[2] Laboratoire associé au CNRS.
[3] Equipe de Recherche associée au CNRS.

$$E\frac{d\sigma}{d^3p}(\gamma p \to hX) = \frac{d\sigma}{dY\, d\boldsymbol{p}_T} \qquad (2)$$

$$= \sum_{\alpha\beta}\frac{1}{\pi}\int dx\, dz\, G_\alpha(x, Q^2)\hat{s}\frac{d\hat{\sigma}_{\alpha\beta}}{d\hat{t}}\delta(\hat{s}+\hat{t}+\hat{u})\frac{D^h_\beta(z)}{z^2},$$

with obvious notations and taking (Y is the center-of-mass rapidity):

$$\hat{t} = (p-K)^2/z = -\sqrt{s}p_T e^{-Y}/z .$$

The subprocess cross sections are given by (figs. 1a,b,c)

$$\frac{d\hat{\sigma}_{q_i q_i}}{d\hat{t}} = \frac{8\pi e_i^2\alpha\alpha_s(Q^2)}{3\hat{s}^2}\left(-\frac{\hat{t}}{\hat{s}}-\frac{\hat{s}}{\hat{t}}\right), \qquad (3a)$$

$$\frac{d\hat{\sigma}_{q_i g}}{d\hat{t}} = \frac{8\pi e_i^2\alpha\alpha_s(Q^2)}{3\hat{s}^2}\left(-\frac{\hat{u}}{\hat{s}}-\frac{\hat{s}}{\hat{u}}\right), \qquad (3b)$$

$$\frac{d\hat{\sigma}_{g q_i}}{d\hat{t}} = \frac{\pi e_i^2\alpha\alpha_s(Q^2)}{\hat{s}^2}\left(\frac{\hat{t}}{\hat{u}}+\frac{\hat{u}}{\hat{t}}\right). \qquad (3c)$$

The running coupling constant is defined as

$$\alpha_s(Q^2) = 12\pi/(33-2N_f)\log(Q^2/\Lambda^2) . \qquad (4)$$

Throughout the paper Λ is taken as 500 MeV and $N_f = 4$.

In eq. (2) the parton transverse momentum has been neglected. We now briefly show that this is justified. It is well known that in large-p_T hadronic collisions the parton transverse momentum may play an important [5] but controversial [6] role, its effect being strongly model dependent. In the reaction considered here we expect a smaller effect since one incident parton, the photon, has no transverse momentum. To test the model independence of our results, we considered on-shell and off-shell kinematics. In both cases we use a gaussian distribution for the parton transverse momentum K_T within the proton. For simplicity we restrict ourselves to the jet production cross section; for the hadron cross section very similar results are expected.

On-shell kinematics. All parton masses are neglected; the initial and final partons are on shell. The divergences which may appear in $d\hat{\sigma}/d\hat{t}$ (eqs. (3a,b,c)) are cured by the substitution $\hat{s}, \hat{t}, \hat{u} \to \hat{s}+M^2, \hat{t}-M^2, \hat{u}-M^2$, with M of the order of a hadronic mass.

Off-shell kinematics. We take the outgoing partons on shell with zero masses. We use off-shell kinematics [7] for the incident parton and put $k^2 \approx -\lambda K_T^2 - \mu^2$; this approximation is valid when the fractional longitudinal momentum x is small. The parameter λ may be estimated from the behaviour of $G_\alpha(x, K_T)$ for small x and large K_T; $\lambda \approx 1.5$ is a reasonable value. The mass μ is taken different from zero so as to prevent divergences from appearing in $d\hat{\sigma}/d\hat{t}$.

Table 1
The ratio r for the jet cross section calculated with off-shell kinematics; $\mu^2 = 0.1$ GeV^2 and $s = 200$ GeV^2.

$\langle K_T\rangle$ (MeV/c)	graph	p_T ($Y=0$)			Y ($p_T=2$)		
		2	3	4	−1	0	+1
900	1a	0.86	0.93	0.97	0.93	0.86	0.71
	1b	1.25	1.09	1.08	1.56	1.25	0.84
500	1a	0.94	0.97	0.99	0.98	0.94	0.88
	1b	1.06	1.03	1.03	1.10	1.06	0.95

Our results for the subprocesses of figs. 1a and b are summarised in table 1 where we show the ratio r of the jet cross section calculated with and without parton transverse momentum. Even with a very large mean value $\langle|K_T|\rangle \approx 900$ MeV/c and a small mass cut off, $\mu^2 = 0.1$ GeV^2, the Fermi motion effect is weak. We get very similar results (within 20%) with on-shell kinematics (with $M^2 \approx 1$ GeV^2). Notice, however, that we found a higher value of r (~ 2–4) for subprocess 1c. This is due to the stronger decrease of the gluon structure function compared to the quark. Anyhow, this subprocess does not contribute to $\Delta^h(p)$. Thus contrarily to the case of hadronic collisions at medium p_T, the effects of parton transverse momenta are well under control in photoproduction.

The input gluon structure and fragmentation functions are unknown and thus a lot of perturbative QCD calculations are somewhat arbitrary. In π^+ photoproduction also, the evaluation of graphs 1b and 1c suffers from this difficulty. A method to circumvent this problem consists in focusing on the difference of cross sections $\Delta^h(\boldsymbol{p})$ defined in eq. (1), which depends only on graph 1a. Moreover only photon–valence-quark scattering contributes. As is well known, the Q^2 evolution of the valence part is decoupled from the evolution of the sea and gluon part. $\Delta^h(\boldsymbol{p})$ is thus completely independent of the poorly determined sea and gluon structure functions.

We shall restrict here on the $\pi^+ - \pi^-$ difference. The resulting $\Delta^\pi(\boldsymbol{p})$ is shown in figs. 2 and 3. In eq. (2) we have used the Buras–Gaemers [8] scale-violating valence structure functions. As there is no experimental

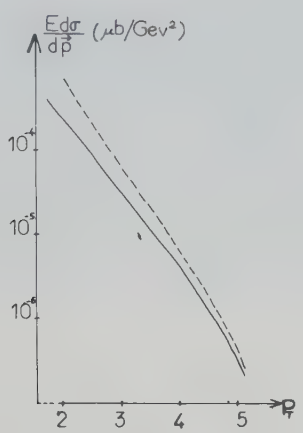

Fig. 2. The p_T dependence of $\Delta^{\pi}(\boldsymbol{p})$ (full curve) and of π^+ photoproduction (dashed curve) at $s = 200\ \mathrm{GeV}^2$ and $Y = 0.5$ (Born terms).

indication of sizable scale violation in the fragmentation functions, we have taken the scaling forms proposed by Field and Feynman [9]. The definition of Q^2 is arbitrary in such a lowest-order calculation. Following Feynman et al. [5] we have taken

$$Q^2 = 2\hat{s}\hat{t}\hat{u}/(\hat{s}^2 + \hat{t}^2 + \hat{u}^2)\,. \tag{5}$$

In fig. 2, we add for comparison the π^+ photoproduction cross section where the three graphs of fig. 1 contribute. For this process we must specify the sea and gluon content of the proton. We have taken the scale-violating parametrization obtained by Owens and Reya [10] as an improvement of the Buras–Gaemers method [8]. At Q_0^2 these structure functions are of the form

$$xG(x, Q_0^2) \sim (1-x)^5\,, \quad xs(x, Q_0^2) \sim (1-x)^7\,. \tag{6}$$

For the gluon fragmentation we have chosen a scale-invariant form,

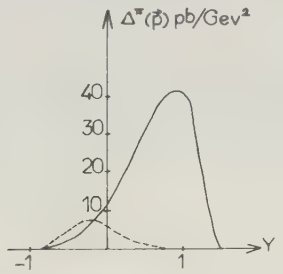

Fig. 3. The angular dependence of $\Delta^{\pi}(\boldsymbol{p})$ at $p_T = 3$ GeV/c and $s = 200\ \mathrm{GeV}^2$. Y is the center-of-mass rapidity, the full curve corresponds to the Born terms and the dashed one to the anomalous part of the hadronized photon.

$$zD_g^{\pi^+}(z) = 2(1-z)^3/3\,. \tag{7}$$

Let us comment on the results:

Due to the charge coefficients in eqs. (3a, b, c), the difference $\Delta^{\pi}(\boldsymbol{p})$ is a large fraction of the π^+ cross section.

The angular distribution is easily understood since the photon interacts with its full energy $\sqrt{s}/2$ with a parton carrying less energy $x\sqrt{s}/2$.

The p_T dependence at fixed s can be described by $p_T^{-n_{\mathrm{eff}}}$ with $n_{\mathrm{eff}} = 5.9$ for $2 < p_T < 4\ \mathrm{GeV}/c$.

The hadronized photon contribution. In addition to the point-like photon Born terms, the hadronic-like terms in the photon should be taken into account. The photon structure function [11] may be viewed as the sum of two terms: the vector dominance contribution and the anomalous component which is derived from the point-like photon coupling to quarks and antiquarks renormalized by the strong interactions. This last component, proportional to $\log Q^2$, is exactly calculated from QCD and is generally believed to dominate [11] at large Q^2. In the Q^2 domain which is investigated here, the VDM component is not negligible. An estimate of its relative importance based on Witten's discussion [11] is of the order of 50%. This spoils the confidence one might have in the predictions for π^+ and π^- cross sections for the medium-p_T range. On the other hand, a favourable situation is obtained by taking the difference of these cross sections where most of both hadronic-like components gets cancelled contrary to the point-like case where the charge factors ensure a sizable value for $\Delta^{\mathrm{h}}(\boldsymbol{p})$. We have calculated the contribution of the anomalous component to $\Delta^{\mathrm{h}}(\boldsymbol{p})$. The only subprocesses which survive involve valence quarks in the proton and either quarks, antiquarks and gluons in the photon. They are drawn in fig. 4. Their cross sections are given in numerous references and were first calculated by Combridge et al. [12]. We use the parametrization of Nicolaidis [13][‡1] for the leading-log photon structure functions. The result of the calculation is plotted in fig. 3 and is indeed found to be small with respect to the Born-term contri-

[‡1] This parametrization gives the quark and gluon distributions correctly summed over color (a factor of 8 is missing for the gluon distribution in Llewellyn Smith's paper of ref. [11]).

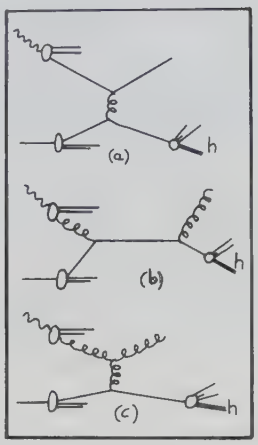

Fig. 4. The graphs with a hadronized photon contributing to $\Delta^h(\boldsymbol{p})$.

bution. Thus even doubling this result in order to roughly take into account the VDM part, we still get a small hadronized photon contribution (negligible at large Y).

Conclusion. The overall value for $\Delta^\pi(\boldsymbol{p})$ is measurable in the conditions of the soon to come experiments at the CERN SPS [14]. As discussed at length, it is free from a list of ambiguities which appear in either π^+ or π^-. On the basis of Owens' calculations of the jet cross section [3] we have estimated that the hadronized photon contribution to the π^+ cross section for $p_T \approx 3$ GeV/c is about twice that of the Born term. This gives $(\pi^+ - \pi^-)/\pi^+ \sim 15$–$25\%$, which means that $\Delta^\pi(\boldsymbol{p})$ is a well-measurable quantity.

It is not easy to determine at which value of p_T the QCD Compton effect will take over from other contributions of the CIM/higher-twist type. We expect a smooth transition from a low-p_T region where a $d\sigma/dp_T \approx Cp_T^{-12}$ law seems to dominate [15] to a QCD region characterized by a p_T^{-6} decreasing law (at fixed s) and the magnitude calculated above. One should keep in mind, however, that all these estimates have been performed in the frame of the leading-log approximation. The problem of incorporating terms beyond the leading log is very delicate. They affect in particular the definition of Q^2 and the value of Λ; for instance, taking $Q^2 = (\hat{s}\hat{t}\hat{u})^{1/3}$ in place of eq. (5) lowers our result by some 30%.

As a final remark, let us stress the fact that we may get completely rid of the hadronized photon contribution by measuring $\Delta^h(\boldsymbol{p})$ on an isoscalar target. In that case also the Born contribution remains sizable due to the charge factors in eq. (3).

We would like to thank the members of the WA4 collaboration at the CERN SPS, especially F. Richards, F. Gorski and D. Treille, for useful discussions.

References

[1] For a recent review, see, for instance: R. Field, lectures at La Jolla Institute Summer Workshop (1978), and references therein.
[2] H. Fritzsch and P. Minkowski, Phys. Lett. 69B (1977) 316.
[3] Tu T.-S., CERN preprint TH 2690 (1979);
J. Owens, Florida State Univ. preprint FSU 790731 (1979).
[4] M. Fontannaz, A. Mantrach, B. Pire and D. Schiff, preprint in prepration.
[5] A. Contogouris, R. Gaskell and S. Papadopoulos, Phys. Rev. D17 (1978) 2314;
R. Feynman, R. Field and G. Fox, Phys. Rev. D18 (1978) 3320.
[6] M. Fontannaz and D. Schiff, Nucl. Phys. B132 (1978) 457;
R. Horgan and P. Sharbach, Phys. Lett. 81B (1979) 215.
[7] D. Sivers, R. Blankenbecler and S. Brodsky, Phys. Rep. 23C (1976) 1, Appendix A.
[8] A. Buras and K. Gaemers, Nucl. Phys. B132 (1978) 249.
[9] R. Field and R. Feynman, Phys. Rev. D15 (1977) 2590.
[10] J. Owens and E. Reya, Phys. Rev. D17 (1978) 3003.
[11] E. Witten, Nucl. Phys. B120 (1977) 189;
C. Llewellyn Smith, Phys. Lett. 79B (1978) 83;
R. de Witt et al., Phys. Rev. D19 (1979) 2046.
[12] B. Combridge, J. Kripfganz and J. Ranft, Phys. Lett. 70B (1977) 234.
[13] A. Nicolaidis, Nucl. Phys. B., to be published.
[14] CERN–Imperial College–LAL Orsay–Saclay–Southampton Collaboration.
[15] A. Eisner et al., Phys. Rev. Lett. 33 (1974) 865.

LARGE P_T PHOTOPRODUCTION AND TESTS OF Q.C.D.

M.Fontannaz, A.Mantrach[+] and D.Schiff
Laboratoire de Physique Théorique et Hautes Energies[*]
Université Paris-Sud 91405 Orsay
France

B.Pire
Centre de Physique Théorique[**] Ecole Polytechnique
91128 Palaiseau Cedex, France

ABSTRACT

A complete investigation of large p_T hadron photoproduction is carried out aiming to isolate and study Q.C.D. predictions concerning both direct coupling and anomalous photon components. Comparison with experimental data shows that these components may be disentangled from a large hadron-like background, provided cross-section differences or symmetric pair correlations are measured. The production of jets is also examined with emphasis on gluon jets.

LPTHE 80/12
A393-0480

[+] On leave of absence from L.P.T.,Faculté des Sciences de Rabat, Maroc.

[*] Laboratoire associé au C.N.R.S.

[**] Groupe de Recherche du C.N.R.S.

Introduction

The interest of photon initiated processes for producing large p_T particles and testing QCD has been emphasized in many places [1-10] . We investigate in this paper what photoproduction of large p_T particles tells us about two aspects of the photon interaction: the direct coupling and the photon structure function contributions, as shown in Fig.1, which are predicted and exactly calculable in the framework of perturbative QCD at sufficiently large Q^2.

In a recent paper[8] we already proposed a way of isolating, among the direct coupling terms, the QCD compton effect (Fig. 1a) by studying the cross-section differences

$$\Delta^h(\vec{p}) = E\frac{d\sigma}{d\vec{p}}(\gamma p \to h^+ X) - E\frac{d\sigma}{d\vec{p}}(\gamma p \to h^- X).$$

The photon structure function contributes very little to $\Delta^h(\vec{p})$ and in lowest order, the prediction of QCD is free from the arbitrariness connected with ill-determined gluon structure and fragmentation functions, so that the measure of $\Delta^h(\vec{p})$ is a clear test of the theory. Moreover, studying, in a second step, differences of double inclusive cross sections is a way of determining specifically the properties of gluon fragmentation [11] .

Furthermore, it is also very interesting to measure the photon structure function[2,12,13] which is completely

calculable at large Q^2. It is usually described as consisting of two terms: the anomalous and hadron-like components. The photon point-like coupling to $q\bar{q}$, renormalized by QCD generates the anomalous component with a specific log Q^2 behaviour, already present at the Born term level. This ensures, at large enough Q^2, the dominance of the anomalous component over the hadron-like component which has the same scaling behaviour as usual hadronic structure functions. At experimentally accessible Q^2, however, both components are at work and we shall be interested in this paper to investigate under which conditions the anomalous component is experimentally accessible, which will provide a stringent test of QCD. We shall thus essentially handle the problems of disentangling the various contributions: the direct photon coupling and the anomalous and hadron-like components of the photon structure function.

Preliminary experimental results[14] for π^+ and π^- photoproduction are already available in the energy domain 45 GeV $< E^{\gamma}_{lab} <$ 70 GeV and $p_T <$ 2.5 GeV/c. We shall show that one-particle inclusive cross-sections are dominated by the hadron-like component, commonly estimated in the VDM framework. This is in some sense a background to the QCD calculable components and forbids a meaningful comparison with the theory. In contrast, the measure of $\Delta^{\pi}(\vec{p})$ is a way of subtracting a large fraction of the hadron-like background; in this sense,this paper contains, in addition to

ref. [8] , a very detailed study of the background in $\Delta^{\pi}(\vec{p})$ and reemphasizes the interest of this quantity. Comparison with existing data for Δ^{π} is indeed satisfactory.

In the next-to-come experiment[15] energy and p_T domain ($E_{lab} \simeq$ 100 GeV, $p_T \lesssim$ 5 GeV/c), we shall find that one particle cross-sections have still an important hadron-like background, so that again, it is very difficult to extract the anomalous component of the photon structure function. Should we wait for higher energies in order to perform this task ? We shall show that a possible way at presently accessible energy is to analyze symmetric pair correlations which are little affected by the hadron-like background .

Finally, we shall study jet cross-sections at very high energies. They provide a stringent test of the non-abelian nature of the theory, being essentially determined by the 3 and 4 gluon couplings. Moreover, they are very sensitive to the gluon content of the photon.

The specificity of the present paper, among others already published on the subject, is the emphasis put on the possibility of isolating each photon component in order to obtain clear tests of QCD. Preliminary experimental data are used to discuss the difficulties of this approach. In particular, we study in detail the hadron-like background which clouds predictions for one-particle cross-sections at presently accessible energies. This problem had been ignored

or underestimated by previous authors. Finally, we mainly focus on particle production in view of the difficulties connected with the experimental definitions of jets in large p_T reactions.

Let us outline the contents of this paper: Section I is devoted to establishing the formalism in order to calculate the direct coupling term and the anomalous component. The hadron-like contribution is discussed and evaluated in the framework of VDM in section II. Section III deals with comparing theoretical calculations to preliminary experimental data on large p_T π^+ and π^- photoproduction. Theoretical predictions are also given, in the next-to-come experiment energy and p_T domain. A complete discussion of the hadron-like background is given. Section IV is devoted to the study of jets, and in particular to the possibility of observing gluon jets after having separated 3 and 4 jet samples. Section V discusses the symmetric pair correlations which provide the way to extract the anomalous component at presently accessible energies. Section VI is devoted to higher energies and section VII is the conclusion.

I. Basic Calculations in QCD.

In this section we present basic formulae for the inclusive cross-section for producing a large p_T hadron. Here, we limit ourselves to the two components that are exactly calculable in QCD, namely the direct coupling terms and the anomalous photon structure function contribution. We perform calculations in the leading logarithm approximation. We also give the relevant equations for differences of cross-section of the type $d\sigma(\gamma p \to h^+ X) - d\sigma(\gamma p \to h^- X)$ which will turn out to provide the most testable predictions.

a) direct coupling terms

In contradistinction with the case of hadron-hadron scattering where both incident particles scatter through their constituents the photon may interact as a whole with the proton partons. The lowest order direct coupling terms which we consider are drawn in fig.1. The one-particle inclusive cross-section may be written as:

$$E\frac{d\sigma^h}{d\vec{p}} = \frac{1}{\pi}\sum_{a,b,c}\int dx\, dz\, G_{a/p}(x,Q^2)\,\hat{s}\frac{d\hat{\sigma}}{d\hat{t}}(\gamma a \to bc)\frac{D_b^h(z)}{z^2}\,\delta(\hat{s}+\hat{t}+\hat{u}) \tag{1}$$

where

$$\frac{d\hat{\sigma}}{d\hat{t}}(\gamma q \to qg) = \left[\frac{4}{3}\right]\frac{2\pi e_q^2 \alpha\,\alpha_s(Q^2)}{\hat{s}^2}\left(-\frac{\hat{t}}{\hat{s}} - \frac{\hat{s}}{\hat{t}}\right)$$

$$\frac{d\hat{\sigma}}{d\hat{t}}(\gamma g \to q\bar{q}) = \left[\frac{1}{2}\right]\frac{2\pi e_q^2 \alpha\,\alpha_s(Q^2)}{\hat{s}^2}\left(\frac{\hat{t}}{\hat{u}} + \frac{\hat{u}}{\hat{t}}\right) \tag{2}$$

numbers in brackets being colour factors, $\hat{s}$,$\hat{t}$ and $\hat{u}$ being the subprocess Mandelstam variables

$$\hat{s} = (p_\gamma + p_a)^2 \qquad \hat{t} = (p_\gamma - p_b)^2 \qquad \hat{u} = (p_\gamma - p_c)^2$$

The running coupling constant is, as usual, given by

$$\alpha_s(Q^2) = 12\pi/(33-2N_f)\,\mathrm{Log}\,(Q^2/\Lambda^2)$$

with $N_f=4$. The definition of Q^2 and Λ is arbitrary in such a leading log calculation. We take $Q^2 = 2\,\hat{s}\,\hat{t}\,\hat{u}/(\hat{s}^2+\hat{t}^2+\hat{u}^2)$ following ref [16] and Λ =0.5 GeV. The trigger rapidity is defined through

$$t = (p - p_\gamma)^2 = -\sqrt{s}\; p_T\; e^{-y}$$

where p_T is the transverse momentum of the observed hadron.

In (1) we have neglected the Fermi motion of partons in the proton. It is well known that such an approximation is unjustified in the case of hadron-hadron scattering. The situation is however very different in photoproduction. We have indeed shown in ref [8] that for direct coupling terms the inclusion of this effect leaves the result unchanged for $p_T \gtrsim$ 2.5 GeV/c, in a model independent way. We refer the reader to this work for more details.

The G's are the gluon and quark structure functions in the proton. The valence quark structure functions are the only well determined ones; we use the Buras-Gaemers [17] parametrization derived in agreement with experiment and

renormalization group equations. Various choices are possible for the sea and gluon content of the proton; we choose the Owens-Reya [18] forms which behave as $(1-x)^7$ and $(1-x)^5$ respectively at $Q_o^2 = 1.8\ GeV^2$ and x near 1. We neglect charmed quarks in the proton. The D's are fragmentation functions. Here again only the quark ones are well-known; we take the Field-Feynman [19] parametrization in agreement with the experiment. For gluon fragmentation we adopt the scale invariant parametrization

$$D_g^{\pi^+}(z) = \frac{2}{3}\frac{(1-z)^3}{z} \qquad (3)$$

In the following we shall comment on the implication of other choices for gluon functions.

It is important to notice, as emphasized in ref [8], that only graph 1a (QCD Compton Effect) contributes to $\Delta^h(\vec{p}) = E\, d\sigma(\gamma p \to h^+X)/d\vec{p} - E\, d\sigma(\gamma p \to h^-X)/d\vec{p}$ and only valence quarks in the proton are to be taken into account. Remembering that the Q^2 evolution of the valence is disconnected from the Q^2 evolution of sea and gluons, one concludes that $\Delta^h(\vec{p})$ does not depend on ill-determined structure or fragmentation functions, at the level of direct processes studied here. Moreover, this difference of cross-sections is not small because of the electric charge coupling of the photon to the quarks.

b) anomalous photon structure function contribution

The photon may also interact through its constituents with the target proton. Both the renormalization group [12] and perturbative QCD [13] approaches lead to distinguish two components in the photon structure function:

i) the anomalous part, exatly calculable which results from renormalization of the point-like photon coupling to quark-anti-quark through strong interactions with the specific $\log Q^2$ behaviour as in the free quark model.

ii) the "hadronic" part which has the same scaling properties as usual hadron structure functions and is commonly parametrized in the framework of Vector Dominance as will be done in detail in section III.

The anomalous part is dominant for large enough Q^2 which makes the photon structure function such an interesting QCD object. Its contribution to the photoproduction cross-section is written under the form

$$E\frac{d\sigma^h}{d\vec{p}} = \frac{1}{\pi}\sum_{a,b,c}\int dx_a\, dx_b\, G_{a/\gamma}(x_a,Q^2)\, G_{b/p}(x_b,Q^2)\left[\frac{dz}{z^2}\, D_c^h(z)\, \hat{s}\,\frac{d\hat{\sigma}}{d\hat{t}}(ab\to cd)\,\delta(\hat{s}+\hat{t}+\hat{u})\right] \qquad (4)$$

The various subprocesses cross-sections have been calculated several times [20] .Three independent photon distribution functions appear : $G_{2/3}(x,Q^2)$ $[G_{1/3}(x,Q^2)]$ for quarks or

antiquarks of fractional charge $\pm$ 2/3 [$\pm$ 1/3] and $G_g(x,Q^2)$ for gluons. We neglect b and t quarks but include charmed quarks in the photon (identifying D_c^π (z) to $D_s^\pi(z)$). Leading log expressions for these G's have been parametrized by Nicolaidis[21]. $G_{2/3}$ and $G_{1/3}$ are remarkably hard: this is responsible for the expected large order of magnitude of high energy high p_T cross-sections and also for the specific shape of the angular distribution peaked in the forward direction. The gluon content of the photon is important at small x and at very high energy it will provide a large amount of the cross-section (so that we disagree with calculations at very high energy given in ref [9] where it is neglected). There are many terms in the sum of (4); let us write explicitly the contribution to $\Delta^\pi(\vec{p})$ under the form:

$$\Delta^\pi(\vec{p}) = \frac{1}{\pi}\int dx_a\, dx_b\, dz \left[D_u^{\pi^+}(z) - D_u^{\pi^-}(z)\right] \hat{s} \sum \delta(\hat{s}+\hat{t}+\hat{u})/z^2 \qquad (5)$$

with

$$\sum = \left[\sigma_1 G_g(x_a,Q^2) + 4\sigma_2 G_{2/3}(x_a,Q^2) + 4\sigma_2 G_{1/3}(x_a,Q^2)\right]\left[G_{u/p}(x_b,Q^2) - G_{d/p}(x_b,Q^2)\right]$$
$$+ \sigma_3\left[G_{2/3}(x_a,Q^2)\, G_{u/p}(x_b,Q^2) - G_{1/3}(x_a,Q^2)\, G_{d/p}(x_b,Q^2)\right] \qquad (6)$$

where

$$\sigma_1 = \frac{\pi \alpha_s^2(Q^2)}{\hat{s}^2}\left(-\frac{4}{9}\,\frac{\hat{t}^2+\hat{s}^2}{\hat{t}\hat{s}} + \frac{\hat{t}^2+\hat{s}^2}{\hat{u}^2}\right)$$

$$\sigma_2 = \frac{\pi \alpha_s^2(Q^2)}{\hat{s}^2}\;\frac{4}{9}\;\frac{\hat{s}^2+\hat{t}^2}{\hat{u}^2} \qquad (7)$$

$$\sigma_3 = \frac{\pi \alpha_s^2(Q^2)}{\hat{s}^2}\left(-\frac{8}{27}\,\frac{\hat{s}^2}{\hat{u}\hat{t}} - \frac{8}{27}\,\frac{\hat{t}^2}{\hat{s}\hat{u}} + \frac{8}{27}\,\frac{\hat{u}^2}{\hat{s}\hat{t}}\right)$$

σ_1 is straightforwardly the contribution of the $qg \to qg$ subprocess σ_2 and σ_3 are the result of all properly symmetrized contributions of the type $q_i q_j \to q_i q_j$ (and $q \leftrightarrow \bar{q}$); all interference terms have been put in σ_3. Apart from this latter contribution, which is small, the integrand in (5) is proportional to $G_{u/p}(x_b) - G_{d/p}(x_b)$, since the photon is not coupled directly to the charge of the constituents in the proton. In absence of the small interference terms, the anomalous photon structure function contribution to $\Delta^{\pi}(\vec{p})$ would vanish when measured on an isoscalar target. This is to be contrasted with the expression of the direct coupling term where the u quark contribution is enhanced by the square charge factor, so that taking the difference is indeed a way of diminishing the anomalous photon contribution, keeping a large fraction of the direct coupling and thus a measurable number for Δ^{π}. This is an interesting feature as it allows to isolate the QCD Compton effect.

In formulae (4) and (5) the initial parton transverse momenta have been neglected. We shall comment on the importance of this effect in section III when dealing with the comparison of predictions and data.

II. VDM estimate of the hadron-like photon contribution

In order to estimate the hadron-like photon contribution, we use the VDM analogy between the photon and the vector mesons as already done by many authors [7,9,12] . We shall deal, here, with the contribution to the one-particle inclusive spectrum. There are actually two possible ways to proceed which are described in turn:

a) the VDM is used to identify the hadron-like part of the photon structure function with the vector meson structure function. We write, as usual, the quark content of the photon as

$$\gamma = g\left(\frac{2}{3}u\bar{u} + \frac{1}{3}d\bar{d} + \cdots\right) = \frac{g}{\sqrt{2}}\left(\rho + \frac{1}{3}\omega + \cdots\right) \qquad (8)$$

We neglect the contribution of heavier resonances like $\rho', \phi, \psi \ldots$ which have smaller couplings to the photons and retain only ρ and ω with $g^2/2 = 4\pi\alpha/f_\rho^2 = \alpha/2.2$. From (8) one relates the momentum distributions of u and d quarks inside the photon and inside $u\bar{u}$ or $d\bar{d}$. These are supposed to be identical to the u quark momentum distribution inside the π^+ so that[1]:

$$u^\gamma(x) = \frac{4}{g}\frac{e^2}{g}u^{\pi^+}(x) = 4\,d^\gamma(x) = \bar{u}^\gamma(x) = 4\,\bar{d}^\gamma(x) \qquad (9)$$

---

[1] We disagree by a factor 2 with the u^γ definition of ref [9].

For u^{π^+} we take the following form in agreement with data of μ pair production in $\pi^- p$ collisions for $x > .25$ [22]

$$u^{\pi^+}(x) = .5\,(1-x)/x \tag{10}$$

We parametrize the gluon distribution by:

$$g^{\gamma}(x) = \frac{5}{9}\,g^2\,2\,(1-x)^3/x \tag{11}$$

in agreement with counting rules and assuming gluons take 50 % of the momentum of either $u\bar{u}$ or $d\bar{d}$. These expressions of the quark and gluon distribution functions in the hadron-like photon are then used to calculate the corresponding inclusive spectrum along the same line as in Ib. In this approximative estimate of the hadron-like component of the photon, we neglect the Q^2-dependence of the structure functions in formulae (10) and (11).

b) A direct phenomenological estimate of the hadron-like photon contribution to $E\,d\sigma(\gamma p \to \pi X)/d\vec{p}$ uses VDM under the form:

$$E\frac{d\sigma}{d\vec{p}}(\gamma p \to \pi X) = \sum_V \frac{4\pi\alpha}{f_V^2}\,E\frac{d\sigma}{d\vec{p}}(V p \to \pi X) \tag{12}$$

We restrict to the ρ for a detailed estimate since in this case, writing as usual $d\sigma(\rho^0 p \to \pi x) = \frac{1}{2}(d\sigma(\pi^+ p \to \pi x) + d\sigma(\pi^- p \to \pi x))$ we may rely on experimentally measured cross-sections. We shall multiply the final result by an overall factor ~ 1.1 to include the ω (neglecting interference terms and heavier vector mesons).

Focusing on π^+ production, we express $E\frac{d\sigma}{d\vec{p}}(pp \to \pi^+ x)$ in terms of $E\frac{d\sigma}{d\vec{p}}(\pi^+ p \to \pi^0 x)$ which has been measured at 90° [23]. It is convenient to define the following cross-sections ratios:

$$\begin{aligned} r_1 &= d\sigma(\pi^+ p \to \pi^+ X)/d\sigma(\pi^+ p \to \pi^- X) \\ r_2 &= d\sigma(\pi^+ p \to \pi^0 X)/d\sigma(\pi^- p \to \pi^0 X) \\ r_3 &= d\sigma(\pi^- p \to \pi^- X)/d\sigma(\pi^- p \to \pi^0 X) \end{aligned} \tag{13}$$

Then

$$E\frac{d\sigma}{d\vec{p}}(pp \to \pi^+ X) = \left(r_1/(1+r_1) + 1/r_2 - r_3/2r_2\right) E\frac{d\sigma}{d\vec{p}}(\pi^+ p \to \pi^0 X) \tag{14}$$

r_2 and r_3 may be calculated from the data of ref [23,24] and depend very little on energy. They are found to be close to 1 at 90° : $r_2 \simeq .95$; $r_3 \simeq 1.1$. r_1 is not experimentally known but may be inferred from the analogous ratio for protons[25]: $r_1 \simeq 1.7$ at 90° and $x_T \simeq .4$. Similarly

$$E\frac{d\sigma}{d\vec{p}}(pp \to \pi^- X) = \left(r_2/(1+r_1) + r_3/2\right) E\frac{d\sigma}{d\vec{p}}(\pi^- p \to \pi^0 X) \tag{15}$$

As a consequence, the cross-section difference Δ^π receives a contribution :

$$\Delta^\pi(\vec{p}) = \frac{4\pi\alpha}{p_T^2 s}\left(\frac{r_1 - 1}{r_1 + 1} + \frac{1}{r_2} - \frac{r_3}{r_2}\right) E\frac{d\sigma}{d\vec{p}}(\pi^+ p \to \pi^0 X) \tag{16}$$

With the above values for r_1, r_2, r_3, this is estimated at 90° to be of the order of 15% of the corresponding hadron-like contribution to

$E \frac{d\sigma}{d\vec{p}}(\gamma p \rightarrow \pi^+ x)$. In the forward direction this ratio should be even smaller since in this region the mean charge is that of the photon.

The advantage of this phenomenological estimate, compared to the first method is that it does not rely on QCD to calculate the hard vector meson-hadron collision. We know indeed that, in the moderate p_T region, QCD has to be supplemented by a phenomenological treatment of constituent transverse motion in order to obtain agreement with the data [16,26,27]. Without playing this game, which appears to be very arbitrary[28,29] one has therefore no chance to evaluate properly the $\rho p \rightarrow \pi x$ cross-section. Thus, as will be shown in the next section, it is not surprising to find that the phenomenological estimate yields a much higher result than the theoretical one, in the moderate p_T region; the ratio is of the order of the enhancement factor due to constituent transverse motion, encountered in the same p_T and energy domain in proton-proton collisions. On the other hand, the theoretical estimate will be useful for correlations which are only little affected by constituent transverse motion[28,30]

III. Comparison with data and predictions for next-to-come experiments

a) comparison with data

Data are already available in the energy range $45 \leqslant E_\gamma^{Lab} \leqslant 70$ GeV for π^+ and π^- photoproduction [14].

- Let us first comment on π^+ photoproduction. One sees from fig.2, which shows the rapidity distribution $\frac{d\sigma}{dy} = \int_{p_T=2.} d\vec{p}_T \frac{d\sigma}{dy d\vec{p}_T}$, that the direct coupling contribution is much larger than the anomalous photon structure function one. The striking feature is the importance of the phenomenological VDM estimate for the hadron-like photon background which appears to represent the main bulk of the cross section. On the other hand, the theoretical VDM contribution is very small (a factor 30 smaller than the phenomenological VDM estimate at y = 0). As indicated in the previous section, this is to be understood as the sign of the importance of the constituent transverse motion, in this p_T range (mean $p_T \simeq 2.3$ GeV), non mentioning the possibility of higher twist /CIM terms [31]. Correlatively we expect that some enhancement factor should also be applied to the QCD anomalous photon structure function calculation. This factor is certainly smaller than in hadron-hadron collisions, since resulting only from gluon bremsstrahlung. To summarize, even if the direct coupling term is little sensitive [8] in this p_T and energy domain to the parton transverse momentum, the other components : anomalous and hadron-like photon structure function contributions are too poorly predicted by the theory for allowing a meaningful comparison with experiment. Notice

however that within uncertainties of the phenomenological estimate of the hadron-like photon background, the agreement with experimental data is altogether obtained.

- The situation is however more favorable for Δ^{π} . As mentioned in section I, both the anomalous and hadron-like contributions are minimized in the cross section difference compared to the direct coupling term. In fig. 2, we draw the phenomenological VDM estimate for the hadron-like background which we obtain from the corresponding contribution to $\gamma p \to \pi^+ X$ by multiplying by .15, as discussed in section II. There we also indicated, however, that such a procedure yields an overestimate for $y > 0$. We are thus left with a situation where the direct coupling term is the dominant contribution so that it is meaningful to compare it to the data. We show $\frac{d\sigma}{dp_T^2}(\pi^+ - \pi^-)$ (integrated on y within the experimental acceptance, $\theta_{lab} < 15°$) on fig.3. The discrepancy in the region $p_T \geq 2$ is consistent with what we expect for the hadron-like background. We have also plotted $\frac{d\sigma}{dp_T^2}(\pi^+ - \pi^-)$ integrated in the region $y \geq .5$ only. This cut presents the advantage of getting rid of most of the VDM background (and also contamination by spectator fragments of the proton). As may be expected, the agreement with corresponding data gets better and quite satisfactory.

To conclude this discussion on Δ^{π} , the lesson of the comparison with data is that in this p_T and energy domain Δ^{π} is a very interesting quantity to measure since it provides a meaningful test of the theory, in contrast with indi-

vidual cross sections which are subject to uncertainties in the treatment of the hadron-like background and of the anomalous component. We shall see, when dealing with the higher energy and p_T range of the next to come experiments, that this is still true.

As a last point, let us comment on contamination of present data by K^+ and K^- due to lack of particle identification. Both positive and negative charged distributions get enhanced by $\sim$ 30 % (the equal status of π^- and K^- compared to π^+ and K^+ is due to the charge factor 4 associated with the u quark and to the relatively moderate value of $\langle z \rangle$ in the fragmentation function)

b) predictions in the intermediate energy domain

The next to come experiments[15] will have most of their statistics in the energy domain $E_\gamma^{lab} = 100$ GeV and it will be possible to explore values of p_T up to 5 GeV/c. In the region $p_T \geq 3$ GeV/c, we expect that the hadron-like background be less important than previously and the more so with increasing p_T.

- Let us first examine the prediction for $E \frac{d\sigma}{dp}(\gamma p \to \pi^+ X)$. We shall perform calculations for $p_T = 3$ GeV/c in order to keep a sizeable anomalous photon structure function contribution compared to the direct coupling terms. Both are shown on fig. 4. For completeness, we indicate the amount of the anomalous photon structure function contribution provided by $qg \to qg$. Also shown is the VDM phenomenological estimate

for the hadron-like background. Although relatively smaller than previously, it is still too large to allow a test of the theory. The theoretical VDM estimate is smaller by a factor 10 which is consistent with parton transverse motion enhancement factors encountered in the same p_T and energy domain in p p collisions. This indicates that the anomalous photon structure function contribution should be also enhanced somehow when considering parton transverse momentum due to gluon bremmstrahlung. In the same line of thought, the difference between theoretical and phenomenological VDM estimates leaves some room for the higher twist/CIM processes. To conclude, the situation is, as previously, such that it is very hard to compare the theoretical prediction to the data and especially to extract the anomalous component of the photon structure function as calculated in Q.C.D.

- In contrast the situation is very favorable for a comparison of Δ^{π} with experiment and specifically a test of the theoretical prediction for the QCD Compton effect. On fig. 4, we show that it provides the essential contribution to Δ^{π} which is a large fraction of the π^+ cross section. The anomalous component is small and vanishes completely in the forward region,[2] and the same is true for the hadron-like background.

In what concerns the anomalous component of the photon structure function, in the p_T and energy domain of the next to come experiments, our conclusion is that it will be difficult to extract it from the data.

---

[2] In formula (7), σ_1 contributes little and σ_2 disappears like $1/\hat{u}^2$ for large y.

Is it, however, possible to find a way of getting rid of the hadron-like background or/and of the parton transverse momentum effects in order to strictly remain with the direct coupling and the anomalous components calculated in leading order QCD ? A means to achieve this goal is to turn to symmetric pair correlations as will be discussed in section V.

IV. Jet Studies

A fairly complete description of jet photoproduction has been given by Owens[7]. We shall not repeat his analysis here, but we want to develop some points which are interesting for our purpose : the identification and the experimental selection of the different components of the photon. We shall also discuss the possibility to observe gluon jets event by event.

The main point is that the final jets produced in the direct coupling reactions and in processes involving the structure function of the photon have a very different topology. The direct coupling results in two large p_T final jets and a backward low p_T jet made of proton fragments, whereas in the second case a fourth jet made of low p_T fragments of the photon is observed in the forward direction[14].

It is important to notice that the transverse momentum and the rapidities of the large angle jets of the 3-jet events have to verify a kinematical constraint. The double jet inclusive cross section is indeed given by

$$\frac{d\sigma}{d\vec{p}_T dy_1 dy_2} = \frac{2}{\pi} \sum_{a,b,c} x_b \, G_{b/p}(x_b) \, \frac{d\hat{\sigma}}{d\hat{t}} \, (\gamma b \to cd) \, \delta(2 - x_T(e^{y_1} + e^{y_2})) \tag{17}$$

where $(\vec{p}_T, y_1)$ and $(-\vec{p}_T, y_2)$ are the transverse momenta and rapidities of the jets.

Thus inspection of the jet structure supplemented by the use of the 3-jet topology kinematical constraint, should allow

one to separate the direct coupling events from the other ones. The interesting consequence of this selection is that we can now compare data and theory within each subset of events independently. Let us illustrate this point by studying the possibility to observe, event by event, a gluon jet.

The jet cross section is, in the direct coupling case,

$$E\frac{d\sigma}{d\vec{p}} = \frac{1}{\pi}\sum_{b,c,d} x_b\, G_{b/p}(x_b,Q^2)\,\frac{2}{2 - x_T\, e^{y}}\,\frac{d\hat{\sigma}}{d\hat{t}}\,(\gamma b \to cd) \qquad (18)$$

with $x_b = x_T\, e^{-y} / (2 - x_T\, e^{y})$. For the reaction involving the photon structure function, we have

$$E\frac{d\sigma}{d\vec{p}} = \frac{1}{\pi}\sum_{a,b,c,d}\int dx_a\, G_{a/\gamma}(x_a,Q^2)\, G_{b/p}(x_b,Q^2)\,\frac{2\,x_a\,x_b}{2\,x_a - x_T e^{y}}\cdot \frac{d\hat{\sigma}}{d\hat{t}}\,(ab \to cd) \qquad (19)$$

with $x_b = x_a\, x_T\, e^{-y} / (2\, x_a - x_T\, e^{y})$

The situation in the next-to-come experiment energy domain ($s \simeq 200$ GeV^2) is interesting. In fig. 5a, we show the different contributions to the jet cross section for a jet of 4 GeV/c transverse momentum. One may observe that the direct coupling terms are dominant for positive rapidity and of the order of the anomalous photon component at negative rapidity. This picture is certainly blurred by the hadron-like background. But we lack experimental data at the corresponding energy and p_T range on jet production in πp collisions in order to evaluate it as in section IIb. Although we expect

a relatively smaller VDM contribution (due to a smaller parton transverse motion enhancement factor in jet than in particle production), it should certainly again forbid comparison with experiment. In fig.5b, we show the ratio of the expected yields of gluon jet to quark jets.

When considering both 3-jet and 4-jet events, this ratio is of order 1 (it should not be much affected by the hadron-like background); thus we have no possibility to observe a pure sample of gluon jets. The situation looks better when focusing on the 3-jet events; gluon jets now dominate over quark jets for negative rapidity. Thus it is possible to observe gluon jets on an event by event basis; the yield should be sufficient to study gluon jet properties.

This conclusion is, however, obtained with a particular choice of the gluon distribution in the proton. We do not have yet any direct experimental information on the shape of this function (although its normalization is fairly well-known from sum rules). The Owens-Reya parametrization we have used may be considered as a mean choice among recently proposed functions[17,30]. For softer choices[17] our results essentially remain unchanged but in the case of harder distributions, as that of ref [30] which decreases as $(1-x)^3$ at $Q_o^2 = 5$ GeV^2, they are drastically different. Indeed, the x region probed by the direct coupling term in the explored kinematical region ranges from about 0.4 to 1. This explains that the harder distribution yields a much more important $(g \to q\bar{q}$ contribution, thus decreasing appreciably the ratio gluon jet/quark jet, as shown in fig.5b. This, in turn, amplifies the need of a direct determination of the gluon content of the proton; we will show in a forthcoming paper[32] that it may be given by the study of correlations in photoproduction.

V. Symmetric pair correlations

In this section we consider the problem of observing the contribution of the anomalous part of the photon. Two obstacles must be overcome before reaching our goal; in a first step we must isolate the photon structure function contribution, and then disentangle the anomalous component from the hadron-like one. We have seen in the preceeding section how it should be possible, on the ground of direct coupling kinematics, to isolate the sample of 4 jet events; we now turn to the second point.

To what concerns the one-particle inclusive cross-section we have shown in section III that it is impossible to safely evaluate and subtract the hadron-like component in order to isolate the anomalous contribution.

Fortunately the situation is much more favorable when looking at two-particle correlations. In this case, by triggering on a symmetric pair of hadrons (hadrons with the same transverse momentum, but in opposite azimuthal hemispheres) one considerably reduces the parton transverse motion effect[30], and the contribution of possible Higher Twist/CIM[31] terms (due to the vanishing of $D(z)$ when $z \to 1$). In the case of hadronic collisions good fits to FNAL and ISR data[33,34] were obtained by Baier et al., within the QCD approach[30].

In the photoproduction of symmetric pairs, the above considerations lead to the following interesting results.

First, on the ground of results of section III we expect the anomalous contribution to be higher than the VDM one, since the parton transverse momentum is now negligible. Correlatively, theoretical predictions (for both the anomalous and the hadron-like parts) are much less model dependent (in the medium p_T range) than the corresponding ones for single inclusive cross-sections. Let us make these points explicit by calculating the double inclusive cross-section:

$$\frac{d\sigma}{dp_T dy dp_{2x} dY} = 2\pi \sum_{\substack{a,b,\\ c,d}} \int \frac{dz_1}{z_1} x_a G_{a/\gamma}(x_a, Q^2)\, x_b G_{b/p}(x_b, Q^2)\, \frac{1}{\pi} \frac{d\hat{\sigma}}{d\hat{t}}(ab \to cd)\, D_c(z_1)\, D_d(z_2) \tag{20}$$

with

$$x_a = \frac{x_T}{2 z_1}\left(e^{y} + e^{Y}\right)$$

$$x_b = \frac{x_T}{2 z_1}\left(e^{-y} + e^{-Y}\right)$$

$$z_2 = \frac{|p_{2x}|}{p_T} z_1$$

The cross-section has been integrated over p_{2y}, the away hadron momentum component perpendicular to the scattering plane. The different building blocks of (20) have already been discussed in sections I and II; Y is the rapidity of the away hadron. In fig.6 we show the results of the calculations done

for $s = 200\ GeV^2$, $p_T = p_{2x} = 3\ GeV/c$, $y=0$, for charged pions.

We find that the anomalous contribution now dominates over the VDM one by an order of magnitude . This is an interesting result in view of the uncertainties associated with the VDM approach (unknown structure functions of the vector mesons and neglect of heavier vector mesons). Changing the VDM predictions by a factor two would not alter our conclusion that the anomalous component is quite observable. Notice that the dominating subprocess is the $qq \to qq$ scattering (q means either quark or antiquark). The subprocess $qg \to qg$ contributes about 3% and the others are negligible.

The p_T dependence of the cross-section (integrated over Y) is shown in fig.7. For $p_T \simeq 2\ GeV/c$, i.e. in a region where the background due to the low p_T photon and proton fragments may already be negligible, the cross-section is fairly large.

VI. Very high energy estimates.

The future of photoproduction experiments relies mostly on very high energy e-p colliding machines. The Tristan project in Japan and the European projects at Hamburg and/or Cern plan center-of-mass energies of the order 100 GeV. We investigate in this section the interest of such almost real photon experiments as QCD tests. We shall show that they mostly probe the gluon content of incident particles. Moreover, the three and four gluon couplings specific of the non-abelian nature of QCD yield the main bulk of the cross-section, which is an almost unique fact in high energy physics[4] . Since luminosities at so high energy are likely to be low, we restrict on large p_T jet production. The drawback of this choice is the unprecise experimental jet definition.

High energy medium p_T events ($x_T \simeq 0.1$) mostly probe the small x content of incident particles. In the photon case, in particular, gluons are predominant. We thus expect to probe this way the gluon content of the photon; moreover, the three gluon coupling specific of the non-abelian nature of the theory plays a very important role in gq scattering, the $gg \to gg$ subprocess being entirely due, to this order in α_s, to 3 and 4 gluon couplings. In fig. 8 the jet inclusive cross-section at $y = 0$ is plotted as a function of the jet transverse momentum. Some of its components are

shown. The gg → gg subprocess yields a significant amount of the cross-section but the gq scattering amplitude dominates for all (reasonable) values of p_T. For this latter subprocess the 3 gluon coupling terms contribute about 90 % of the cross-section. Also shown is the cross-section one would obtain if 3 and 4 gluon couplings were put equal to zero. At large enough p_T, since most of the uncertainties relative to the magnitude of the cross-section (effect of parton transverse motion, next to leading terms, mismatch of background and genuine jet particles) are expected to die away, we thus handle a very clear test of the non-abelian nature of the underlying theory.

In these energies and transverse momenta regions and in the light of our results at lower energy, one can safely ignore the hadron-like part of the structure function of the photon. Direct coupling terms only contribute about 1 % of the cross-section.

The rapidity distribution at p_T = 6 GeV/c is shown in fig.9. As expected the gg → gg contribution is almost symmetric. The input used here for the gluon structure function in the proton [18] has a somewhat similar shape as the QCD calculated gluon in the photon. The q g scattering subprocess is very different since quarks have much harder distribution in the photon than in a hadron, yielding a rapidity distribution peaked in the direction of the incident

photon. Because of the dominance of $qg \to qg$ and $gg \to gg$ subprocesses, as discussed above, gluon jets dominate the final state.

In conclusion, let us stress that very high energy photoproduction provides tests of QCD which are different from those at lower energy. It mostly allows to measure the strength of the 3 and 4 gluon couplings specific of the non-abelian nature of the theory.

VII. Conclusion

We have investigated in detail various tests of QCD in large p_T photoproduction. We have shown that it is possible to study separately the direct photon coupling by measuring cross-section differences. On the other hand, a careful investigation of the possibility of measuring the photon structure function at presently accessible energies has been carried out. We have shown that the hadron-like background is very important in single particle cross-sections and forbids to extract the anomalous photon structure function. We have proposed a way to perform this task which is to measure symmetric pair correlations. Furthermore, we have also studied reactions at very high energy and emphasized that they should provide a direct test of the non-abelian nature of the theory. The present analysis has been carried in the leading log approximation. The various tests,which we propose to perform, remain valid and feasible if next-to- leading corrections are incorporated. These may be eventually quite large and should be calculated when accurate experimental data become available

Acknowlegements

We acknowledge useful discussions with F.Gorski, F.Richard and D.Treille and thank them for communication of the WA4 collaboration results prior to publication.

REFERENCES

[1] H.Fritzsch and P.Minkowski, Phys.Lett.69B(1977)316.

[2] C.H.Llewellyn-Smith, Phys.Lett.79B (1978)83.

[3] Tu Tung Sheng and Wu Chi Min, Nucl.Phys.B156(1979)493.

[4] E.Gotsman, D.Silverman and A.Soni, Phys.Rev.D20(1979)2220
A.Soni, Slac Pub 2398(1979) and Irvine preprint 79-45(1979)

[5] T.Chandramohan Phys.Lett. 88B(1979)163.

[6] K.Ishida, T.Kobayashi and T.Yoshino KEK preprint 79-14(1979)

[7] J.Owens, Phys.Rev.D21(1980) 54.

[8] M.Fontannaz, A.Mantrach, B.Pire and D.Schiff, Phys.Lett 89B (1980) 263.

[9] I.Kang and C.H.Llewellyn-Smith Oxford preprint 62/79(1979)

[10] K.Iguchi, A.Niegawa and Y.Uranishi, Osaka City University preprint OCU-61 (1979)

[11] M.Fontannaz, A.Mantrach, B.Pire and D.Schiff, Ecole Polytechnique preprint A381-0380 (1980).

[12] E.Witten, Nucl.Phys. B120 (1977)189

[13] R.DeWitt et al., Phys.Rev.D19(1979)2046, D20(1979)1751(E)
W.Frazer and J.Gunion Phys.Rev.D20(1979)147.

[14] WA4 collaboration preliminary results. We thank F.Gorski and F.Richard for communication of their results prior to publication. These results are quoted in details in M.Fontannaz, Proceedings of the XV Rencontre de Moriond,1980 to be published, ed.J.Tran Thanh Van.

[15] NA14 experiment of the CERN-London-Orsay-Saclay-Southampton collaboration.Wide band beam and tagged photon beam FNAL facilities.

[16] R.Feynman, R.Field and G.Fox, Phys.Rev. D18 (1978)3320.

[17] A.Buras and K.Gaemers, Nucl.Phys.B132(1978)249.

[18] J.Owens and E.Reya, Phys.Rev.D17 (1978)3003.

[19] R.Field and R.Feynman, Phys.Rev.D15(1977) 2590.

[20] B.Combridge, J.Kripfganz and J.Ranft, Phys.Lett.70B(1977)234.

[21] A.Nicolaidis, Nucl.Phys. B163 (1980) 156.

[22] C.B.Newman et al., Phys.Rev.Lett.42 (1979) 951
J.Badier er al., Phys.Lett.88B (1979) 145.

[23] G.Donaldson et al., Phys.Lett. 73B (1978) 375.

[24] H.J.Frish et al., Phys.Rev.Lett.44(1980)511 .

[25] D.Antreasyan et al., Phys.Rev. Lett.38(1977) 112 .

[26] A.Contogouris, R.Gaskell and S.Papadopoulos, Phys.Rev. D17 (1978)2314.

[27] J.Owens and J.Kimel Phys.Rev.D18(1978) 3313.

[28] M.Fontannaz and D.Schiff, Nucl.Phys. B132(1978) 457.

[29] R.Horgan and P.Sharbach, Phys.Lett. 81B(1979) 215.

[30] R.Baier, J.Engels and B.Petersson, Z.Physik C2 (1979)265.

[31] D.Sivers, R.Blankenbecler and S.Brodsky, Phys.Reports 23C (1976) 1.

[32] M.Fontannaz, A.Mantrach, B.Pire and D.Schiff, Orsay preprint in preparation.

[33] H.Jöstlein et al., Phys.Rev.Lett. 42 (1979)146.

[34] M.Jacob "High p_T and Jets", Proceedings of the International Conference on High Energy Physics, Geneva 1979.

F I G U R E C A P T I O N S

Fig.1 The graphs contributing to large p_T photoproduction: a,b) direct coupling terms; c) photon structure function terms (the dashed lines represent quarks or gluons).

Fig.2 The contribution of the various photon components to $d\sigma^{\pi^+}/dy$ (upper figure) and $d\sigma^{\pi^+-\pi^-}/dy$ (lower figure) for 45 GeV $\leqslant E^{\gamma} \leqslant$ 70 GeV and $p_T \geqslant$ 2 GeV/c : the direct coupling term (dashed line), the anomalous term (dotted line) and the phenomenological VDM term (full line). The dash-dotted is the sum of the various components. Data are from ref [14].

Fig.3 The y-integrated cross-section differences $d\sigma^{\pi^+-\pi^-}/dp_T^2$ for $\theta_{Lab} < 15°$ (full curve and full dots) and $y \geqslant .5$ (dashed curve and open dots) and for 45 GeV $\leqslant E^{\gamma} \leqslant$ 70 GeV. Data are from ref [14].

Fig.4 The cross-sections $d\sigma^{\pi^+}/d\vec{p}_T dy$ (upper figure) and $d\sigma^{\pi^+-\pi^-}/d\vec{p}_T dy$ (lower figure) for p_T= 3GeV/c and s= 200 GeV^2. The direct coupling contribution: $\gamma q \to gq$ contribution (-··—··) and total (——·——·); the anomalous component contribution: total (—— —— ——) and neglecting the

qg → qg subprocess (·····); the phenomenological VDM contribution (———).

Fig.5 (a) The various contributions to the jet cross-section at p_T= 4 GeV/c and s = 200 GeV^2; direct coupling contribution : gluon and quark jets (———) and quark jets only (— — —); anomalous component contribution: gluon and quark jets (—·—·—·)and quark jets only (· · · · · ·).

(b) The gluon jet to quark jet ratio; direct coupling and anomalous component contributions (—·—·—), and direct coupling only (———) ((· · · · ·) with the gluon distribution of ref. [30]).

Fig.6 The double inclusive cross-section $d\sigma/dp_T dy\, dp_{2x} dY$ as a function of Y for y=0, p_T= p_{2x}= 3 GeV/c and s=200 GeV^2 anomalous component contribution (———) and VDM contribution (— — —).

Fig.7 The double inclusive cross-section $d\sigma/dp_T dy\, dp_{2x}$ (integrated over Y) anomalous component contribution (———) and VDM contribution (— — —).

Fig.8 The jet cross-section at very high energy (———): $\sqrt{s}$ = 100 GeV and y =0; various contributions shown are qg → qg (— — —), gg → gg (· · · ·) and gg → $q\bar{q}$ (—··———··), the cross-section obtained by putting

to zero the 3 and 4 gluon couplings (——·—·).

Fig.9 The rapidity distribution of the jet cross-section at $\sqrt{s}$ = 100 GeV and p_T= 6 GeV/c. Total (———) $gg \to gg$ (· · · ·) and $qg \to qg$ (— — —) contributions are shown.

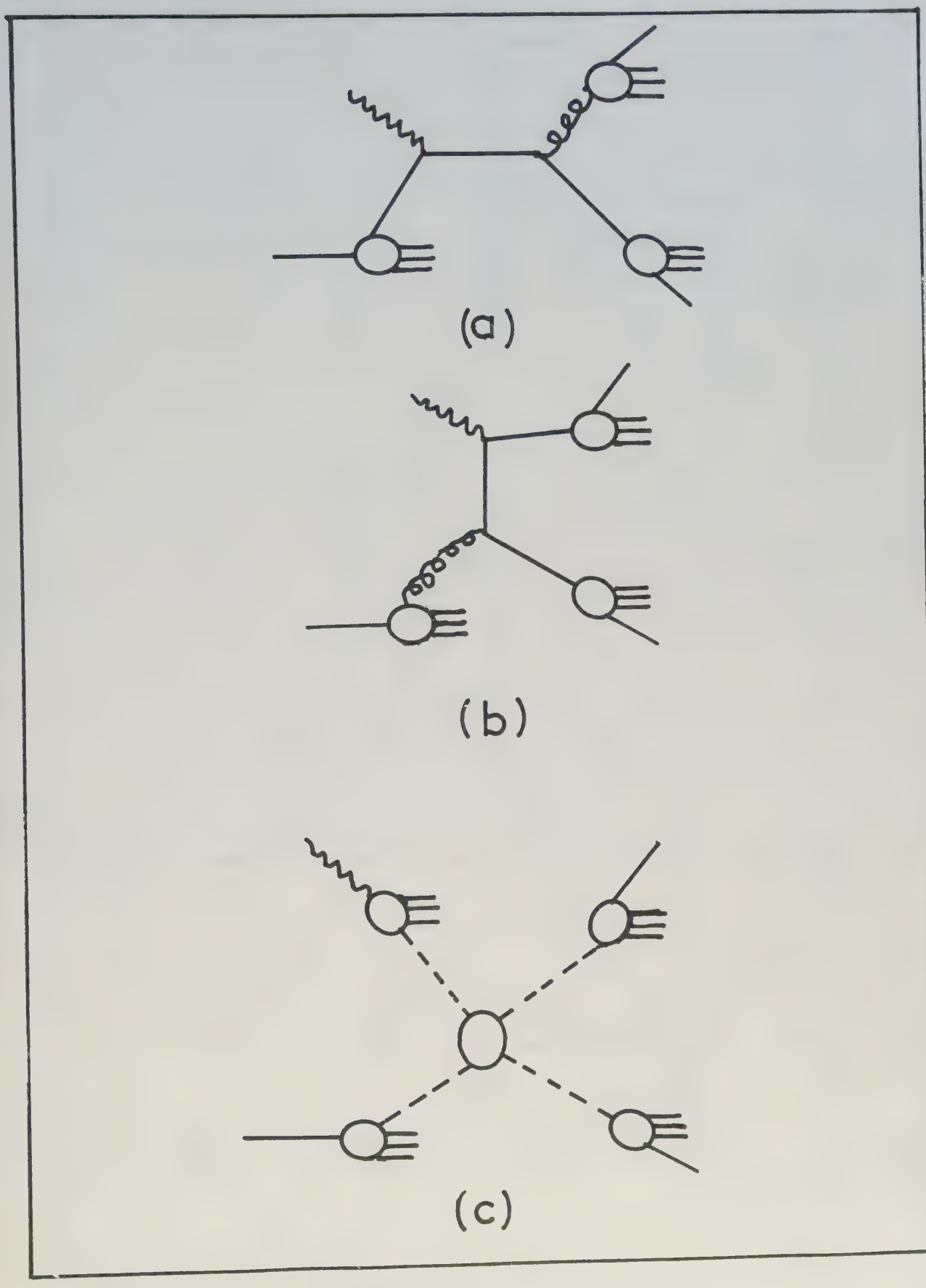

FIG. 1

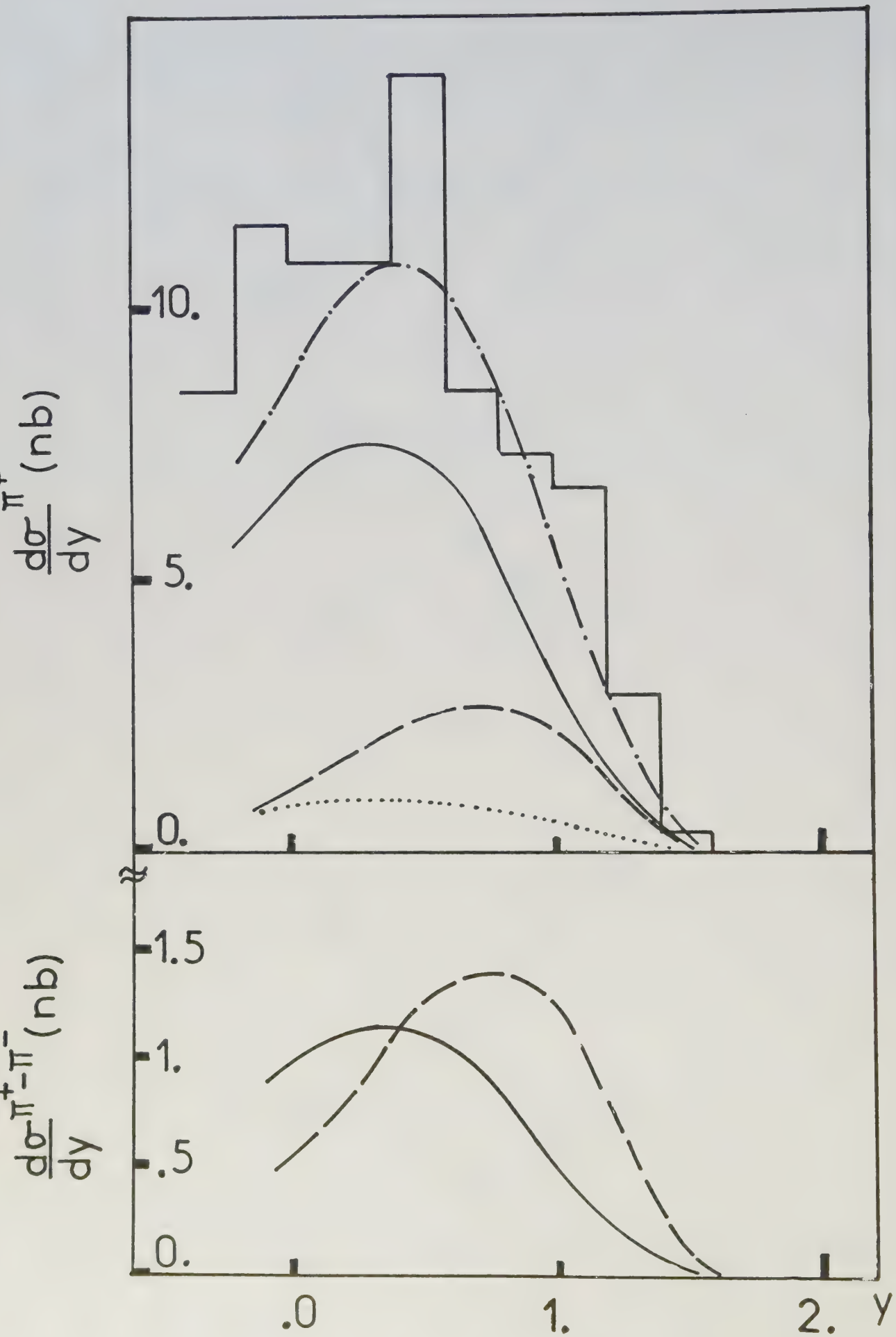

FIG. 2

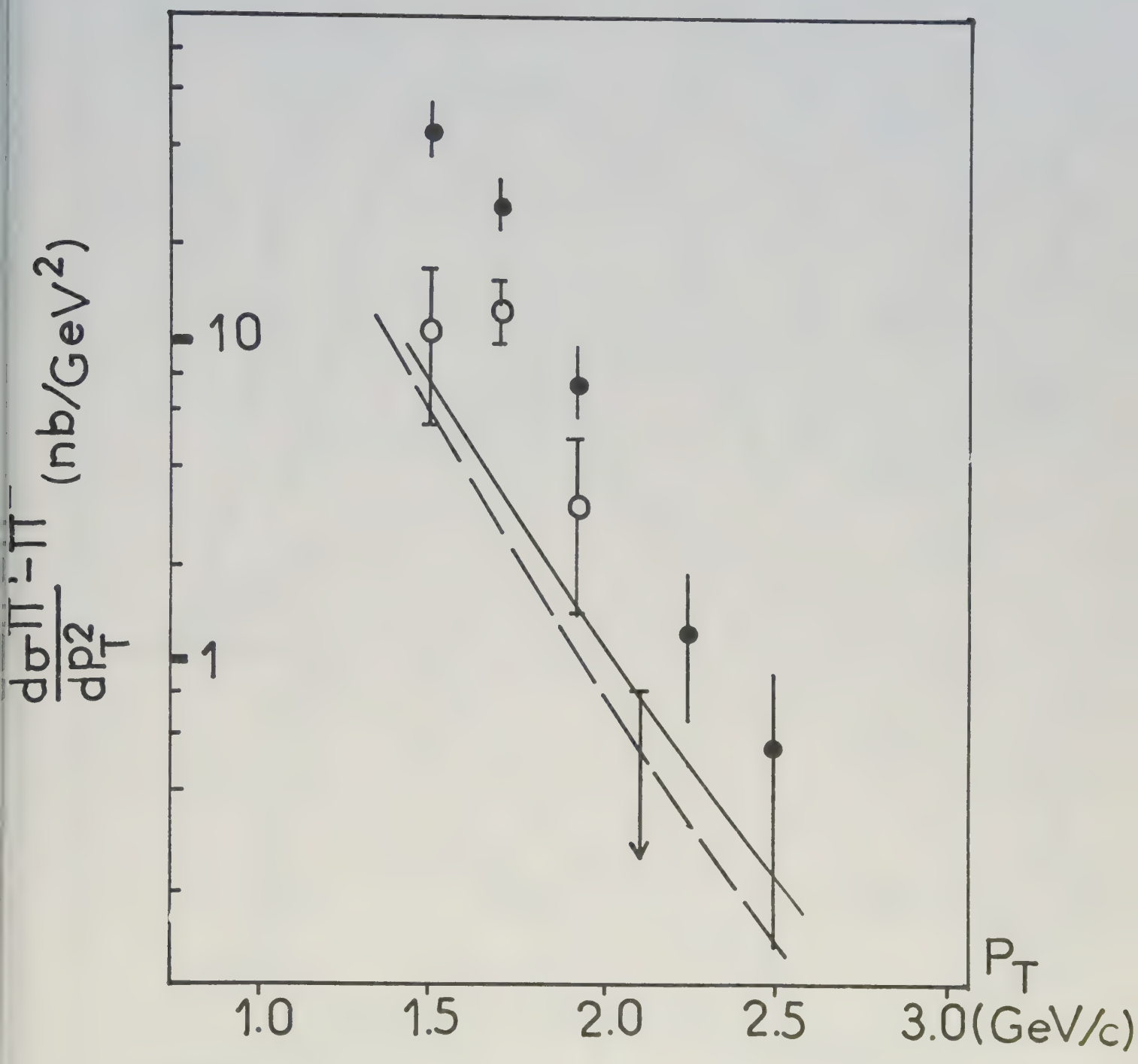

FIG. 3

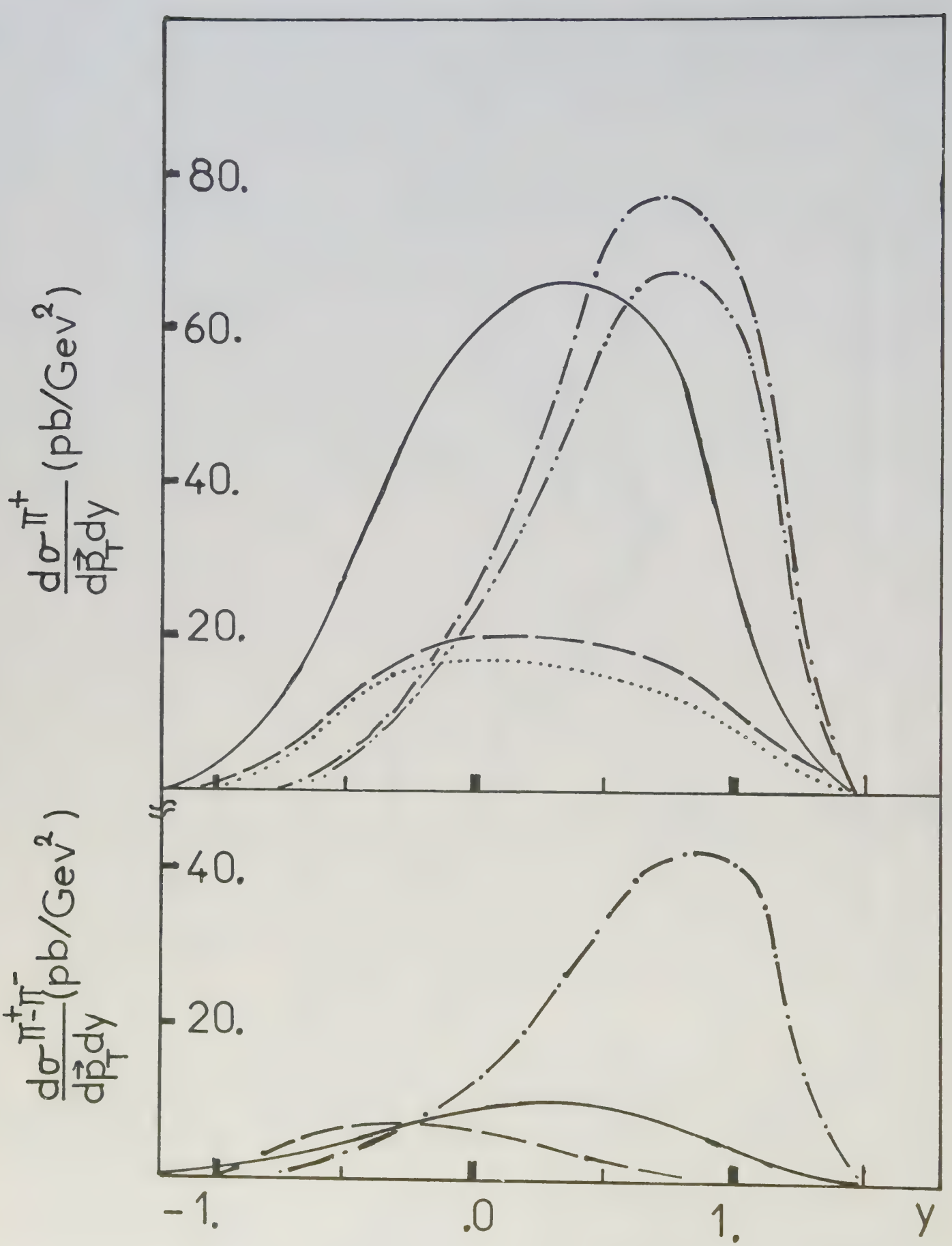
80.
60.
40.
20.
$\frac{d\sigma^{\pi^+}}{d\vec{p}_T dy}$ (pb/Gev^2)
40.
20.
$\frac{d\sigma^{\pi^+\pi^-}}{d\vec{p}_T dy}$ (pb/Gev^2)
-1.
.0
1.
y

FIG. 4

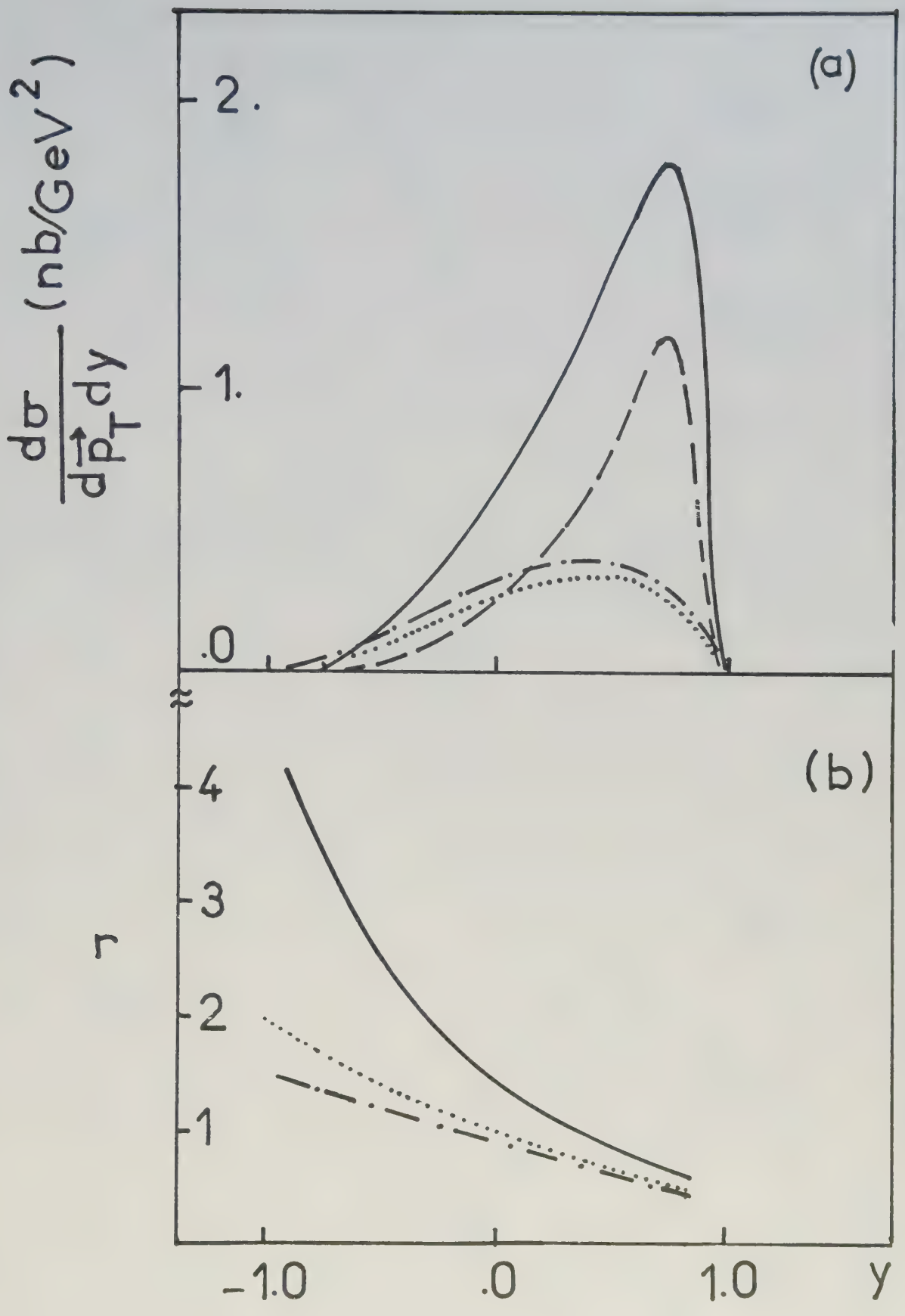

FIG 5

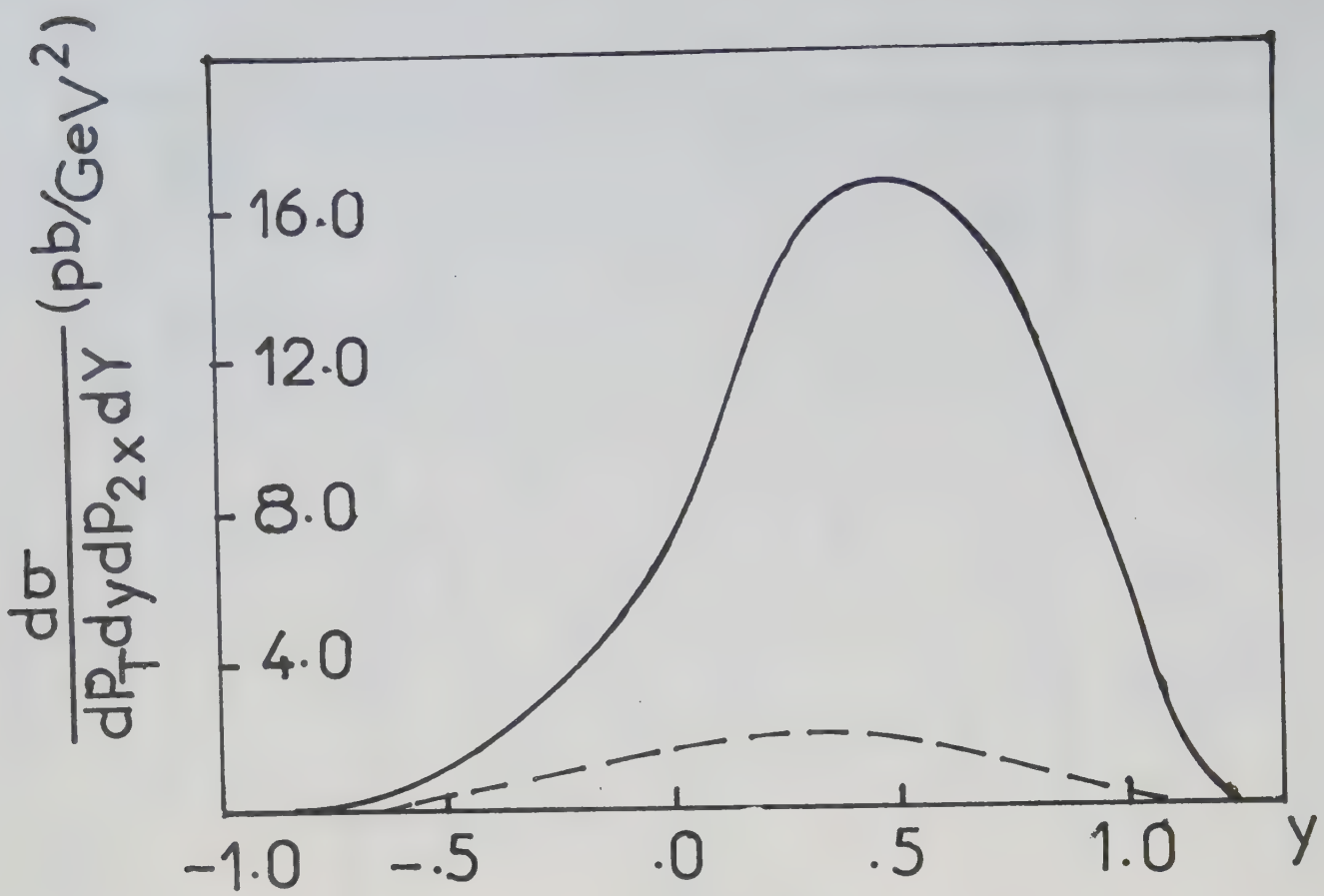
$\frac{d\sigma}{dP_T dy dP_{2x} dY}$ (pb/GeV^2)
16·0
12·0
8·0
4·0
-1.0
-.5
.0
.5
1.0
y

FIG 6

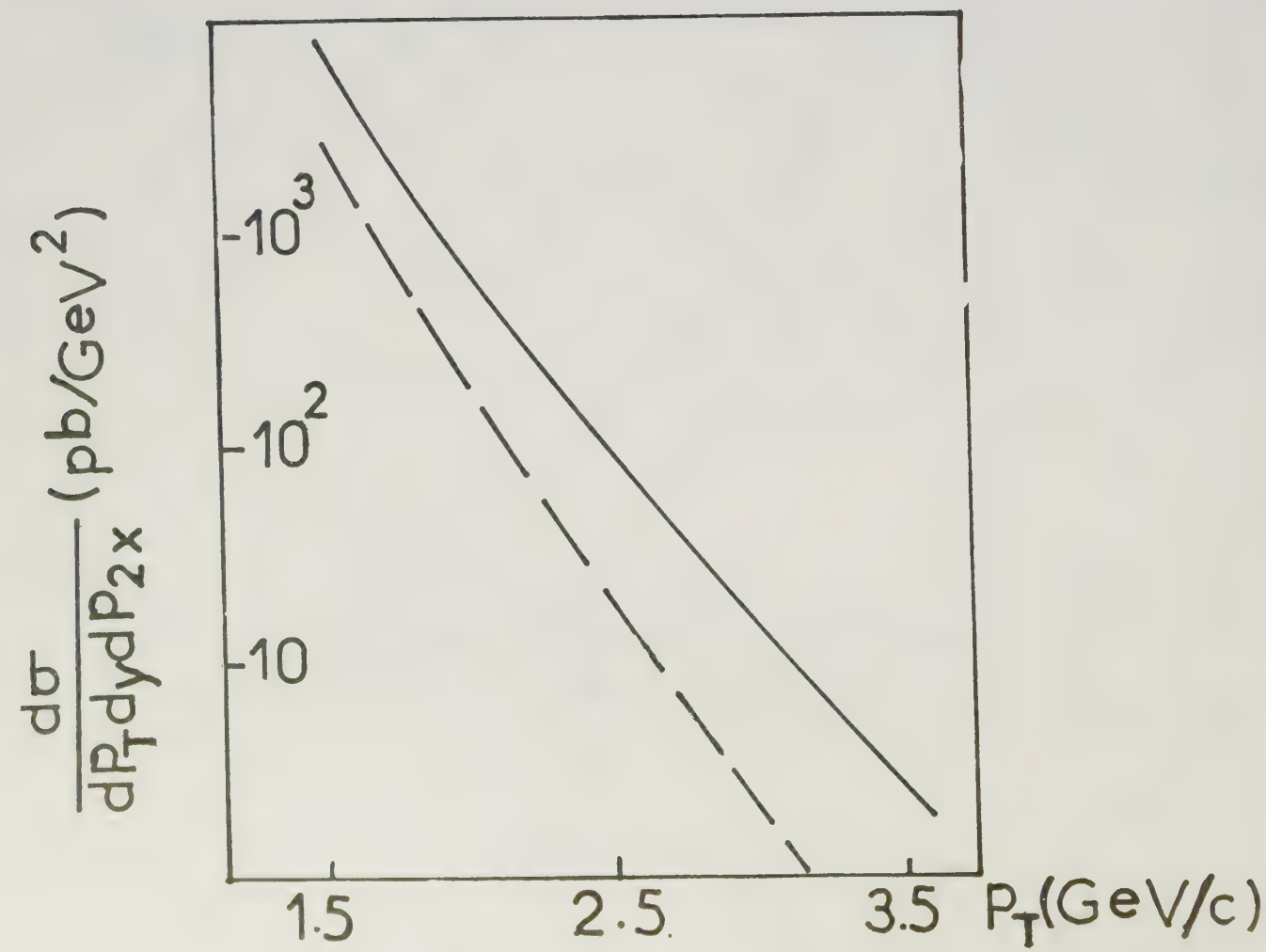
$\frac{d\sigma}{dP_T dy dP_{2x}}$ (pb/GeV^2)
10^3
10^2
10
1.5
2.5
3.5
P_T(GeV/c)

FIG 7

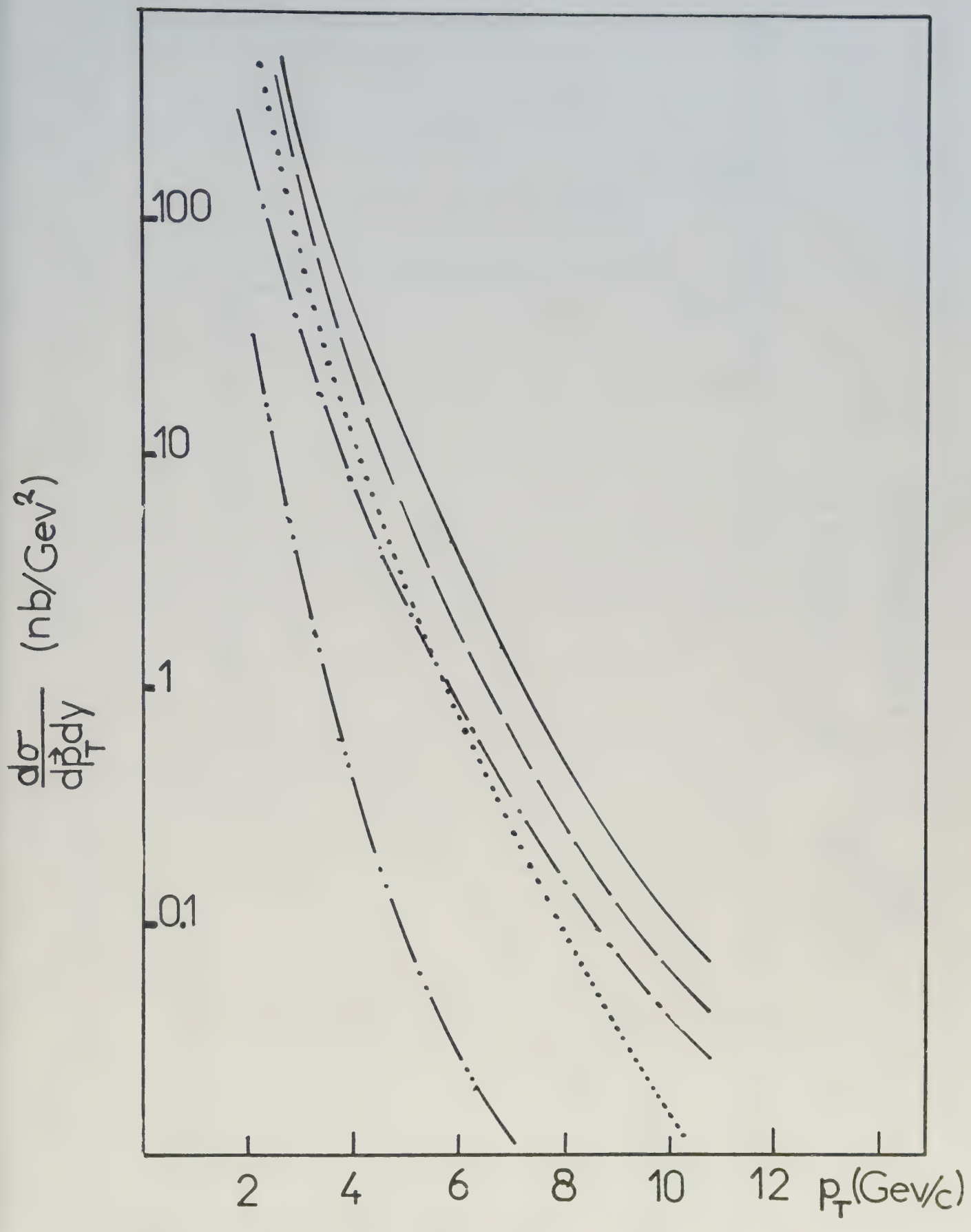

FIG. 8

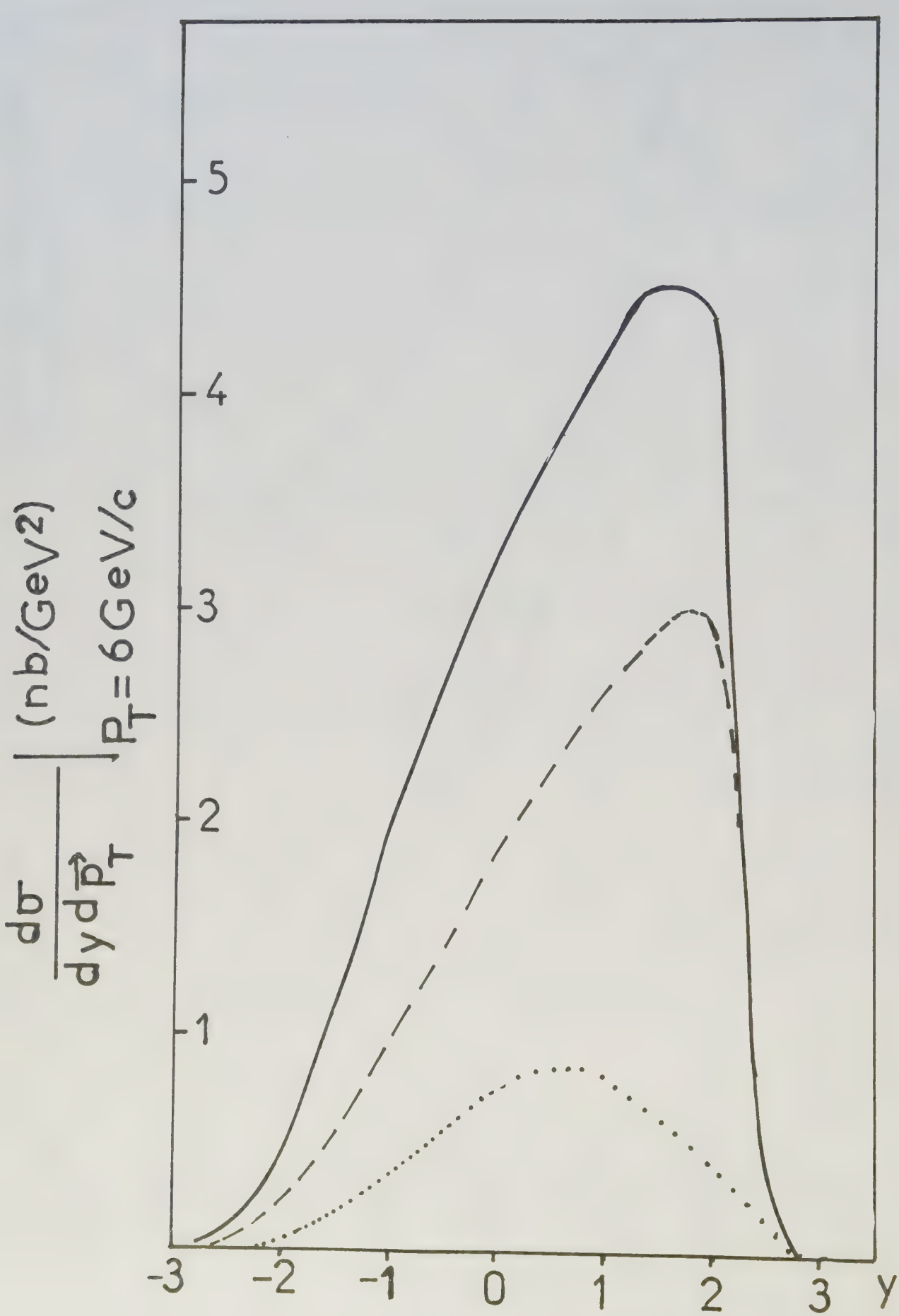

FIG. 9

QUATRIEME PARTIE

LA PHYSIQUE DU GLUON ET LA PHOTOPRODUCTION DE HADRONS A GRANDE IMPULSION TRANSVERSE

HOW TO EXTRACT THE GLUON FRAGMENTATION FUNCTION FROM LARGE $p_\perp$ PHOTOPRODUCTION

M. FONTANNAZ [a], A. MANTRACH [a,1], B. PIRE [b] and D. SCHIFF [a]
[a] *LPTHE [2], Université Paris Sud Orsay, 91405 Orsay, France*
[b] *CPT [3], Ecole Polytechnique, 91128 Palaiseau Cedex, France*

Received 21 March 1980

A clear determination of the gluon fragmentation function $D_g^h(z, Q^2)$ is accessible in near to come large $p_\perp$ photoproduction experiments. This is done by analyzing differences of double inclusive cross sections. The scale invariance breaking effect is shown to be measurable.

The observation of gluon jets and of their properties is crucial for the verification of perturbative quantum chromodynamics ideas. The three jet structures discovered in e^+e^- annihilation have been a very beautiful confirmation of the existence of gluons. It is, however, difficult to go further in this reaction and to study the gluon properties. On the other hand, large $p_\perp$ photoproduction has the very interesting feature of producing gluons at the Born term level through the QCD Compton effect $\gamma q \to qg$ [1]. We have shown in a preceding paper [2] that this reaction provides a very clear test of QCD and allows a direct experimental approach of the QCD Compton cross section. The purpose of this letter goes further and aims to show that large $p_\perp$ photoproduction provides a determination of the gluon fragmentation function $D_g^h(z, Q^2)$ which is very clean and accessible to the next to come experiments [‡1].

Let us briefly recall the basic features of the QCD description of large $p_\perp$ photoproduction. In fig. 1 we show the contributing graphs: direct coupling processes (figs. 1a,b) and the photon structure function [3] terms (fig. 1c). The trick for picking up only the contribution of subprocess 1a, cancelling those of 1b and minimizing those of 1c, consists in taking the difference $\Delta^{h_1 h_2}$ of the double inclusive cross sections,

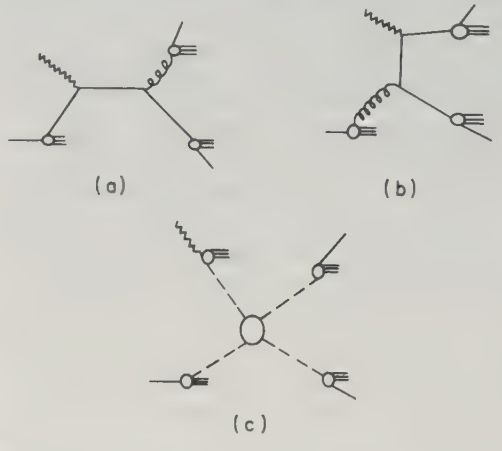

Fig. 1. The graphs contributing to large $p_\perp$ photoproduction: (a), (b) direct coupling terms; (c) photon structure function terms. In this last graph dashed lines represent quarks or gluons.

$$\Delta^{h_1 h_2} = \frac{E_1 E_2 \, d\sigma^{(2)}(\gamma p \to h_1^+ h_2 X)}{dp_1 \, dp_2} - \frac{E_1 E_2 \, d\sigma^{(2)}(\gamma p \to h_1^- h_2 X)}{dp_1 \, dp_2}, \quad (1)$$

[1] On leave from LPT, Faculté des Sciences de Rabat, Morocco.
[2] Laboratoire associé au CNRS.
[3] Groupe de Recherche du CNRS.
[‡1] NA 14 experiment of the CERN–London(Imp.Coll.)–Orsay(LAL)–Saclay–Southampton collaboration and wide band beam and tagged photon beam FNAL facilities. These experiments will have $s \approx 200$ GeV^2 and a yield of 5–50 particles/pb is expected in the CERN experiment.

where $h_1^{\pm}$ are the positively and negatively charged triggers at large $p_{\perp 1}$ and h_2 a hadron observed in the hemisphere away from the trigger; h_2 is either neutral or represents the sum $h_2^+ + h_2^-$. Then it is clear that of the direct coupling terms only the subprocess $\gamma q \to qg$ contributes to $\Delta^{h_1 h_2}$; moreover the particle h_1 may only come from the quark fragmentation; this means that in the away hemisphere one observes gluon fragments only.

In addition to selecting the subprocess $\gamma q \to qg$, the differences $\Delta^{h_1 h_2}$ present many interesting features that were described in a preceding letter [2]; let us briefly recall them:

(i) All terms which enter the theoretical prediction are well known (the distributions of valence quarks in the proton and the fragmentation functions of the u and d quarks are well determined from experiment).

(ii) The u quark contribution is strongly enhanced by the QED coupling, compared to that of the d quark; therefore, the cross section difference is a large fraction of the cross section itself.

(iii) Taking the difference $\Delta^{h_1 h_2}$ reduces the contributions due to the anomalous and VDM components of the photon structure function [3] to a negligible background (at $s \approx 200\ \mathrm{GeV}^2$, $p_{\perp 1} \gtrsim 3\ \mathrm{GeV}/c$).

Postponing to the end of this letter a more complete discussion of the background, let us now present some quantitative results for the direct coupling term. We consider the case where h_1 and h_2 are pions ($h_2 = \pi^+ + \pi^-$); the inclusion of kaons is straightforward. The cross section difference is written, with the usual notations (we have integrated over the $\boldsymbol{p}_2$ component perpendicular to the scattering plane; p_{2x} is the component perpendicular to the beam axis in the scattering plane) as

$$\begin{aligned}\frac{\mathrm{d}\sigma^{\Delta}}{\mathrm{d}\boldsymbol{p}_{\perp 1}\,\mathrm{d}y_1\,\mathrm{d}p_{2x}\,\mathrm{d}y_2} &= \frac{x}{p_{\perp 1}}\left[\tfrac{4}{9}G_{\mathrm{u}}^{\mathrm{val}}(x,Q^2) - \tfrac{1}{9}G_{\mathrm{d}}^{\mathrm{val}}(x,Q^2)\right] \\ &\times \left[D_{\mathrm{u}}^{\pi^+}(z_1,Q^2) - D_{\mathrm{u}}^{\pi^-}(z_1,Q^2)\right] \\ &\cdot \frac{1}{\pi}\frac{\mathrm{d}\hat{\sigma}}{\mathrm{d}\hat{t}}\left[D_{\mathrm{g}}^{\pi^+}(z_2,Q^2) + D_{\mathrm{g}}^{\pi^-}(z_2,Q^2)\right],\end{aligned} \tag{2}$$

with

$$\frac{1}{\pi}\frac{\mathrm{d}\hat{\sigma}}{\mathrm{d}\hat{t}} = \tfrac{8}{3}\alpha\alpha_{\mathrm{s}}(Q^2)\frac{1}{\hat{s}^2}\left(\frac{\hat{s}}{-\hat{u}} + \frac{-\hat{u}}{\hat{s}}\right),$$

$$\begin{aligned} z_1 &= p_{\perp 1}(\mathrm{e}^{y_1} + \mathrm{e}^{y_2})/\sqrt{s}\,, \\ z_2 &= |p_{2x}|(\mathrm{e}^{y_1} + \mathrm{e}^{y_2})/\sqrt{s}\,, \\ x &= \mathrm{e}^{-y_1 - y_2}\,. \end{aligned} \tag{3}$$

The Mandelstam invariant $\hat{u}$ is the square of the momentum transfer between the gluon and the incident quark and $\hat{s} = xs$ where $\sqrt{s}$ is the γ–p c.m. energy. For $\alpha_{\mathrm{s}}(Q^2)$ we take the canonical value $12\pi/[25 \times \log(Q^2/0.25)]$. The leading logarithm approach used here does not specify the expression of Q^2. We use that of ref. [4]: $Q^2 = 2\hat{s}\hat{t}\hat{u}/(\hat{s}^2 + \hat{t}^2 + \hat{u}^2)$. Notice that we have not taken into account the incident quark Fermi motion. It is indeed known that double inclusive cross sections are little sensitive to its effects [5,6]. Moreover we have shown in ref. [2] that already at the one particle level the Fermi motion is negligible as soon as $p_{\perp} > 2.5\ \mathrm{GeV}/c$ contrary to the case of hadron–hadron collisions. We have also neglected the hadron transverse momentum with respect to the away jet axis. The magnitude of this spread is unknown. If it is large, it might show up in a kinematical scale breaking of the fragmentation function for relatively small $p_{\perp 1}$. Such an effect has been studied in hadronic reactions by Alonso et al. [7]. This should be kept in mind when analyzing data.

Expression (2) exhibits a remarkable feature: the subprocess kinematics are completely fixed by observing $\boldsymbol{p}_{\perp 1}, y_1, p_{2x}$ and y_2. No integration is needed; the extraction of $D_{\mathrm{g}}^{\mathrm{h}}(z,Q^2)$ is thus straightforward. In order to get $D_{\mathrm{g}}^{\mathrm{h}}(z,Q^2)$ from experiment, we make use of the peculiar direct coupling kinematics by defining a cross section at fixed $\sqrt{s}/(\mathrm{e}^{y_1} + \mathrm{e}^{y_2})$ which is the outgoing jet transverse momentum $p_{\perp}^{\mathrm{jet}}$:

$$\begin{aligned}\frac{\mathrm{d}\sigma^{\Delta}}{\mathrm{d}z_2\,\mathrm{d}p_{\perp}^{\mathrm{jet}}} &= \int_{p_{\perp 1}^{\min}} \mathrm{d}\boldsymbol{p}_{\perp 1}\int \mathrm{d}p_{2x}\,\delta\left(z_2 - \frac{|p_{2x}|}{p_{\perp}^{\mathrm{jet}}}\right) \\ &\times \int_{y_1^{\min}}^{y_1^{\max}} \mathrm{d}y_1\,\mathrm{d}y_2\,\delta\left(p_{\perp}^{\mathrm{jet}} - \frac{\sqrt{s}}{\mathrm{e}^{y_1} + \mathrm{e}^{y_2}}\right) \\ &\times \frac{\mathrm{d}\sigma^{\Delta}}{\mathrm{d}\boldsymbol{p}_{\perp 1}\,\mathrm{d}y_1\,\mathrm{d}p_{2x}\,\mathrm{d}y_2}\,,\end{aligned} \tag{4}$$

which can be written as

$$\frac{d\sigma^{\Delta}}{dz_2\, dp_{\perp}^{jet}} = D_g^{h_2}(z_2, \bar{Q}^2) \times d(p_{\perp 1}^{min}, p_{\perp}^{jet}, s, y_1^{min}, y_1^{max}), \quad (5)$$

with

$$d = 2\pi\sqrt{s} \int_{z_1^{min}}^{1} dz_1 \int_{y_1^{min}}^{y_1^{max}} dy_1\, e^{-y_2} D_u^{\pi^+ - \pi^-}(z_1, Q^2) \times x[\tfrac{4}{9} G_u^{val}(x, Q^2) - \tfrac{1}{9} G_d^{val}(x, Q^2)]\, \frac{1}{\pi} \frac{d\hat{\sigma}}{d\hat{t}}, \quad (6)$$

where $e^{y_2} = \sqrt{s}/p_{\perp}^{jet} - e^{y_1}$ and $z_2 = |p_{2x}|/p_{\perp}^{jet}$. In expression (4) we integrate over a y_1 range fixed by theoretical or experimental considerations.

The interest of eq. (5) comes from the fact that in the y_1 range where the cross section is important, Q^2 is nearly constant depending only on the value of $p_{\perp}^{jet}$ [‡2]. Therefore the gluon fragmentation function may safely be factored out. With the definition of ref. [4] for Q^2, we find $\bar{Q}^2 \approx \frac{4}{3}(p_{\perp}^{jet})^2$.

In order to show that $d\sigma^{\Delta}/dz_2\, dp_{\perp}^{jet}$ is fairly large and thus should allow a precise measurement of $D_g(z, Q^2)$, we perform the calculations at $s = 200$ GeV^2 with the proton structure functions of ref. [8], the quark fragmentation functions of ref. [9] (without scale breaking in agreement with e^+e^- data) and the gluon fragmentation function $D_g^h(z, Q^2)$ of ref. [4].

We integrate over the range $y_1 > 0$ where the direct coupling term is peaked and fix $p_{\perp 1}^{min} = 2$ GeV/c. The results are shown in fig. 2. The use of a different parametrization [6] for $D_g^h(z, Q^2)$ gives quite different results as shown in fig. 2.

The factorized form (4) allows us to go further and define the ratio

$$r_1(z_2, z_2', \bar{Q}^2) = \frac{d\sigma^{\Delta}/dz_2\, dp_{\perp}^{jet}}{d\sigma^{\Delta}/dz_2'\, dp_{\perp}^{jet}} = \frac{D_g^h(z_2, \bar{Q}^2)}{D_g^h(z_2', \bar{Q}^2)}, \quad (7)$$

in which many of the experimental and theoretical uncertainties cancel; then the z_2 dependence at fixed $\bar{Q}^2$ may be investigated very clearly. The Q^2 dependence may be studied by means of the double ratio

$$r_2 = \frac{r_1(z_2, z_2', \bar{Q}^2)}{r_1(z_2, z_2', \bar{Q}'^2)} = \frac{D_g(z_2, \bar{Q}^2)/D_g(z_2', \bar{Q}^2)}{D_g(z_2, \bar{Q}'^2)/D_g(z_2', \bar{Q}'^2)}. \quad (8)$$

Using the parametrization of ref. [5] we show in fig. 3 that we get a quite observable effect when fixing $\bar{Q}^2 = 10$ GeV^2, $z_2 = 0.2$ (a value at which D_g is almost Q^2 independent) and $z_2' = 0.8$; this large effect is intimately related to the QCD three gluon coupling [10] and provides a stringent test of this latter. A more standard approach consists in taking moments of eq. (5), the ratio of which are directly given in terms of experimental data:

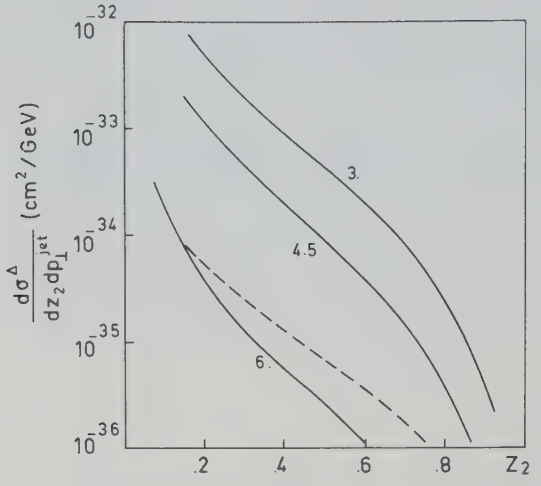

Fig. 2. The differential cross section $d\sigma^{\Delta}/dz_2\, dp_{\perp}^{jet}$. Full (dashed) curves correspond to the gluon fragmentation function of ref. [5] ([7]). Curves are labelled with the value of $p_{\perp}^{jet}$.

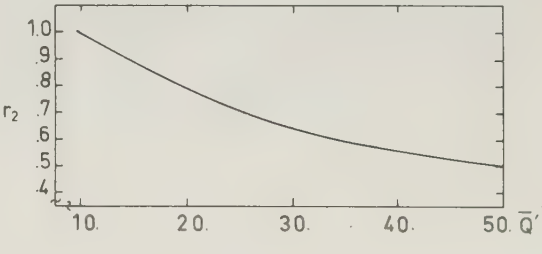

Fig. 3. The expected scaling violation as measured by the double ratio r_2 defined in the text for $z_2 = 0.2$, $z_2' = 0.8$ and $\bar{Q}^2 = 10$ GeV^2.

‡2 This statement is true for a very large class of definitions of Q^2 due to the sharp peaking in y_1 of the cross section.

$$\frac{M_g^n(Q^2)}{M_g^m(\bar{Q}^2)} = \frac{\int_0^1 dz_2\, z_2^{n-1}\, d\sigma^{\Delta}/dz_2\, dp_\perp^{jet}}{\int_0^1 dz_2\, z_2^{m-1}\, d\sigma^{\Delta}/dz_2\, dp_\perp^{jet}}. \quad (9)$$

Let us now comment on the background. Before the collision, the photon may, briefly speaking, transform in an almost collinear $q\bar{q}$ pair subsequently renormalized by the strong (QCD) interaction [3] or in a vector boson. Then large angle scattering takes place between gluons and/or quarks exactly as in hadron–hadron collisions. In hadron–hadron reactions, it was found that the incident parton Fermi motion does not strongly modify the double (toward–away) inclusive cross section [5,6]. We shall therefore neglect it in our estimate. Neglecting also the VDM contribution which is much smaller (see Kang and Llewellyn-Smith [1]) than the anomalous one, we estimated the contribution of this latter and found that it represents roughly 10–20% of the direct coupling one. This small background may again be experimentally reduced by using veto-counters forbidding forward jets. Another source of background is the presence of proton fragments; they may obscure the measurement of $D_g^h(z, Q^2)$ at small values of z and must be subtracted. It should be possible, by inspection of the y_2 behaviour of $d\sigma^{\Delta}/d\boldsymbol{p}_{\perp 1}\, dy_1\, dp_{2x}\, dy_2$ to disentangle their contribution – a flat curve – from that of the gluon jet – a marked peak, the position of which can be fixed by the trigger rapidity.

To conclude, we have indicated a clear way to extract the gluon fragmentation function: orders of magnitude are such that it is measurable as is also the scaling violation effect. Of course, one should keep in mind that in a second step it will be necessary to bypass the leading logarithm approximation and calculate the next to leading terms.

We acknowledge useful discussions with F. Gorski and F. Richard.

References

[1] H. Fritzsch and P. Minkowski, Phys. Lett. 69B (1977) 316;
Tu Tung-Sheng and Wu Chi-Min, Nucl. Phys. B156 (1979) 493;
Tu Tung-Sheng, Nucl. Phys. B161 (1979) 417;
J. Owens, Phys. Rev. D21 (1980) 54;
I. Kang and C. Llewellyn-Smith, Oxford preprint 62/79;
E. Gotsman, D. Silverman and A. Soni, Phys. Rev. D20 (1979) 2220.
[2] M. Fontannaz, A. Mantrach, B. Pire and D. Schiff, Phys. Lett. 89B (1980) 26.
[3] E. Witten, Nucl. Phys. B120 (1977) 189;
C. Llewellyn-Smith, Phys. Lett. 79B (1978) 83;
R. De Witt et al., Phys. Rev. D19 (1979) 2046;
W. Frazer and J. Gunion, Phys. Rev. D20 (1979) 147.
[4] R. Feynman, R. Field and G. Fox, Phys. Rev. D18 (1978) 3320.
[5] M. Fontannaz and D. Schiff, Nucl. Phys. B132 (1978) 457.
[6] R. Baier, J. Engels and B. Petersson, Z. Phys. C2 (1979) 265.
[7] J.L. Alonso, A. Cruz, G. Ringland and R. Roberts, Nucl. Phys. B157 (1979) 498.
[8] A. Buras and K. Gaemers, Nucl. Phys. B132 (1978) 249.
[9] R. Field and R. Feynman, Nucl. Phys. B136 (1978) 1.
[10] K. Koller, T. Walsh and P. Zerwas, Phys. Lett. 82B (1979) 263.

GLUON PHYSICS IN LARGE $p_\perp$ PHOTOPRODUCTION

M. FONTANNAZ[*], A. MANTRACH[*+], B. PIRE[**] and D. SCHIFF[*]

[*] L.P.T.H.E., Université Paris-Sud Orsay, Bât. 211,
91405 ORSAY, Cedex, France.
Laboratoire associé au C.N.R.S.

[**] C.P.T., Ecole Polytechnique, 91128 PALAISEAU Cedex, France.
Equipe de Recherche associée au C.N.R.S.

ABSTRACT : Large $p_\perp$ photoproduction turns out to be a beautiful laboratory for gluon physics. The gluon properties namely the distribution function inside the proton and the fragmentation function may be studied by measuring two particle correlations. It is also possible to extract the anomalous photon structure function. The orders of magnitude encountered for the various cross sections are shown to be measurable by the present generation of photoproduction experiments.

LPTHE 80/21
A406.0680 June 1980

+ On leave from L.P.T., Faculté des Sciences de Rabat, Maroc.

Introduction.

As already pointed out [1-4] , large $p_\perp$ photoproduction is a very good place to test the validity of perturbative Q.C.D. The point-like coupling of the photon to charged partons results in completely calculable amplitudes assuming the proton structure functions are known from deep inelastic experiments ; these amplitudes are reliable provided one is in the hard scattering regime, ($p_\perp^2 \gg M^2$). It is moreover remarkable that the lowest order graphs which describe the hard subprocesses involve gluons and therefore comparison between theory and experiment allows detailed studies of the gluon properties. In this respect, large $p_\perp$ photoproduction may be viewed as a laboratory to study gluon physics.

The way the photon interacts with the proton may be described under two categories :

1) the direct coupling terms of fig. 1a and 1b : the Compton and fusion graphs.
2) the photon structure function [5] contribution represented on fig. 2 which describes the interaction of the partons in the photon with partons inside the proton. The photon structure function is usually described as being made of two parts : the anomalous component which is completely calculable in Q.C.D. and dominates at large Q^2 over the hadron like component. This last one may be estimated in the frame-

work of the vector dominance model and contributes as a background to the other parts which are in principle completely described by the theory.

In paper I [4] we discussed in detail how these various components might be disentangled. In particular, we showed under which conditions the background might be sufficiently suppressed in order not to spoil the Q.C.D. predictions.

In this paper we address ourselves to a complete study of gluon physics in large $p_\perp$ photoproduction. We will show that the direct coupling terms may be separated in a way which allows to study the gluon fragmentation function and the gluon distribution in the proton. Large p_T photoproduction indeed appears as one of the best places where to measure this latter. On the other hand, it is possible to isolate the anomalous photon term and thus study the parton content of the photon. A detailed discussion of the background will be given in each case. We shall work in the energy and p_T domain of the coming CERN-SPS and FNAL experiments [6], that is $s \simeq 200\ GeV^2$ and $p_T \lesssim 5\ GeV/c$.

Let us outline the content of this paper. In section I, we discuss the possibility to isolate and observe the various contributions to the cross-sections. In section II, we focus on the measurement of $D_g^h(z,Q^2)$ whereas section III deals with the gluon content of the proton. Section IV is a brief comment about the study of the quark and gluon content of the photon. Section V is the conclusion.

I. Observing the photon components.

In this section, we recall the results of paper I in which the possibility to observe the different photon components is studied in detail ; we have shown that various tricks such as cross-section differences, symmetric pairs correlations, kinematical constraints must be used in order to disentangle the contributions of the photon components and to isolate them. Let us briefly describe these results which are the starting point of this paper.

We begin by the separation of 3 jet events, corresponding to fig. 1a and 1b, from 4 jet events (fig. 2) in which a fourth forward jet made of the photon fragments can be observed. These two types of events have a very different jet topology ; moreover, it is important to notice that the 3 jet events have to verify the following kinematical constraint

$$p_\perp \left(e^{y_1} + e^{y_2} \right) / \sqrt{s} = 1 \qquad (1)$$

where $p_\perp, y_1$ and y_2 are respectively the transverse momentum and the rapidities of the two large $p_\perp$ jets ; $\sqrt{s}$ is the energy of the reaction in the overall CMS. Thus inspection of the jet structure, supplemented by the use of the 3 jet topology kinematical constraint (1), should allow one to separate the direct coupling events from the other ones. The interesting consequence of this selection is that we can now compare data and theory within each subset of events indepen-

dently.

The 4-jet sample is populated by the contribution of the anomalous and of the hadron-like component of the photon. The one particle inclusive cross-section is dominated, as shown in I, by the hadron-like component which hides the anomalous one. This dominance of the hadron-like part is explainable by the parton Fermi motion enhancement effect. However, when symmetric pairs are observed (two hadrons with the same $p_\perp$, but in opposite azimuthal hemispheres), the Fermi motion effect is considerably reduced and the anomalous component of the photon now dominates. Thus there is a possibility to isolate this component, which opens the way to interesting experimental tests of perturbative Q.C.D. (see section IV).

The method described above for disentangling 3 jet from 4 jet events evidently requires sophisticated experiments observing jets and measuring most particle momenta. However it is possible to isolate the 3 jet event contributions by simply taking cross-section difference [2] . For instance, for the one particle inclusive cross-section, taking the difference

$$E d\Delta^{\pi}/d\vec{p} = E d\sigma(\gamma p \to \pi^+ X)/d\vec{p} - E d\sigma(\gamma p \to \pi^- X)/d\vec{p} \qquad (2)$$

enhances the 3 jet contributions compared to the 4 jet contributions, as shown in detail in I. This comes from the photon direct coupling to the quark charge which conside-

rably enhances the u-quark jets (thus the π^+ production) compared to the d-quark jets ; this effect is not present for the graphs of fig. 2.

Let us end this section by noting that cross-section differences also allow, within the 3 jet sample, to disentangle the Q.C.D. Compton contribution form the fusion one. We define the double inclusive cross-section

$$\frac{d\Delta^{\pi,h}}{d\vec{p}_{\perp 1}\, dy_1\, dp_{2x}\, dy_2} = \frac{d\sigma(\gamma p \to \pi^+ h X)}{d\vec{p}_{\perp 1}\, dy_1\, dp_{2x}\, dy_2} - \frac{d\sigma(\gamma p \to \pi^- h X)}{d\vec{p}_{\perp 1}\, dy_1\, dp_{2x}\, dy_2} \quad (3)$$

where the hadron h of momentum $\vec{p}_2$ is measured in the hemisphere away from the trigger π^+ or π^- (with transverse momentum $\vec{p}_{\perp 1}$ and rapidity y_1).

When $h = \pi^{\pm}$, it may be written :

$$\frac{d\Delta^{\pi,\pi^{\pm}}}{d\vec{p}_{\perp 1}\, dy_1\, dp_{2x}\, dy_2} = \frac{x}{p_{\perp 1}} \left(\frac{4}{9} G_u^{val}(x,Q^2) - \frac{1}{9} G_d^{val}(x,Q^2) \right) D_u^{\pi^{\pm}-\pi^-}(z_1,Q^2)$$

$$D_g^{\pi^{\pm}}(z_2,Q^2) \frac{1}{\pi} \frac{d\hat{\sigma}^C}{d\hat{t}} + \frac{x}{p_{\perp 1}} G_g(x,Q^2) \frac{5}{9} D_u^{\pi^+-\pi^-}(z_1,Q^2) D_u^{\pi^{\pm}-\pi^-}(z_2,Q^2) \frac{1}{\pi} \frac{d\hat{\sigma}^F}{d\hat{t}} \quad (4)$$

with

$$x = e^{-(y_1+y_2)}$$

$$z_1 = p_{\perp 1} (e^{y_1} + e^{y_2})/\sqrt{s}$$

$$z_2 = p_{2x} (e^{y_1} + e^{y_2})/\sqrt{s}$$

In (4), we have integrated over the component p_{2y} perpendicular to the scattering plane and used the notation $D_q^{\pi^+-\pi^-}(z,Q^2) = D_q^{\pi^+}(z,Q^2) - D_q^{\pi^-}(z,Q^2)$. The subprocess cross-sections are given by :

$$\frac{1}{\pi}\frac{d\hat{\sigma}^C}{d\hat{t}} = \frac{8}{3}\frac{\alpha\alpha_s(Q^2)}{\hat{s}^2}\left(\frac{\hat{s}}{-\hat{u}} + \frac{-\hat{u}}{\hat{s}}\right)$$

$$\frac{1}{\pi}\frac{d\hat{\sigma}^F}{d\hat{t}} = \frac{\alpha\alpha_s(Q^2)}{\hat{s}^2}\left(\frac{\hat{u}}{\hat{t}} + \frac{\hat{t}}{\hat{u}}\right) \qquad (5)$$

with $\alpha_s(Q^2) = (12\pi/25) \;/\; \mathrm{Log}(Q^2/\Lambda^2)$ and

$$\hat{s} = x\,s$$

$$\hat{t} = -x\,s\,e^{y_1}/(e^{y_1}+e^{y_2}) \qquad (6)$$

$$\hat{u} = -s\,e^{-y_1}/(e^{y_1}+e^{y_2})$$

We use the definition [7]

$$Q^2 = 2\hat{s}\hat{t}\hat{u}/(\hat{s}^2+\hat{t}^2+\hat{u}^2) \qquad (7)$$

and Λ = 500 MeV. It is now clear, from (4), that the sum

$$\frac{d\Delta^{\pi,\pi^+\pi^-}}{d\vec{p}_{1\perp}\,dy_1\,dp_{2x}\,dy_2} = \frac{d\Delta^{\pi,\pi^+}}{d\vec{p}_{1\perp}\,dy_1\,dp_{2x}\,dy_2} + \frac{d\Delta^{\pi,\pi^-}}{d\vec{p}_{1\perp}\,dy_1\,dp_{2x}\,dy_2} \qquad (8)$$

allows a direct determination of the gluon fragmentation function $D_g(z,Q^2)$, whereas the difference

$$\frac{d\Delta^{\pi,\pi^-\pi^+}}{d\vec{p}_{\perp 1}\,dy_1\,dp_{2x}\,dy_2} = \frac{d\Delta^{\pi,\pi^-}}{d\vec{p}_{\perp 1}\,dy_1\,dp_{2x}\,dy_2} - \frac{d\Delta^{\pi,\pi^+}}{d\vec{p}_{\perp 1}\,dy_1\,dp_{2x}\,dy_2} \quad (9)$$

allows the measurement of the gluon distribution within the proton $G_g(x,Q^2)$.

II. The fragmentation fonction of the gluon.

As shown in the previous section, the fragmentation function of the gluons is directly accessible through the cross-section combination :

$$\frac{d\Delta^{\pi,\pi^+\pi^-}}{d\vec{p}_{\perp 1}\,dy_1\,dp_{2x}\,dy_2} = \frac{x}{p_{\perp 1}}\left(\frac{4}{9}G_u^{val}(x,Q^2) - \frac{1}{9}G_d^{val}(x,Q^2)\right) D_u^{\pi^+\pi^-}(z_1,Q^2)\, D_g^{\pi^+\pi^-}(z_2,Q^2)\,\frac{1}{\pi}\,\frac{d\hat{\sigma}^{QC}}{d\hat{t}} \quad (10)$$

This determination of D_g turns out to be very clear [3] : a) The building blocks entering (10) are well-known : only the valence quark distributions are needed. b) No integration is involved in (10) and the variables z_2 and Q^2 are fixed by the momenta $\vec{p}_1$ and $\vec{p}_2$ of the observed hadrons. c) the Fermi motion of the incident partons has a negligible effect. A possible background may come from the 4-jet events, if these latter have not been discarded as

described in section I. However, we are going to show that such a background is rather small.

In order to study the gluon fragmentation function, it is useful to define

$$\frac{d\Delta^{\pi,\pi^+\pi^-}}{d\vec{p}_{\perp 1}\, dy_1\, dp_{\perp jet}\, dz_2} = \frac{\sqrt{s}}{p_{\perp jet}} \frac{1}{e^{y_2}} \frac{d\Delta^{\pi,\pi^+\pi^-}}{d\vec{p}_{\perp 1}\, dy_1\, dp_{2x}\, dy_2} \qquad (11)$$

where

$$p_{\perp jet} = \sqrt{s} / (e^{y_1} + e^{y_2})$$

$$z_2 = p_{2x} / p_{\perp jet} \qquad (12)$$

The quantity $p_{\perp jet}$ is nothing else than the quark or gluon jet transverse momentum. Such a variable is useful in that it fixes almost completely the value of Q^2 which depends very weakly on y_1 in the region where the cross-section is non negligible. For instance, with our choice (7) for Q^2, we have $Q^2 \simeq \frac{4}{3} (p_{\perp jet})^2$

The contribution of the anomalous component of the photon is given by

$$\frac{d\Delta^{\pi,\pi^+\pi^-}}{d\vec{p}_{\perp 1}\, dy_1\, dp_{\perp jet}\, dz_2} = \frac{\sqrt{s}}{p_{\perp jet}} \frac{1}{e^{y_2}} \frac{1}{p_{\perp 1}} \frac{1}{s^2} \int \frac{dz_1}{z_1} D_u^{\pi^+-\pi^-}(z_1, Q^2) \alpha_s^2(Q^2) \cdot$$

$$\left\{ \left[\left(u_\gamma(x_a, Q^2) \left(1 + c(\tilde{z}_2)\right) + d_\gamma(x_a, Q^2)\left(1 + s(\tilde{z}_2)\right)\right) \left(G_u^{val}(x_b, Q^2) - G_d^{val}(x_b, Q^2)\right) \cdot 2|A_1|^2 + \left(u_\gamma(x_a, Q^2)\, G_u^{val}(x_b, Q^2) - d_\gamma(x_a, Q^2)\, G_d^{val}(x_b, Q^2)\right) I \right] D_u^{\pi^+\pi^-}(\tilde{z}_2, Q^2) \right.$$

$$\left. + q_\gamma(x_a, Q^2) \left(G_u^{val}(x_b, Q^2) - G_d^{val}(x_b, Q^2)\right) |A_2|^2 D_q^{\pi^+\pi^-}(\tilde{z}_2, Q^2) \right\} / x_a x_b \qquad (13)$$

where

$$|A_1|^2 = \frac{4}{9}(\hat{s}^2+\hat{u}^2)/\hat{t}^2$$

$$|A_2|^2 = (\hat{u}^2+\hat{s}^2)/\hat{t}^2 - 4(\hat{u}^2+\hat{s}^2)/9\hat{u}\hat{s}$$

$$I = -8(s^3+\hat{u}^3-\hat{t}^3)/27\hat{s}\hat{t}\hat{u} \qquad (14)$$

We have the following kinematical relations

$$x_a = x_{\perp 1}(e^{y_1}+e^{y_2})/2z_1 \qquad \hat{s} = x_a x_b s$$

$$x_b = x_{\perp 1}(e^{-y_1}+e^{-y_2})/2z_1 \qquad \hat{t} = -x_b x_{\perp 1} s e^{y_1}/2z_1$$

$$\tilde{z}_2 = z_1 |p_{2x}|/p_{\perp 1} \qquad \hat{u} = -x_a x_{\perp 1} s e^{-y_1}/2z_1$$

$$x_{\perp 1} = 2p_{\perp 1}/\sqrt{s} \qquad (15)$$

In expression (13), u_γ, d_γ and g_γ are the distribution functions within the photon of quarks of charge 2/3, 1/3 and of the gluons. We use here the parametrization of ref. [8] : for the distributions G_q^{val} , we use the parametrization of Buras and Gaemers [9] and for the quark fragmentation functions, the expressions of Field and Feynman [10] (without scale breaking in agreement with e^+e^- data). $c(\tilde{z}_2)$ and $s(\tilde{z}_2)$ in (13) mean $D_c^{\pi^+ +\pi^-}(\tilde{z}_2)/D_u^{\pi^+ +\pi^-}(\tilde{z}_2)$ and $D_s^{\pi^+ +\pi^-}(\tilde{z}_2)/D_u^{\pi^+ +\pi^-}(\tilde{z}_2)$; we take $c(\tilde{z}_2) = s(\tilde{z}_2)$. For $D_g(\tilde{z}_2, Q^2)$ we use the parametrization of ref [7] . Notice also that we have not taken into account the Fermi motion

of the incident parton in (13) ; we know indeed that the Fermi motion effect is small in double inclusive cross-sections[11] .

The results of our calculations (done for E_{Lab}^{γ} = 100 GeV, as everywhere in this paper) are shown in fig. 3. We see that the direct coupling term dominates over the anomalous one for $p_{\perp jet} \lesssim$ 5 GeV/c, provided we choose $y_1 \gtrsim 0$. On the other hand, we have not considered the VDM background, since we already know from I that it is smaller in double inclusive cross-sections than the anomalous component contribution. We conclude from these calculations that the direct coupling contribution to $d\Delta^{\pi,\pi^+ + \pi^-}/dp_{\perp 1} dy_1 dp_{\perp jet} dz_2$ is quite observable, for $p_{\perp jet}$ not too large, even if the 4-jet events have not been discarded.

To extract $D_g(z,Q^2)$ from (10), we integrate over y_1 and $\vec{p}_{\perp 1}$ defining

$$\frac{d\Delta^{\pi,\pi^+ + \pi^-}}{dz_2\, dp_{\perp jet}} = D_g(z_2,\bar{Q}^2)\, d(p_{\perp 1}^{min}, y_1^{min}, y_1^{max}, p_{\perp jet}, s) \qquad (16)$$

with

$$d = 2\pi\sqrt{s}\int_{z_1^{min}}^{1} dz_1 \int_{y_1^{min}}^{y_1^{max}} dy_1\, e^{-y_2}\, D_u^{\pi^+ - \pi^-}(z_1,Q^2) \times \left(\frac{4}{9} G_u^{val}(x,Q^2) - \frac{1}{9} G_d^{val}(x,Q^2)\right) \cdot \frac{1}{\pi}\frac{d\hat{\sigma}^c}{dt}$$

and $\bar{Q}^2 \simeq 4(p_{\perp jet})^2/3$ (17)

This cross-section is fairly large and should be quite observable, as shown in fig. 4. These results are obtained by integrating over $y_1 > 0$ and taking $p_{\perp 1}^{min} = 2$ GeV/c. We show also in Fig. 4 the curve obtained with another parametrization of the gluon fragmentation function [12] . The results are very different, which emphasizes the sensitivity of this approach for measuring $D_g(z,Q^2)$.

The factorized form (16) allows us to go further and to define ratios in which many of the experimental and theoretical uncertainties cancel. By defining

$$r_1(z_2,z_2',\bar{Q}^2) = \frac{d\Delta^{\pi,\pi^+\pi^-}/dz_2\,dp_{\perp jet}}{d\Delta^{\pi,\pi^+\pi^-}/dz_2'\,dp_{\perp jet}} = \frac{D_g^{\pi^+\pi^-}(z_2,\bar{Q}^2)}{D_g^{\pi^+\pi^-}(z_2',\bar{Q}^2)} \qquad (18)$$

the z_2 dependence of $D_g(z_2,Q^2)$ at fixed Q^2 may be investigated very clearly. Similarly the ratio

$$r_2 = \frac{r_1(z_2,z_2',\bar{Q}^2)}{r_1(z_2,z_2',\bar{Q}'^2)} = \frac{D_g(z_2,\bar{Q}^2)}{D_g(z_2,\bar{Q}'^2)} \Big/ \frac{D_g(z_2',\bar{Q}^2)}{D_g(z_2',\bar{Q}'^2)} \qquad (19)$$

allows the observation of scale breaking effect, as explicitly shown in ref. [3] .

To end this section, let us comment on two effects which could obscure the measurement of $D_g(z_2,Q^2)$.

One effect comes from the transverse spread of the final hadrons in the gluon jet. In that case, the measured value $z_2^m = |p_{2x}|/p_{\perp jet}$ does not coincide with the definition $z_2 = \frac{\vec{p}_2 \cdot \vec{p}_{jet}}{\vec{p}^2_{jet}}$ and a bias is thus introduced in the measurement of $D_g(z_2, Q^2)$. It is however possible to get rid of this effect, extensively studied in ref. [13] for hadron-hadron collisions, if the jet axis is experimentally determined, which allows to use the true definition of z_2.

A second effect comes from the background due to the proton low $p_\perp$ fragments in the backward direction ; the fragments may be confused with gluon jet fragments at low p_{2x} . We estimate this background by the approximation

$$\frac{d\Delta^{\pi, \pi^+ + \pi^-}}{d\vec{p}_{\perp 1}\, dy_1\, dp_{2x}\, dy_2} = \frac{dN^{\pi^+ + \pi^-}}{dp_{2x}\, dy_2} \; \frac{d\sigma^{\pi}}{d\vec{p}_{\perp 1}\, dy_1} \qquad (20)$$

where $dN^{\pi^+ + \pi^-}/d\vec{p}_{\perp 2}\, dy_2$ describes the spectator diquark fragmentation [14,15]

$$dN^{\pi^+ + \pi^-}/d\vec{p}_{\perp 2}\, dy_2 = \frac{A}{\pi} e^{-A\vec{p}_{\perp 2}^{\,2}} x_2 D_{qq}^{\pi^+ + \pi^-}(x_2)$$

$$x_2 D_{qq}^{\pi^+ + \pi^-}(x_2) = \left[(1-x_2)^3 + (1-x_2)^5\right]/2$$

$$x_2 \simeq 2 p_{\perp 2} \operatorname{sh} y_2 / \sqrt{s} \qquad (21)$$

$$dN^{\pi^+ + \pi^-}/dp_{2x}\, dy_2 = \int dp_{2y}\; dN^{\pi^+ + \pi^-}/d\vec{p}_{\perp 2}\, dy_2$$

For A we take the value A = 6 which gives $< p_{\perp 2} > \simeq$ 360 MeV/c.

The results of our calculations are shown[1] in fig. 5a and 5b. The diquark background is negligible, even for p_{2x} = 300 MeV/c. Moreover, it contributes only for negative values of y_2, whereas the signal is important for positive y_2.

This approximate treatment of the background is very crude in the $y_2 \simeq 0$ region. A better description of the background would be obtained by following the approach developed in ref. [15] ; in that approach, the hadrons are considered as fragments of a string which stretches between colored charges, and a satisfying description of the $y_2 \simeq 0$ region can be obtained. We do not however expect (ref. [15]) the relative value of the signal over the background to be changed.

III. The gluon content of the proton.

In this section, we turn to the possibility to measure the gluon distribution within the proton in photoproduction experiment. The cross-section difference

$$\frac{d\Delta^{\pi,\pi^-\pi^+}}{d\vec{p}_{\perp 1}\, dy_1\, dp_{2x}\, dy_2} = \frac{2x}{p_{\perp 1}}\, G_g(x,Q^2)\, \frac{1}{\pi}\, \frac{d\hat{\sigma}^F}{d\hat{t}}\, \frac{5}{9}\, D_u^{\pi^+\pi^-}(z_1,Q^2)\, D_u^{\pi^+\pi^-}(z_2,Q^2) \qquad (22)$$

---

1 - The peculiar shape of the Compton curves near the upper value of y_2 is due to the behaviour of the fragmentation function $D_u^{\pi^+\pi^-}(z_1)$ when $z_1 = p_{\perp 1}(e^{y_1} + e^{y_2})/\sqrt{s}$ goes to 1 ; in the Field-Feynman parametrization which we use here this difference does not vanish at $z_1 = 1$.

is directly proportional to the gluon distribution $G_g(x,Q^2)$ and the variables x and Q^2 are fixed by the rapidities y_1 and y_2 of the observed π's. Thus we have a way to directly observe the gluon content of the proton ; the cross-section differences must, of course, be sizeable and not small compared to various backgrounds. We are going to show that this measurement is indeed possible.

Let us begin by estimating the relative magnitude of the Compton and fusion contributions, using two somewhat extreme parametrizations of $G_g(x,Q^2)$[12,16]. As the cross-section differences (4) , read :

$$\frac{d\Delta^{\pi,\pi^{\pm}}}{d\vec{p}_{\perp 1}\, dy_1\, dp_{2x}\, dy_2} = \frac{d\Delta^{\pi,\pi^{+}}_{\text{(Compton)}}}{d\vec{p}_{\perp 1}\, dy_1\, dp_{2x}\, dy_2} \mp \frac{d\Delta^{\pi,\pi^{-}}_{\text{(fusion)}}}{d\vec{p}_{\perp 1}\, dy_1\, dp_{2x}\, dy_2} \tag{23}$$

a necessary condition to observe $G_g(x,Q^2)$ is that $d\Delta^{\pi,\pi^-}$(fusion) is not too small compared to $d\Delta^{\pi,\pi^+}$(Compton) It is useful to let the x variable appear through

$$\frac{d\Delta^{\pi,\pi^+}}{d\vec{p}_{\perp 1}\, dy_1\, dp_{2x}\, dx} = \int dy_2\ \delta(x - e^{-y_1 - y_2})\ \frac{d\Delta^{\pi,\pi^+}}{d\vec{p}_{\perp 1}\, dy_1\, dp_{2x}\, dy_2} \tag{24}$$

The dependence of this cross-section on $p_{\perp 1}$ and p_{2x} ,

through the quark and gluon fragmentation functions, is trivial and of no interest here ; we fix $p_{\perp 1}$ = 2.5 GeV/c and p_{2x} = 1 GeV/c. The Compton and fusion cross-sections are shown[1] in Fig. 6a,b,c as functions of y_1 for x = ·2, ·4 and ·6. We have used the quark structure and fragmentation functions defined in the preceeding section and two different parametrizations for the gluon distribution within the proton, that of ref. [16] and that of ref. [12] . We see that the contribution of the fusion term may be sizable for x up to ·6.

We already know that taking cross-section differences enhances the ratio of the 3 jet signal to the 4 jet one. However, the 4 jet events may still produce an appreciable background in some kinematical regions. Let us, for instance, study the contribution of the anomalous component of the photon to the difference $d\Delta^{\pi,\pi^-\pi^+}/d\vec{p}_{\perp 1} dy_1 dp_{2x} dx$ and see how it compares to the direct coupling contribution. The results of our calculations, done with the gluon distribution of ref. [16] are shown[1] in Fig. 7a and 7b. We see that for the higher value the background due to the anomalous component of the photon may be large.

We have however, in section II, shown that it was possible to completely eliminate the 4 jet event background. Another and may be simpler way to discard the 4 jet events consists in putting a forward veto counter allowing to discard events with a forward jet. Thus eliminating events with forward jets carrying more than 10 % of the incident photon momentum (this amounts to require

the variable x_a of the photon constituent (fig. 2) be bigger than ·9), we considerably reduce the anomalous component contribution as shown in Fig. 7.

Thus our conclusion is that, as long as $x \lesssim \cdot 6$, the fusion term can be safely isolated.

In order to extract the gluon distribution function, it is useful to define the cross-section (22) as function of x and Q^2, where Q^2 is a given expression of s, e^{y_1} and e^{y_2}. With our choice (7) for Q^2, it is simpler to introduce as in section III, the variable $p_{\perp jet} = \sqrt{s}/(e^{y_1} + e^{y_2})$. The value of Q^2 is now essentially fixed by $p_{\perp jet}$ and varies very little with x for $\cdot 1 < x < \cdot 8$; we found, within 20 %, that $Q^2 \simeq 4\, p^2_{\perp jet}/3 - 1$. Integrating (22) over $p_{\perp 1}$ and p_{2x}, and expressing the result as a function of x and $x_{\perp jet} = 2p_{\perp jet}/\sqrt{s}$, we get the simple form :

$$\left.\frac{d\Delta^{\pi,\pi^- - \pi^+}}{dy_1\, dy_2}\right| = \frac{20\pi\alpha}{9s}\left(1 - \frac{x^2_{\perp jet}}{2x}\right)\alpha_s(Q^2)\, \mathcal{D}_u^{\pi^+ - \pi^-}(z_1^{min}, Q^2)\, \mathcal{D}_u^{\pi^+ - \pi^-}(z_2^{min}, Q^2)\, G_g(x, Q^2)$$

$$\left| \begin{array}{l} y_1 = \bar{y}_1(x, x_{\perp jet}) \\ y_2 = \bar{y}_2(x, x_{\perp jet}) \end{array} \right. \qquad (25)$$

where we have defined

$$\mathcal{D}_q^h(z_1^{min}, Q^2) = \int_{z_1^{min}} dz_1\, D_q^h(z_1, Q^2) \qquad (26)$$

In (25), the values of the rapidities are connected with x and $x_{\perp jet}$ by the relation

$$\bar{y}_{1\atop 2} = \ln \left\{ 1/x_{\perp jet} \pm \left(1/x^2_{\perp jet} - 1/x \right)^{1/2} \right\} \tag{27}$$

Notice that expression (25) is invariant under the substitution $y_1 \rightarrow y_2$.

In fig. 8, we show the cross-sections $d\Delta^{\pi,\pi^- - \pi^+}/dy_1 dy_2$ as function of x and $p_{\perp jet}$ for $p^{min}_{\perp 1} = 2$ GeV/c, $p^{min}_{2x} = 1$ GeV/c and the structure function of. ref. [16] . These cross-sections are fairly large for x up to about ·5 and should allow a direct measure of $G(x,Q^2)$. The Q^2 evolution of $G(x,Q^2)$ is related to the variation of $d\Delta^{\pi,\pi^- - \pi^+}/dy_1 dy_2$ with $p_{\perp jet}$ as written in (25). For illustration we also plot in Fig. 8 the value obtained for $d\Delta^{\pi,\pi^- - \pi^+}/dy_1\, dy_2$ when the scaling violation in $G(x,Q^2)$ is frozen by taking $Q^2(p_{\perp jet}) = Q^2(2.5) = 7.33$ GeV^2. We find that scaling violation effects are relatively small and should thus be difficult to detect.

Of course these results strongly depend on the parametrization of $G_g(x,Q^2)$. To see the effect of another choice for $G_g(x,Q^2)$, we present in Fig. 9, results for the cross-section

$$\frac{d\Delta^{\pi,\pi^-\pi^+}}{dx} = \int dy_1\, dy_2\, \delta(x - e^{-y_1 - y_2}) \int_{p^{min}_{\perp 1}} d\vec{p}_{\perp 1} \int_{p^{min}_{\perp 2}} d\vec{p}_{\perp 2}\, \frac{d\Delta^{\pi,\pi^-\pi^+}}{d\vec{p}_{\perp 1}\, dy_1\, dp_{2x}\, dy_2} \tag{28}$$

with $p_{\perp 1}^{min} = 2.0$ GeV/c, $p_{2x}^{min} = 1$ GeV/c and $-1 < y_1 < 2$. The great difference between the curves obtained with the parametrizations of ref [12] and [16] is the effect of the current ignorance of the gluon distribution within the proton and a good illustration of the method we propose to measure it.

IV. Quark and gluon content of the photon.

We already indicated in paper (I) how it is possible to isolate the contribution of the anomalous photon component in the 4-jet event sample. This is done by measuring symmetric pair correlations which are found to be fairly large for $E_{Lab}^{\gamma} = 100$ GeV and $p_{\perp} = 2.5$ GeV/c. In this case the dominant subprocess is the qq → qq scattering, and qg → qg contributes only 3 % which means that this measurement will not yield information on the gluon content of the photon.

In order to obtain this, we propose to measure the difference of opposite side double inclusive cross-sections :

$$\frac{d\Delta^{g}}{dp_{\perp 1}\, dy_1\, dp_{2x}\, dy_2} = \frac{d\sigma(\gamma p \to \gamma \pi^{+} X)}{dp_{\perp 1}\, dy_1\, dp_{2x}\, dy_2} - \frac{d\sigma(\gamma p \to \gamma \pi^{-} X)}{dp_{\perp 1}\, dy_1\, dp_{2x}\, dy_2}$$

where the photon and the pions are detected at large $p_\perp$ in opposite hemispheres with rapidity y_1 and y_2 and transverse momenta $p_{\perp 1}$ and p_{2x} respectively. It is straightforward to see (fig. 10) that only the gluon content of the photon contributes to the difference. This difference is written under the simple expression

$$\frac{d\Delta^g}{dp_{\perp 1}\,dy_1\,dp_{2x}\,dy_2} = \frac{2}{3}\,\frac{\pi\alpha\alpha_s(Q^2)}{\hat{s}^2}\,x_a\,g_\gamma(x_a,Q^2)\cdot$$

$$\left[\frac{4}{9}x_b G_u(x_b,Q^2) - \frac{1}{9}x_b G_d(x_b,Q^2)\right] D_u^{\pi^+-\pi^-}(z_2)\left(\frac{\hat{s}}{-\hat{t}} + \frac{-\hat{t}}{\hat{s}}\right) \qquad (30)$$

where

$$x_a = x_{\perp 1}\left(e^{y_1} + e^{y_2}\right)/2$$

$$x_b = x_{\perp 1}\left(e^{-y_1} + e^{-y_2}\right)/2$$

$$z_2 = |p_{2x}| / p_{\perp 1}$$

The results of the calculations done with the same ingredients as defined in previous section are shown in Fig. 11. They turn out to be very small (E^γ_{lab} = 100 GeV, $p_{\perp 1}$ = 2.5 GeV/c p_{2x} = 1 GeV/c and y_1 = 0). Thus the measurement of the gluon content of the photon would require very high statistics experiments.

V - CONCLUSION

We have shown in this paper how large $p_\perp$ photoproduction should in the near future reveal very interesting results on the gluon properties. The orders of magnitude which come out of the calculations are all large enough to yield sufficient counting rates within the expected experimental luminosities.

Let us conclude by some remarks about the next steps in the study of gluon physics in photoproduction.

i) on the experimental side, very high energy photon beams (as the HERA project in Europe and the TRISTAN project in Japan) would allow the anomalous contribution to dominate much over the direct coupling and hadron-like terms. Moreover, as shown in I the processes contributing mainly are $qg \to qg$ and $gg \to gg$ provided $p_\perp$ is not too large (say $p_\perp < 10$ GeV/c for $\sqrt{s} \simeq 100$ GeV).

ii) The use of polarized photon beams either on unpolarized targets [17] or on polarized ones [18] should provide new tests of QCD and more precisely of the vector nature of the gluon.

iii) On the theoretical side, a deeper understanding of the applicability of perturbative QCD is needed. The problem of next to leading terms which have been shown to yield a very significant correction to the leading log approximation [19] is as sharp in photoproduction as in other reactions. Some of the conclusions of this paper

may well be invalidated if it turns out that these next to leading corrections completely destroy the simple picture of hard processes we have been used to.

We indeed are just at the beginning of the study of large $p_\perp$ photoproduction. The preliminary data of the WA4 collaboration at CERN show an encouraging trend. More data at higher energy will be available in the near future which should help the gluon properties to be better known.

ACKNOWLEDGEMENTS

We wish to thank M. Gorski and F. Richard for helpful discussions.

REFERENCES.

1. H. Fritzsch and P. Minkowski, Phys. Lett. 69B (1977)316.
   C.H. Llewellyn-Smith, Phys. Lett. 79B (1978)83.
   Tu Tung Sheng and Wu Chi Min, Nucl. Phys. B156 (1979)493.
   J. Owens, Phys. Rev. D21(1980)54
   K. Ishida, T. Kobayashi and T. Yoshino KEK preprint 79-14(1979)
   I. Kang and C.H. Llewellyn-Smith, Nucl. Phys. B166(1980) 413.
2. M. Fontannaz, A. Mantrach, B. Pire and D. Schiff, Phys. Lett. 89B(1980), 263
3. M. Fontannaz, A. Mantrach, B. Pire and D. Schiff, Ecole Polytechnique preprint A381(1980) to appear in Phys. Lett. B.
4. M. Fontannaz, A. Mantrach, B. Pire and D. Schiff, Orsay preprint LPTHE 80/12(1980) to appear in Z. Physik, C. This paper is hereafter called I.
5. E. Witten, Nucl. Phys. B120(1977),189.
   C.H. Llewellyn Smith, Phys. Lett. 79B,(1978)83
   R. DeWitt et al, Phys. Rev. D19(1979)2046, D20(1979) 1751(E)
   W. Frazer and J. Gunion, Phys. Rev. D20(1979)147
6. NA14 experiment of the CERN-London-Orsay-Saclay-Southampton collaboration. Wide band beam and tagged photon beam FNAL facilities.
7. R. Feynman, R. Field and G. Fox, Phys. Rev. D18(1978) 3320
8. A. Nicolaïdis, Nucl. Phys. B163(1980)156
9. A. Buras and K. Gaemers, Nucl. Phys. B132(1978)249
10. R. Field and R. Feynman, Nucl. Phys. B136(1978)1.
11. M. Fontannaz and D. Schiff, Nucl. Phys. B132(1978)457.
12. R. Baier, J. Engels and B. Petersson, Z. Physik C2 (1979)265.
13. J.L. Alonso, A. Cruz, G. Ringland and R. Roberts, Nucl.

Phys. B157(1979)498.

14. M. Fontannaz, B. Pire and D. Schiff, Phys. Lett. 77B (1978)315.

15. M. Fontannaz, B. Pire and D. Schiff, Nucl. Phys.B162 (1980)317.

16. J. Owens and E. Reya, Phys. Rev. D17(1978) 3003.

17. B. Petersson and B. Pire, Ecole Polytechnique preprint A394(1980) to appear in Phys. Letters B.

18. M. Fontannaz, B. Pire and D. Schiff, Ecole Polytechnique preprint under preparation

19. J. Abad and B. Humpert, Phys. Lett. 78B(1978)627, 80B (1979)433(E)

G. Altarelli, R. Ellis and G. Martinelli, Nucl. Phys. B143(1978)521,B157(1979)461

J. Kubar-André and F. Paige, Phys. Rev. D19(1979)221

W. Bardeen and A. Buras, Phys. Rev. D20(1979)166

D. Duke and J. Owens, FSV preprint HEP 802401(1980).

Figure Captions

Fig. 1 : The direct coupling graphs a) Compton b) fusion

Fig. 2 : The photon structure function contribution

Fig. 3 : The double inclusive cross-section $d\Delta^{\pi,\pi^+ + \pi^-}/d\vec{p}_{\perp 1} dy_1 dp_{\perp jet} dz_2$ for $s = 200\ GeV^2$, $p_{\perp 1} = 2.5$ GeV/c, $z_2 = \cdot 4$ and a) $p_{\perp jet} = 3$ GeV/c, b) $p_{\perp jet} = 5$ GeV/c. The Compton graph contribution (-) and the anomalous photon contribution (---).

Fig. 4 : The differential cross-section $d\Delta^{\pi,\pi^+ + \pi^-}/dz_2 dp_{\perp jet}$. Full and dashed curves correspond to the parametrizations of ref [16] and [12] respectively for the gluon distribution function. Curves are labelled with the value of $p_{\perp jet}$.

Fig. 5 : Comparison of the Compton graph contribution (-) to the double inclusive cross-section $d\Delta^{\pi,\pi^+ + \pi^-}/d\vec{p}_{\perp 1} dy_1 dp_{2x} dy_2$ with the corresponding background due to low $p_\perp$ proton fragments ($s = 200\ GeV^2$, $p_{\perp 1} = 3$ GeV/c, $p_{2x} = \cdot 3$ GeV/c and a) $y_1 = \cdot 5$; b) $y_1 = -\cdot 5$)

Fig. 6 : Comparison between the Compton graph (-) and the fusion graph contributions to the double inclusive cross-section $d\Delta^{\pi,\pi^-}/d\vec{p}_{\perp 1}, dy_1 dp_{2x} dx$. The dashed and dash-dotted lines correspond to

the fusion graph evaluated with the parametrization of ref. [16] and [12] respectively for the gluon distribution function. ($s = 200$ GeV^2, $p_{\perp 1} = 2$ GeV/c, $p_{2x} = 1$ GeV/c and a) $x = \cdot 2$, b) $x = \cdot 4$, c) $x = \cdot 6$).

Fig. 7 : The double inclusive cross-section $d\Delta^{\pi,\pi^-\pi^+}/d\vec{p}_{\perp 1} dy_1 dp_{2x} dx$ for $s = 200$ GeV^2, $p_{\perp 1} = 2.5$ GeV/c, $p_{2x} = 1$ GeV/c and a) $x = \cdot 4$, b) $x = \cdot 6$. The fusion graph contribution (-) is compared to the anomalous photon contribution (-•-•). The dashed curve is the anomalous photon contribution with the condition $x_a > \cdot 9$.

Fig. 8 : The differential cross-section $d\Delta^{\pi,\pi^-\pi^+}/dy_1 dy_2$ ($s = 200$ GeV^2, $p_{\perp 1}^{min} = 2$ GeV/c, $p_{2x}^{min} = 1$ GeV/c) as a function of x for 2 values of $p_{\perp jet}$: $p_{\perp jet} = 2.5$ GeV/c(-) and $p_{\perp jet} = 4.5$ GeV/c (-•-). The dashed curve is obtained for $p_{\perp jet} = 4.5$ GeV/c, with no scaling violation in the gluon distribution function when Q^2 is held fixed $Q^2 = Q_o^2 = 7.33$ GeV^2.

Fig. 9 : The differential cross-section $d\Delta^{\pi,\pi^-\pi^+}/dx$ for $s = 200$ GeV^2, $p_{\perp 1}^{min} = 2$ GeV/c, $p_{2x}^{min} = 1$ GeV/c, y_1 integrated between -1 and 2. Comparison between the parametrization of ref. 16 (-•-) and ref. 12 (-) for the gluon distribution function.

Fig. 10 : The contribution of the gluon in the photon to the large $p_\perp$ photon inclusive production.

Fig. 11 : The double inclusive cross-section $d\Delta^g/dp_{\perp 1} dy_1 dp_{2x} dy_2$ for $s = 200$ GeV^2, $p_{\perp 1} = 2.5$ GeV/c, $p_{2x} = 1.$ GeV/c and $y_1 = 0$.

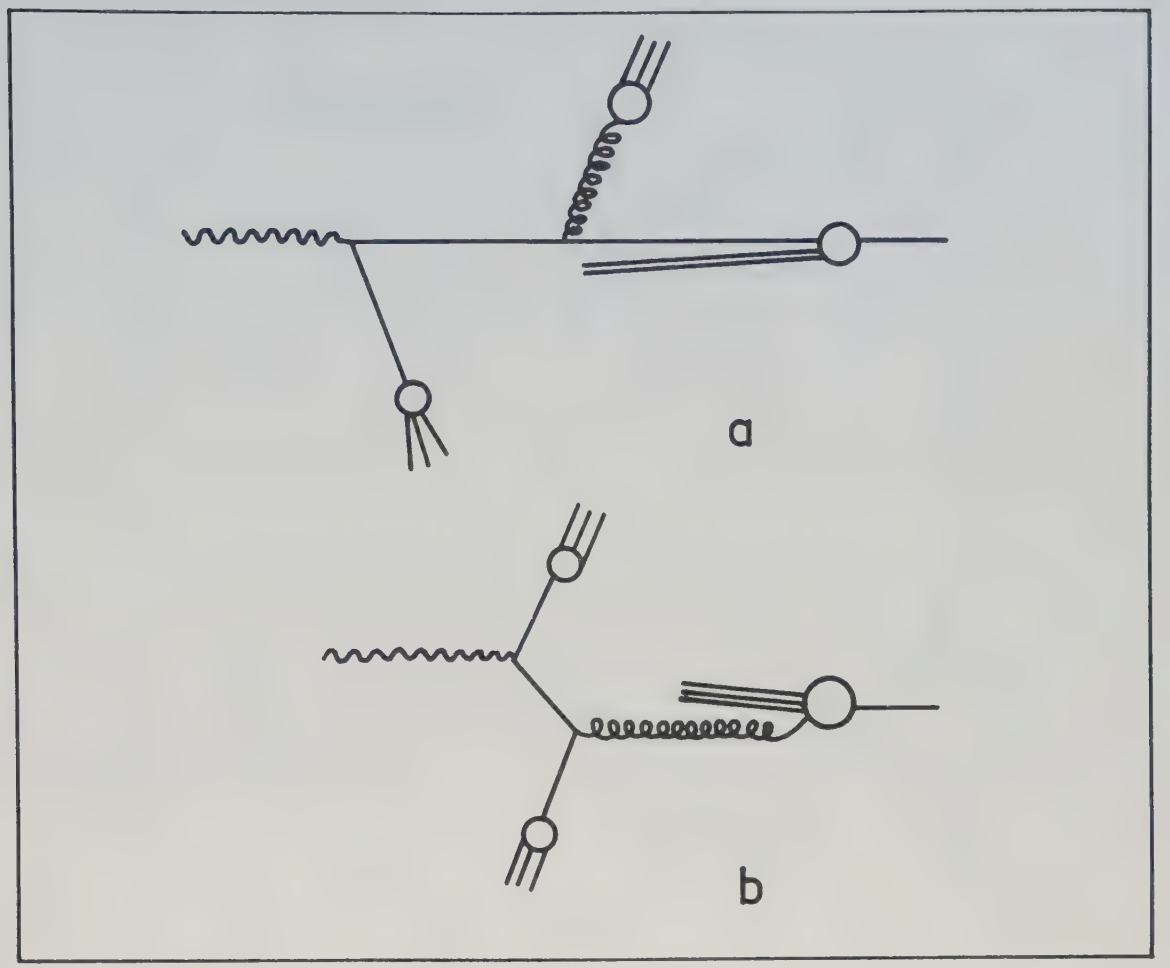

Fig.1

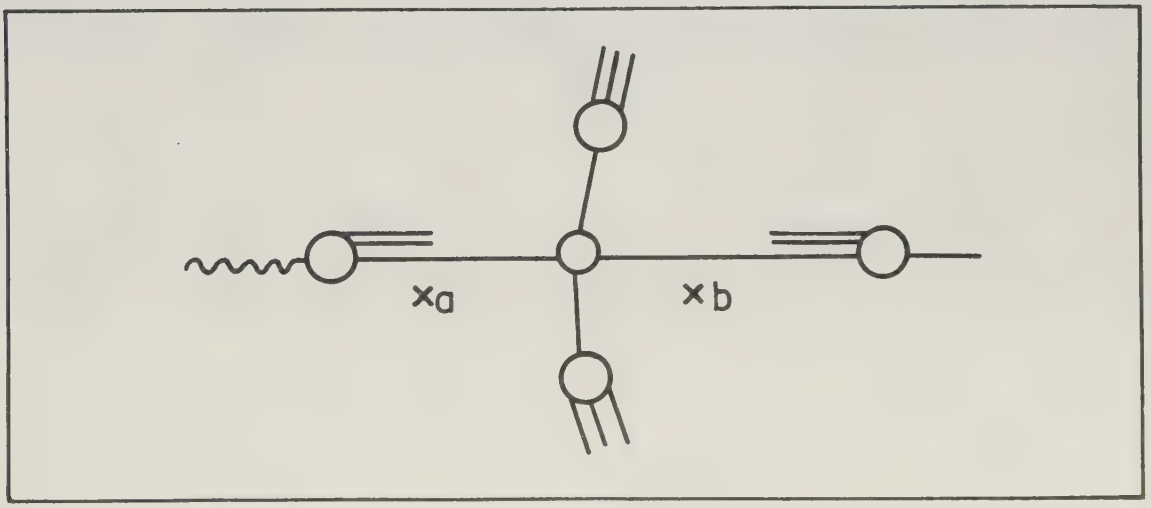

Fig.2

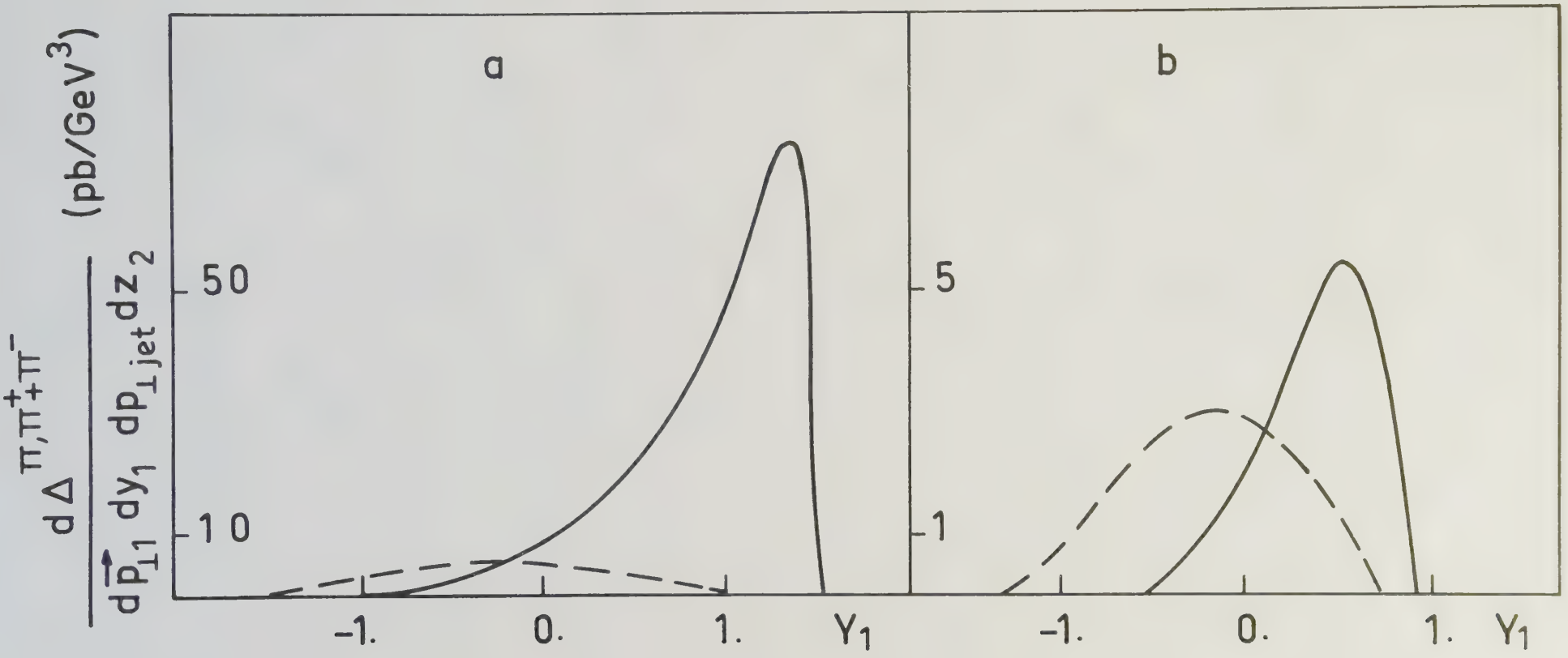
a
b
50
10
5
1
-1.
0.
1.
Y_1
$\frac{d\Delta^{\pi,\pi^+\pi^-}}{d\vec{P}_{\perp 1}\, dy_1\, dp_{\perp jet}\, dz_2}$ (pb/GeV^3)

Fig. 3

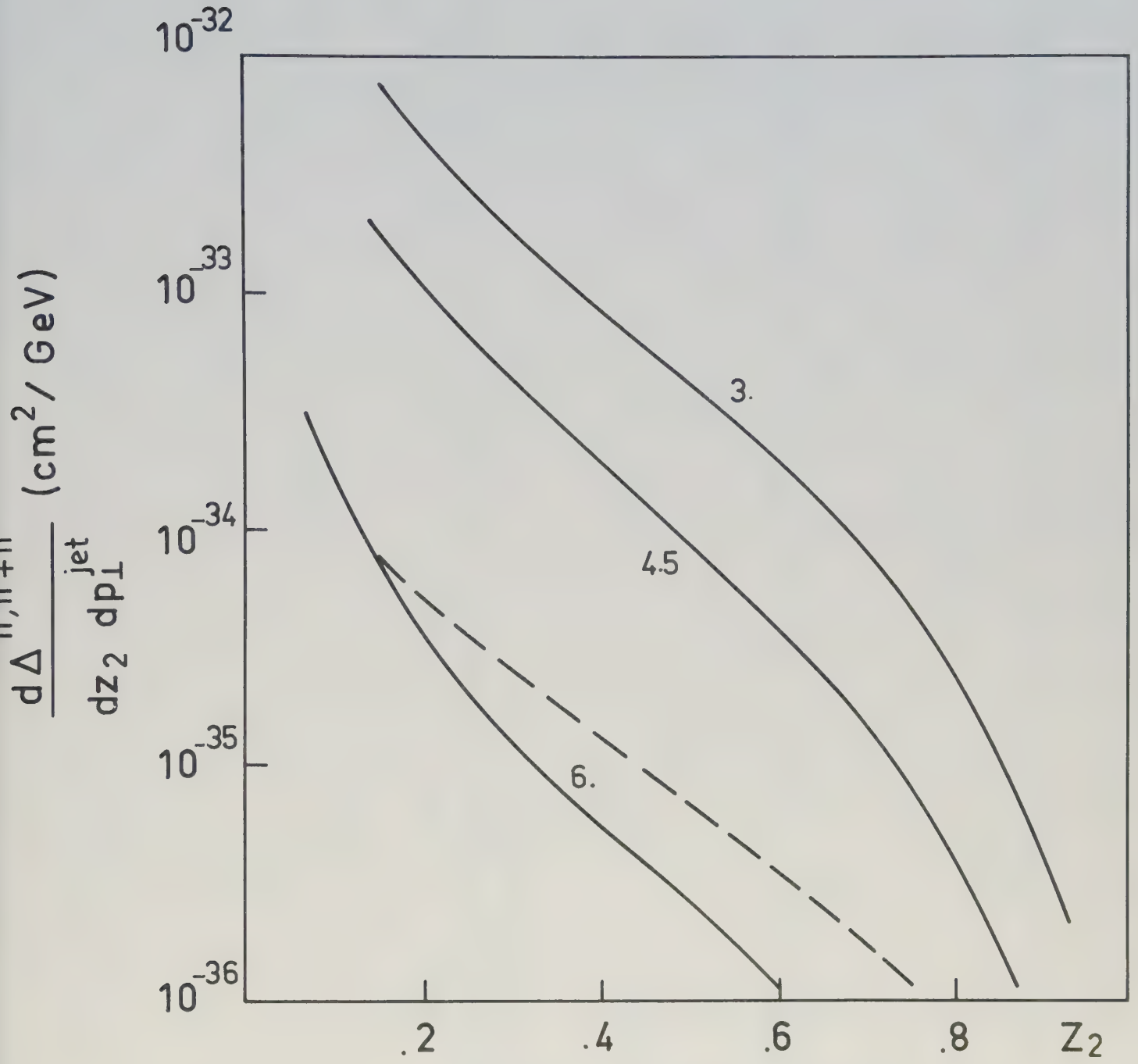
10^{-32}
10^{-33}
10^{-34}
10^{-35}
10^{-36}
$\frac{d\Delta^{\pi,\pi^+\pi}}{dz_2\ dp_\perp^{jet}}$ (cm^2/ GeV)
3.
4.5
6.
.2
.4
.6
.8
Z_2

Fig. 4

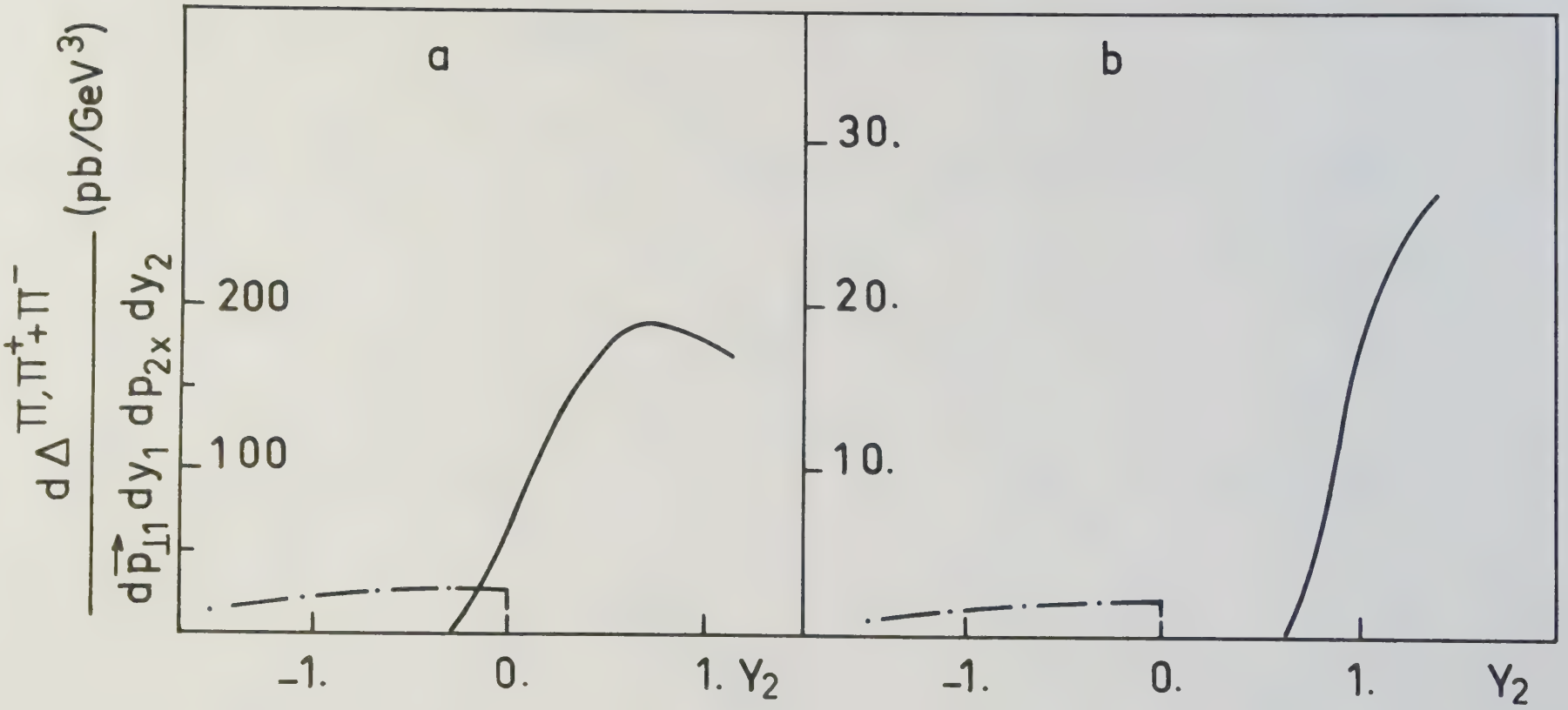
a
b
200
100
30.
20.
10.
-1.
0.
1. Y_2
-1.
0.
1.
Y_2
$\frac{d\Delta^{\pi,\pi^+\pi^-}}{d\vec{p}_{\perp 1}\, dy_1\, dp_{2x}\, dy_2}$ (pb/GeV^3)

Fig. 5

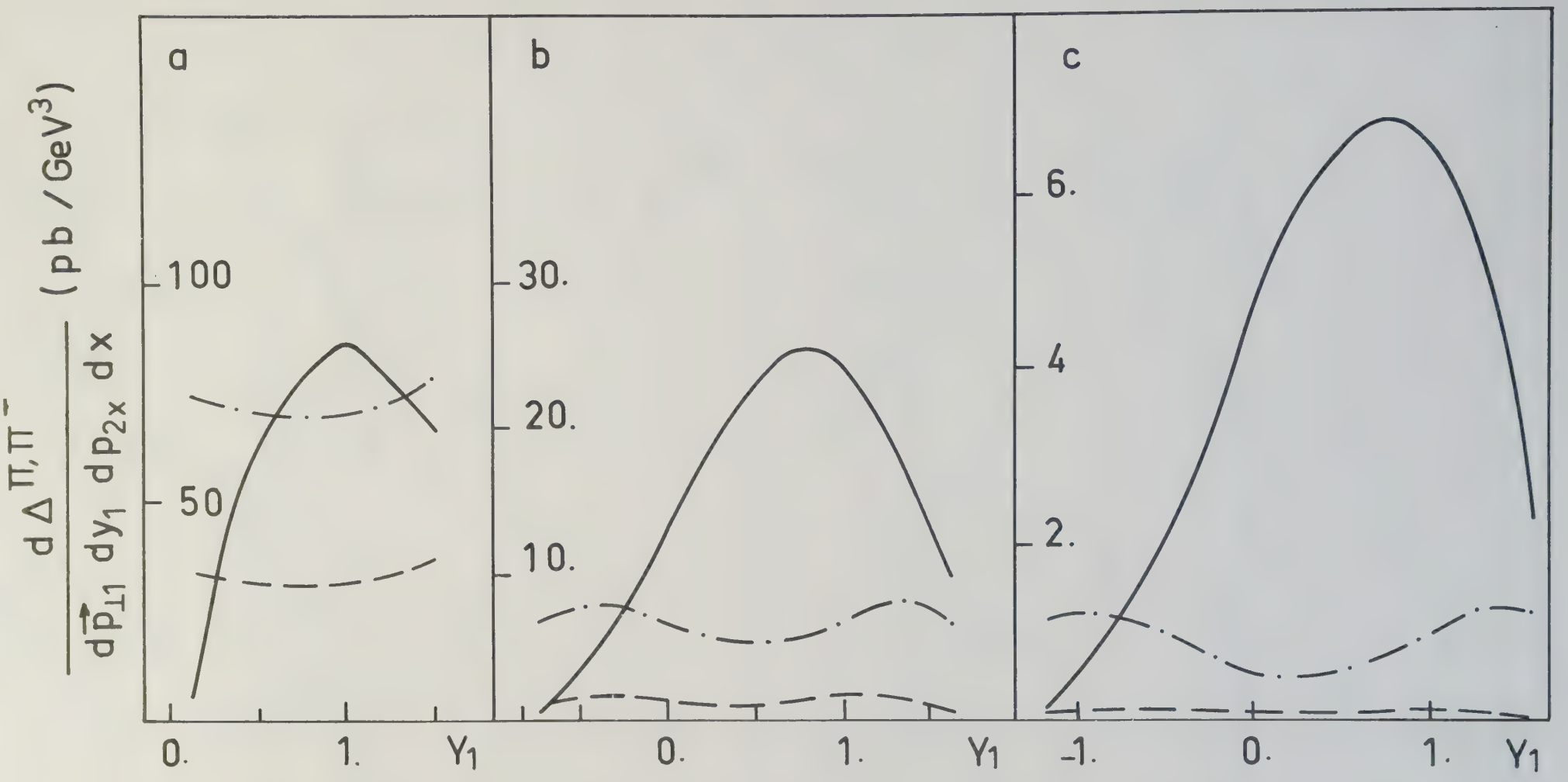
a
b
c
100
50
30.
20.
10.
6.
4
2.
0.
1.
Y1
0.
1.
Y1
-1.
0.
1.
Y1
$\frac{d\Delta^{\pi,\pi^-}}{d\vec{p}_{\perp 1}\, dy_1\, dp_{2x}\, dx}$ (pb / GeV^3)

Fig. 6

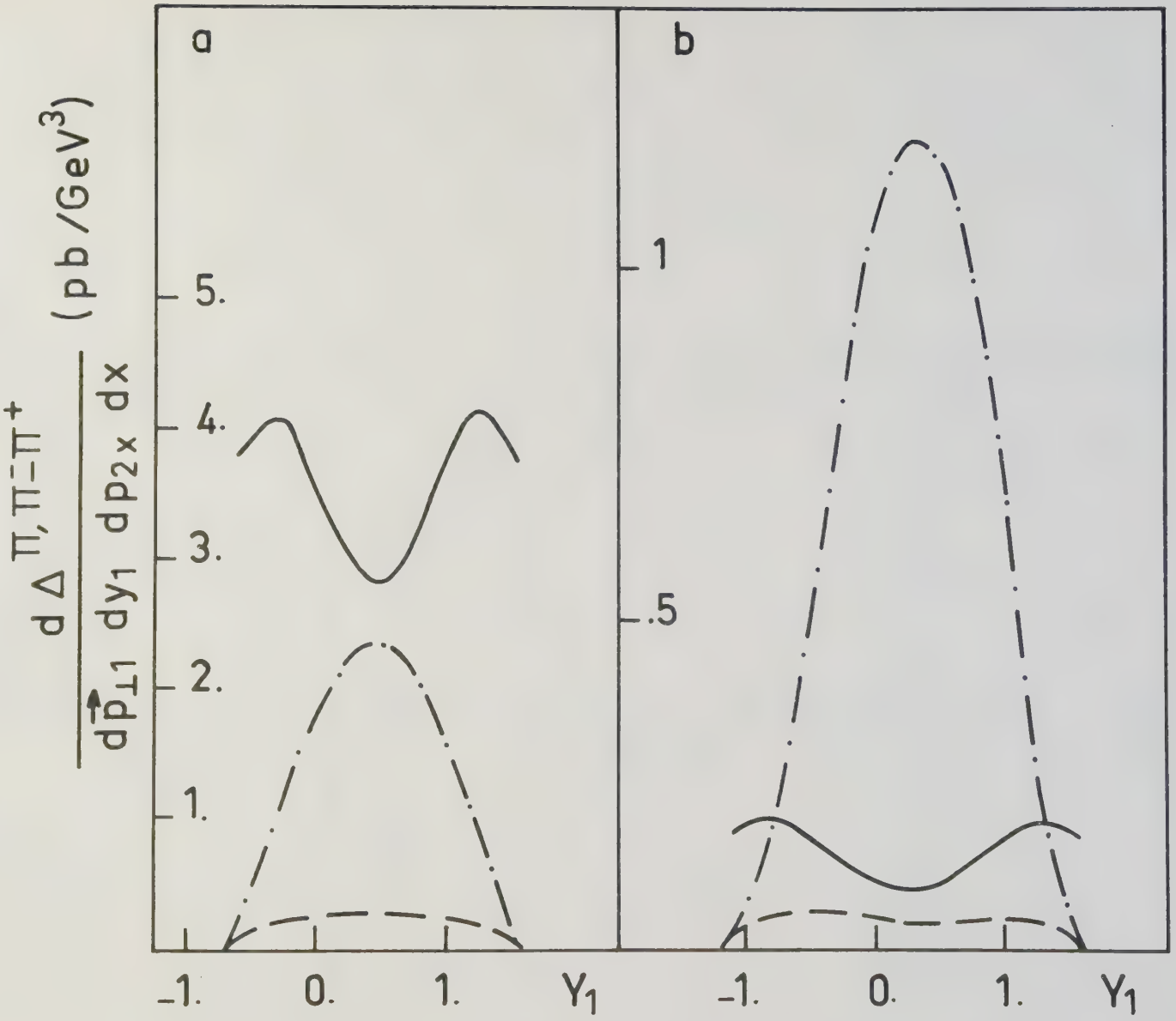
a
b
5.
4.
3.
2.
1.
1
.5
-1.
0.
1.
Y1
-1.
0.
1.
Y1
$\frac{d\Delta^{\pi,\pi^-\pi^+}}{d\vec{p}_{\perp 1}\, dy_1\, dp_{2x}\, dx}$ (pb/GeV^3)

Fig. 7

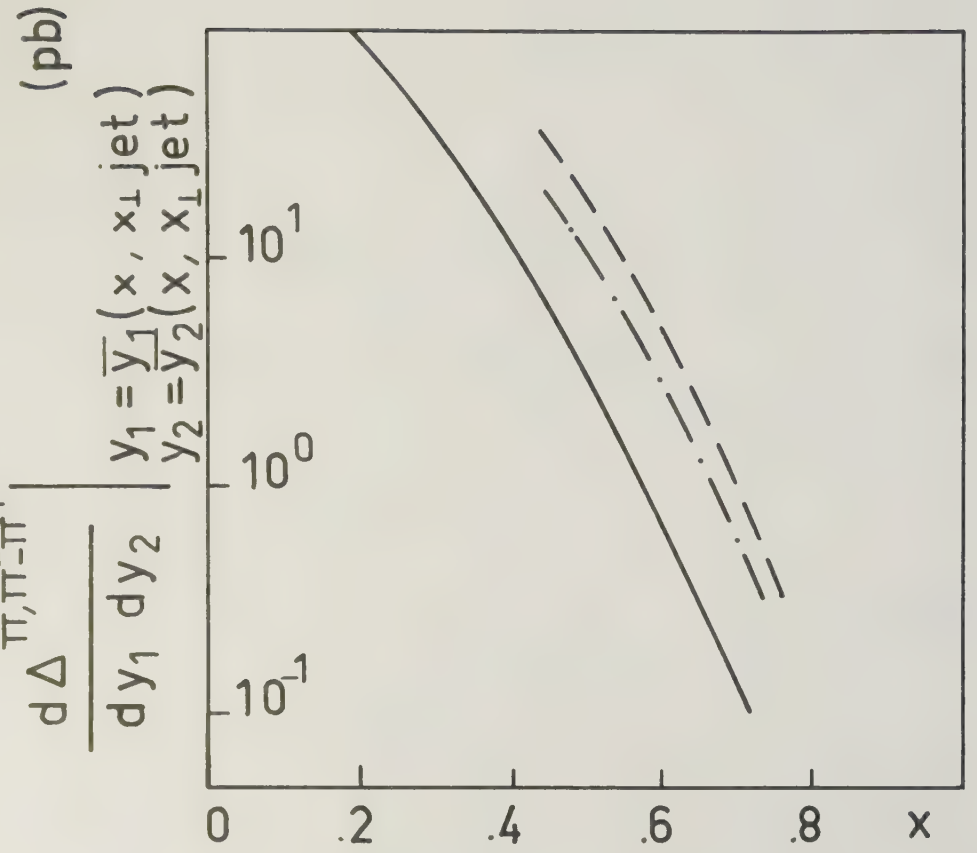
(pb)
$\frac{d\Delta^{\pi,\pi^-\pi^+}}{dy_1\ dy_2}$
$y_1 = \overline{y_1}(x, x_\perp \text{ jet})$
$y_2 = \overline{y_2}(x, x_\perp \text{ jet})$
10^1
10^0
10^{-1}
0
.2
.4
.6
.8
x

Fig. 8

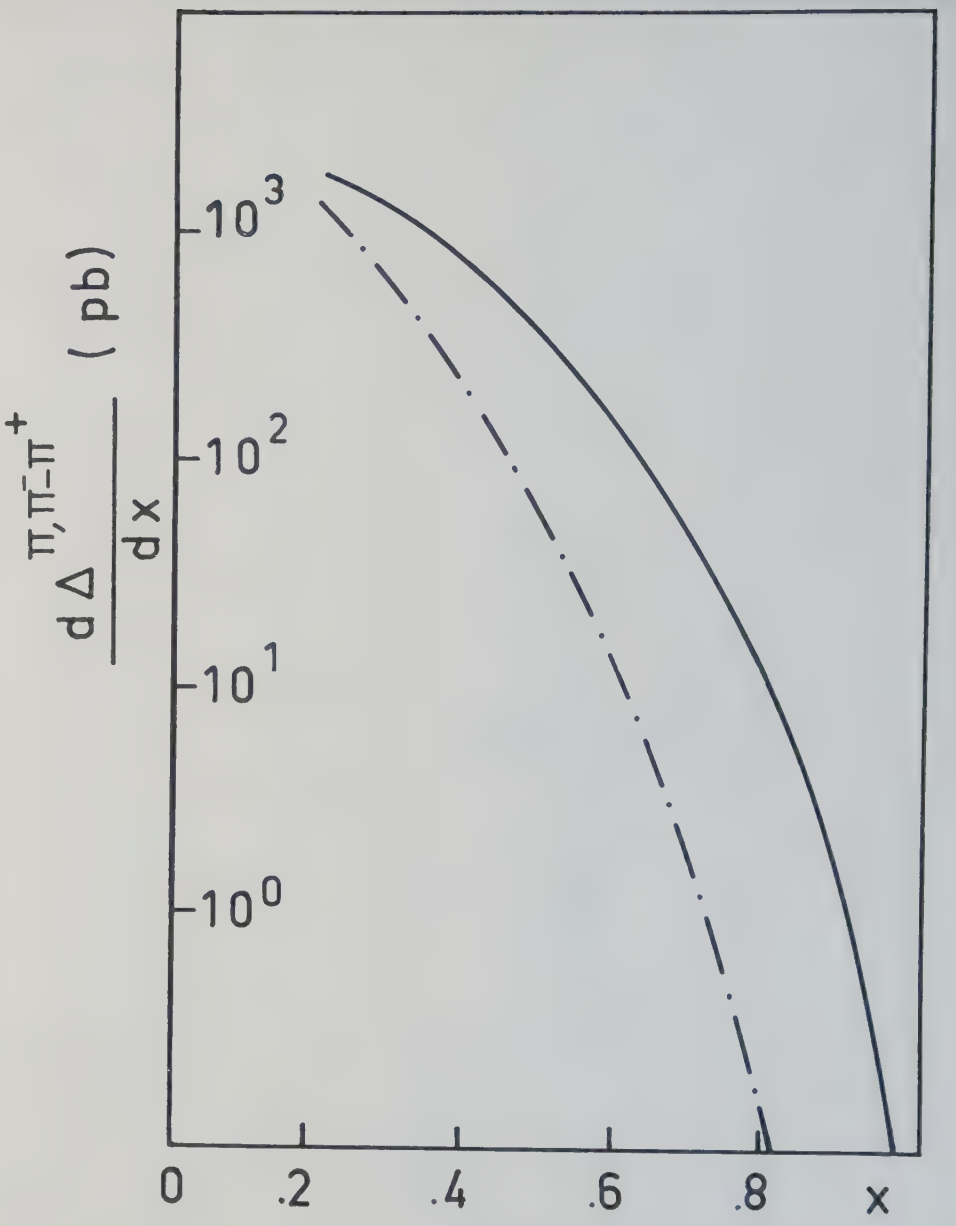
$\frac{d\Delta^{\pi,\pi^-\pi^+}}{dx}$ (pb)
10^3
10^2
10^1
10^0
0
.2
.4
.6
.8
x

Fig. 9

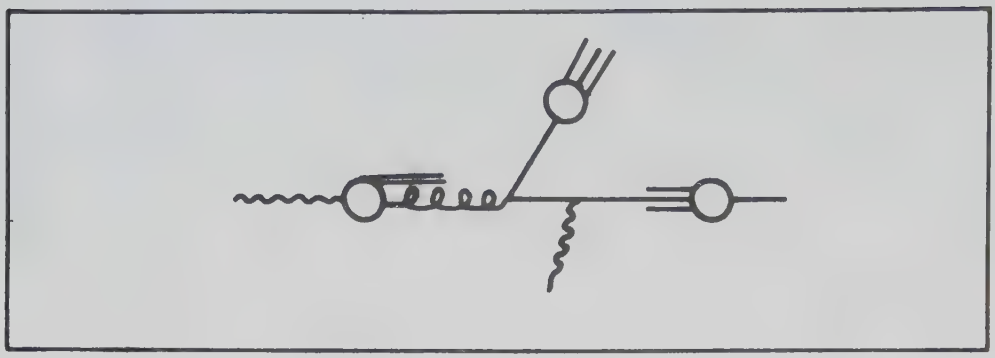

Fig.10

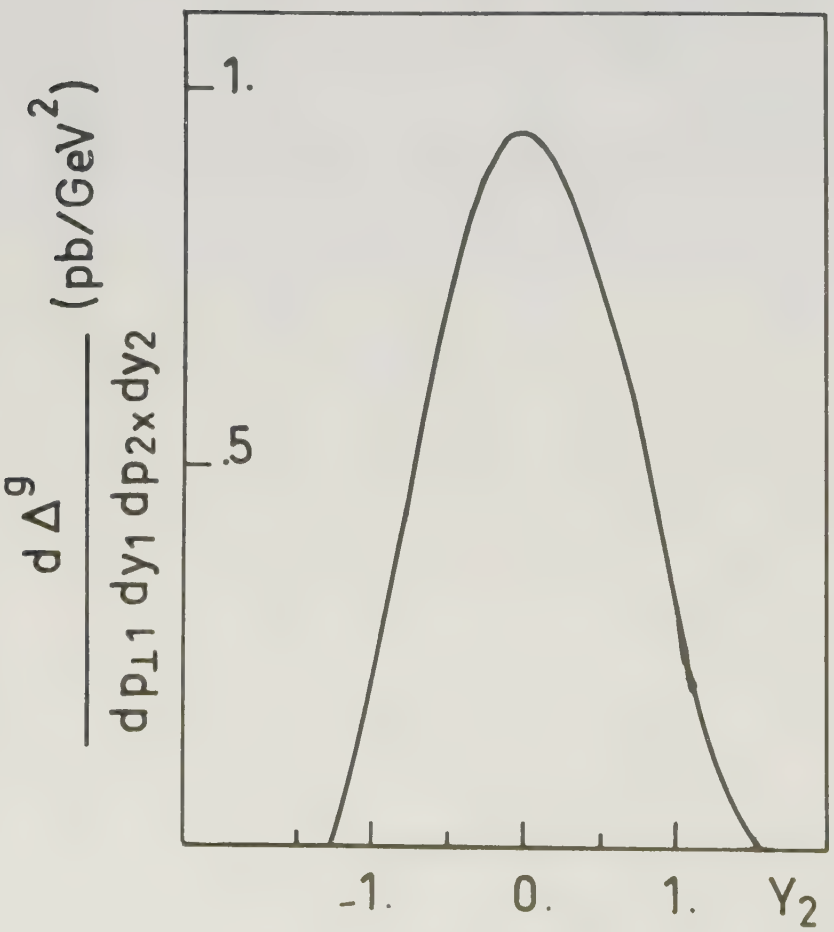

Fig.11

C I N Q U I E M E P A R T I E

LA PHOTOPRODUCTION DE HADRONS A GRANDE IMPULSION TRANSVERSE AVEC DES PHOTONS POLARISES

PHOTOPRODUCTION WITH POLARIZED PHOTONS AS A SOURCE OF POLARIZED GLUON JETS

B. PETERSSON
Fakultät für Physik, Universität Bielefeld, Germany

and

B. PIRE
Centre de Physique Théorique, Ecole Polytechnique, Palaiseau, France

Received 9 May 1980

We show that, according to QCD, the direct Compton process $\gamma q \to qg$ in polarized photoproduction leads to strongly polarized gluon jets. We also show that this process is expected to dominate in the reaction $\gamma p \to \pi^+ +$ opposite side jet + X. The study of the opposite side jet will give direct evidence for the spin of the gluon.

The realization of the Parton Model by a field theory, Quantum Chromo-Dynamics (QCD), which for hard scattering processes may be treated in perturbation theory, has been very successful especially in the confrontation with experiments on deep inelastic scattering and e^+e^- annihilation [‡1]. In fact QCD stands now as the best candidate for a theory of strong interactions. The basic feature in this theory is the introduction of the spin one gluon. Therefore it is of paramount importance to obtain more direct evidence for the manifestation of the gluon and its spin [2–5]. In this connection, one should preferentially study processes where, according to QCD, gluons participate in the same order in the coupling constant as quarks. This is the case e.g. for hadronic large p_T reactions [1,6]. Another process, specific of QCD, is the "Gluon Compton Effect" $\gamma q \to qg$ and its crossed versions [7]. It has recently been shown that a promising way of isolating this process is given by photoproduction of large p_T hadrons [8,9].

In this letter we show that an extension of such experiments to a polarized photon beam is expected to give crucial evidence for the gluon spin. We point out that, at the level of constituents, a strong correlation will exist between the direcitons of the gluon and photon linear polarizations. We further show that under certain trigger conditions, the processes $\gamma q \to qg$ gives the dominant contribution. We finally discuss the situation as regards the observation of the gluon polarization from the properties of its fragments.

A straightforward calculation gives the cross section for the process $\gamma q \to qg$ for given photon (gluon) linear polarizations ϵ (ϵ'). The gluon is put on mass shell. We get

$$\frac{d\hat{\sigma}}{d\hat{t}} = \frac{4\pi e_q^2 \alpha \alpha_s(Q^2)}{3\hat{s}^2}\left[\left(-\frac{\hat{t}}{\hat{s}}-\frac{\hat{s}}{\hat{t}}-2\right) + 4\left(\epsilon\cdot\epsilon' - \frac{2\epsilon\cdot p\,\epsilon'\cdot p'}{\hat{s}} - \frac{2\epsilon'\cdot p\,\epsilon\cdot p'}{\hat{t}}\right)^2\right], \quad (1)$$

where p (p') is the 4-momentum of the incoming (outgoing) quark and $\hat{t}$ is the momentum transfer from the photon to the outgoing quark. Neglecting the transverse momentum of the quark in the proton, which will be a good approximations for the reactions we will propose, we have $\epsilon\cdot p = 0$. Denoting the normal to the scattering plane as $\hat{n}$ and defining the angles α and α' by

$$\cos\alpha = \hat{n}\cdot\hat{\epsilon}, \qquad \cos\alpha' = \hat{n}\cdot\hat{\epsilon}',$$

‡1 For a review see e.g. ref. [1].

we get the more transparent expression

$$\frac{d\hat{\sigma}}{d\hat{t}} = \frac{16\pi e_q^2 \alpha \alpha_s(Q^2)}{3\hat{s}^2} \times [\tfrac{1}{4}(-\hat{s}/\hat{t} - \hat{t}/\hat{s} - 2) + \cos^2(\alpha - \alpha')]. \quad (2)$$

The first term in the bracket is small when $\hat{s} \simeq -2\hat{t}$, i.e. at 90° in the γ–q C.M.S. The second term gives a strong correlation between the directions of ϵ and ϵ'.

The next important point is to show how one may isolate the gluon jet in large p_T photoproduction experiments [9,10]. Such reactions are described by:

a) direct coupling processes of fig. 1a, b, c,

b) indirect processes of fig. 1d where the photon interacts through its constitutents.

Its structure function is usually divided into an anomalous part which grows like $\log Q^2$ and a hadron-like part estimated through VDM [11]. Indirect processes have the qualitative difference of giving a 4-jet structure as opposed to the 3-jet structure (one backward and two transverse jets) of direct coupling events.

We propose that an experiment studying the reaction

$$\gamma(\text{pol}) + p \to \pi^+ + \text{opposite side jet} + X, \quad (3)$$

measuring a large p_T pion in the forward hemisphere and investigating the properties of the opposite side jet, will be a good laboratory for the study of polarized gluon jets. Other trigger conditions, e.g. $\gamma + p \to$ two large p_T jets in forward hemisphere, may also be contemplated. As the discussion will be similar, we restrict ourselves to the first mentioned reaction (3). We shall first show that subprocess 1a where the π^+ is a fragment of the quark and the opposite side jet comes from a gluon, is expected to be the dominant direct process.

It has been shown in ref. [9] that the primordial transverse momentum is negligible for the direct coupling processes. We neglect also the transverse momentum of the π^+ in its parent jet. Then the differential cross sections corresponding to reaction (3) take the following simple forms for the direct subprocesses 1a–1c:

$$d\sigma/dy\, d\boldsymbol{p}_T\, dy' = \sum_{q,\bar{q}} F e_q^2 x G_{q/p}(x,Q^2) \frac{D_q^{\pi^+}(z,Q^2)}{z} \left(-\frac{\hat{s}}{\hat{t}} - \frac{\hat{t}}{\hat{s}}\right), \quad (4a)$$

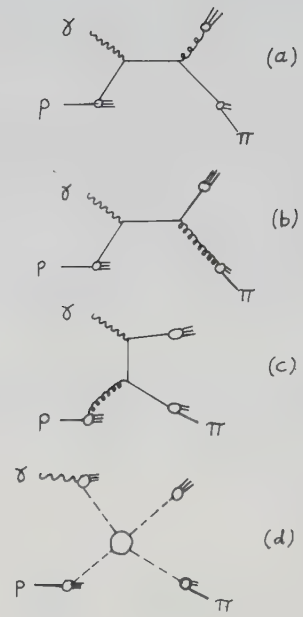

Fig. 1. The subprocesses contributing to large p_T photoproduction. (a), (b), (c) Direct coupling processes, (d) indirect coupling processes. In this last figure dashed lines represent any type of parton.

$$d\sigma/dy\, d\boldsymbol{p}_T\, dy' = \sum_{q,\bar{q}} F e_q^2 x G_{q/p}(x,Q^2) \frac{D_g^{\pi^+}(z,Q^2)}{z} \left(-\frac{\hat{s}}{\hat{u}} - \frac{\hat{u}}{\hat{s}}\right), \quad (4b)$$

$$d\sigma/dy\, d\boldsymbol{p}_T\, dy' = \tfrac{3}{8} F x G_{g/p}(x,Q^2) \sum_{q,\bar{q}} \frac{D_q^{\pi^+}(z,Q^2)}{z} \left(\frac{\hat{t}}{\hat{u}} + \frac{\hat{u}}{\hat{t}}\right), \quad (4c)$$

where

$$F = 8\alpha\, \alpha_s(Q^2)/3\hat{s}^2.$$

The functions $G(x,Q^2)$ and $D(x,Q^2)$ are the usual non-invariant structure and fragmentation functions. In these formulae, y is the rapidity and $\boldsymbol{p}_T$ the transverse momentum of the trigger π^+ and y' the rapidity of the opposite side jet. We further define $\hat{t}$ to be the momentum transfer from the photon to the jet containing the trigger π^+ and $x_T = 2p_T/\sqrt{s}$. We get the following kinematic relations

$$x = \exp(-y - y'), \qquad z = x_T(e^y + e^{y'})/2.$$

Table 1
The relative contributions to the photoproduction of a $\pi^+(p_T = 3\ \mathrm{GeV}/c$, rapidity y) and an away side jet (rapidity y') from subprocesses 1a, b, c [$s = 200\ \mathrm{GeV}^2$].

	$y = 0.5$			$y = 1$	
y'	0.3	0.6	0.9	0.3	0.6
a	87%	84%	77%	84%	78%
b	8%	5%	1%	1%	0%
c	5%	11%	21%	15%	22%
$\frac{d\sigma}{dy\,dp_T\,dy'}$ (pb/GeV^2)	45.5	64.7	62.5	69.5	87.1

One may notice that $\sqrt{x}z \geqslant x_T$; from eqs. (4) it is easy to see that the maximum of the cross sections will indeed be at $\sqrt{x}z \simeq x_T$ (giving $\hat{t} \simeq -\hat{s}/2$) corresponding to 90° scattering in the photon–parton CMS. At $s = 200\ \mathrm{GeV}^2$ and $p_T = 3\ \mathrm{GeV}/c$, typical values at the maximum are $x \simeq 0.3$, $z \simeq 0.75$ corresponding to $y = y' \simeq 0.6$. The ratio of (4b) to (4a) is approximately given by $D_g^{\pi^+}(z)/D_u^{\pi^+}(z)$ and the ratio of (4c) to (4a) by $3G_{g/p}(x)/8G_{u/p}(x)$. These ratios are expected to be small if the gluon distribution and fragmentation functions are softer than the corresponding ones for the u-quark. A more quantitative estimate using the same distribution and fragmentation functions as utilized in ref. [9] is shown in table 1.

As discussed in ref. [12], the indirect contributions of fig. 1d may be important in single particle spectra for medium p_T. For $s = 200\ \mathrm{GeV}^2$ and $p_T = 3\ \mathrm{GeV}/c$ they are estimated to be about equal to the direct contribution. In the reaction discussed here, however, they can be considerably suppressed. Firstly the recoil jets from direct coupling processes will go in the forward hemisphere while for the indirect contribution they will be approximately symmetric around $y' = 0$. Thus constraining the jet to be in the forward hemisphere gives a reduction of about a factor 2. Secondly, in the phenomenological QCD approach the contributions for single particle spectra are only big because of the internal transverse momenta in the wave functions. Thus the recoil jets for indirect processes will be considerably more diffuse, giving much less hard opposite side particles [‡2]. Thirdly, as mentioned above the indirect processes give rise to a forward jet initiated by the spectators of the hadronized photon. A veto trigger in the forward direction will further discriminate against such events. In conclusion, indirect processes contributions may be reduced significantly to the order 20–30% of the direct Compton process or less, especially by demanding the opposite jet to contain a relatively large p_T particle.

The polarization of the gluon jet may manifest itself e.g. in an azimuthal asymmetry [2,14] or in the decay properties of vector mesons from the jet [4]. Quantitative estimates of these effects are quite model dependent [‡3]. One quantity which may be the easiest to measure is the variation with the photon polarization of the mean momentum of particles in the gluon jet out of the reaction plane, $\langle P_{out} \rangle$ [3]. It is clear that any correlation between the properties of the jet and the photon polarization would be an evidence for non-zero spin of the parent constituent.

In our opinion, only experiment can presumably settle the last question. However, in order to answer it, one should preferally study the most promising reaction. We have shown that large p_T photoproduction with polarized photons is a good candidate for such a reaction.

We acknowledge useful discussions with M. Fontannaz, F. Richard, D. Schiff and D. Treille.

[‡2] The similar case in hadronic collisions is discussed in ref. [13].

[‡3] For a recent discussion, see ref. [3].

References

[1] R. Field, Lectures at La Jolla Institute Summer Workshop (1978).
[2] S. Brodsky, T. De Grand and R. Schwitters, Phys. Lett. 79B (1978) 255.
[3] T. De Grand and B. Petersson, Proc. Workshop on Lepton pair production in hadron–hadron collisions, ed. J. Cleymans (Bielefeld, 1978); and UCSB preprint TH-19 (1979), to be published in Phys. Rev. D.
[4] H. Olsen, P. Osland and I. Øverbø, Phys. Lett. 89B (1980) 221.
[5] A. Devoto, J. Pumplin, W. Repko and G. Kane, Phys. Lett. 90B (1980) 436.
[6] B. Combridge, J. Kripfganz and J. Ranft, Phys. Lett. 70B (1977) 234.
[7] H. Fritzsch and P. Minkowski, Phys. Lett. 69B (1977) 316.

[8] C. Llewellyn Smith, Phys. Lett. 79B (1978) 83;
Tu Tung Sheng and Wu Chi Min, Nucl. Phys. B156 (1979) 493;
J. Owens, Phys. Rev. D21 (1980) 54.
[9] M. Fontannaz, A. Mantrach, B. Pire and D. Schiff, Phys. Lett. 89B (1980) 263.
[10] M. Fontannaz, A. Mantrach, B. Pire and D. Schiff, Ecole Polytechnique preprint A381-0380 (1980).
[11] E. Witten, Nucl. Phys. B120 (1977) 189;
C. Llewellyn Smith, Phys. Lett. 79B (1978) 83;
R. De Witt et al., Phys. Rev. D19 (1979) 2046;
W. Frazer and J. Gunion, Phys. Rev. D20 (1979) 147.
[12] M. Fontannaz, A. Mantrach, B. Pire and D. Schiff, Orsay preprint LPTHE 80/12;
M. Fontannaz, talk at the XV Rencontre de Moriond, to be published.
[13] R. Baier, J. Engels and B. Petersson, Z. Phys. C2 (1979) 265.
[14] A. Smilga and M. Vysotsky, preprint ITEP-12 (1979).

ASYMMETRIES IN LARGE P_T PHOTOPRODUCTION AND THE POLARIZED GLUON STRUCTURE FUNCTION

M. FONTANNAZ*, B. PIRE** AND D. SCHIFF*

* L.P.T.H.E., Université Paris Sud Orsay, Bât. 211
91405 Orsay, France
Laboratoire associé au C.N.R.S.

** C.P.T., Ecole Polytechnique, 91128 Palaiseau Cedex, France
Groupe de Recherche associé au C.N.R.S.

ABSTRACT. QCD predictions for asymmetries in large p_T polarized photon reactions on a polarized target are given. Taking cross-section differences is shown to yield new tests of QCD. Double inclusive cross section measurements provide a direct way to measure the distribution function of polarized gluons in the proton.

LPTHE 80/25
September 1980
A416.0780

Introduction

Large p_T photoproduction provides very clear tests of QCD [1] in particular when the direct coupling terms of fig. 1 are isolated. These contributions are generally mixed with terms in which the photon fragments before interacting (fig. 2)(photon structure function [2]). But we have previously shown [1] that a clear separation of these various contributions could be achieved by taking advantage of the following features :

- the direct coupling terms correspond to a specific event topology : 3 jet (two large p_T final jets and a backward low p_T jet made of proton fragments) as opposed to the 4 jet topology induced by the photon structure function (the 4th jet being made of forward moving photon fragments).

- moreover, the direct coupling kinematics are characterized by the constraint [1] : $p_{Tjet}(e^{y_1} + e^{y_2}) = \sqrt{s}$ where y_1 and y_2 are the rapidities of the jets with large transverse momentum p_{Tjet}.

- differences of cross sections select, among the direct coupling terms, either the Compton (fig. 1a) or the Fusion subprocess (fig. 1b) ; namely $d\sigma(\gamma p \to \pi^+ X) - d\sigma(\gamma p \to \pi^- X)$ receives contribution from the Compton graph only whereas only the Fusion graph contributes to $d\sigma(\gamma p \to \pi^+\pi^+ X) - d\sigma(\gamma p \to \pi^+\pi^- X) + d\sigma(\gamma p \to \pi^-\pi^- X) - d\sigma(\gamma p \to \pi^-\pi^+ X)$, where the two pions are detected at

large p_T in opposite azimuthal hemispheres.

In this paper , we shall study the spin-spin asymmetries predicted by QCD for the direct coupling subprocesses of fig. 1, thus gaining further accurate tests of QCD. We shall thus suppose that the strategy described above has been used to isolate their contributions.

I - Asymmetries in the QCD Compton Effect

Let us first write the unpolarized cross section difference to which only the Compton graph contributes

$$\Delta^{\pi}(\vec{p}) = \frac{E\,d\sigma}{d\vec{p}}(\gamma p \to \pi^+ X) - \frac{E\,d\sigma}{d\vec{p}}(\gamma p \to \pi^- X)$$

$$= \frac{1}{\pi}\int dx \frac{dz}{z^2}\left[\frac{4}{9}G_u^{val}(x,Q^2) - \frac{1}{9}G_d^{val}(x,Q^2)\right] \cdot \quad (1)$$

$$\hat{s}\,\frac{d\hat{\sigma}^c}{d\hat{t}}\left[D_u^{\pi^+}(z,Q^2) - D_u^{\pi^-}(z,Q^2)\right]\delta(\hat{s}+\hat{t}+\hat{u})$$

with

$$\frac{d\hat{\sigma}^c}{d\hat{t}} = \frac{8\pi\alpha\alpha_s(Q^2)}{3\hat{s}^2}\left(-\frac{\hat{u}}{\hat{s}} - \frac{\hat{s}}{\hat{u}}\right)$$

with usual notations ($\hat{t}$ is the transfer momentum squared between the photon and the gluon). The running coupling constant is defined as

$$\alpha_s(Q^2) = 12\pi/25\,Log(Q^2/\Lambda^2)$$

with

$$Q^2 = 2\,\hat{s}\,\hat{t}\,\hat{u} \Big/ (\hat{s}^2 + \hat{t}^2 + \hat{u}^2)$$

and Λ will be taken as 500 MeV. We have shown in ref. [1] that the parton Fermi motion inside the proton might be safely ignored in Eq.(1). Let us turn to the polarized case ; the Compton cross sections for longitudinally polarized incoming particles (summed over final polarizations) are :

$$\frac{d\hat{\sigma}^c_{++}}{d\hat{t}} = \frac{16\pi}{3}\,\frac{\alpha\,\alpha_s(Q^2)}{\hat{s}^2}\,\frac{\hat{s}}{-\hat{u}} \qquad (2)$$

$$\frac{d\hat{\sigma}^c_{+-}}{d\hat{t}} = \frac{16\pi}{3}\,\frac{\alpha\,\alpha_s(Q^2)}{\hat{s}^2}\,\frac{-\hat{u}}{\hat{s}} \qquad (3)$$

where indices describe the helicity components. The asymmetry at the subprocess level is thus given by

$$\hat{A} = \frac{d\hat{\sigma}_{++}/d\hat{t} - d\hat{\sigma}_{+-}/d\hat{t}}{d\hat{\sigma}_{++}/d\hat{t} + d\hat{\sigma}_{+-}/d\hat{t}} = \frac{\hat{s}^2 - \hat{u}^2}{\hat{s}^2 + \hat{u}^2} \qquad (4)$$

This asymmetry is always positive and is close to 1 when the outgoing quark makes a small angle with the photon direction ($-\hat{u} \ll \hat{s}$).

Let us show that this statement is still valid at the hadron level, under reasonable assumptions for the polarized proton structure function.

Defining $G_{q_+/p_+}(x,Q^2)$ and $G_{q_-/p_+}(x,Q^2)$ with obvious notations and denoting their difference by $\Delta G_q(x,Q^2)$, it is straightforward to obtain, using T and P invariance,

$$A(\vec{p}) = \frac{1}{2\,\Delta^\pi(\vec{p})} \int dx \frac{dz}{z^2} \left[\frac{4}{9}\Delta G_u^{val}(x,Q^2) - \frac{1}{9}\Delta G_d^{val}(x,Q^2)\right] \cdot$$

$$\cdot\, \hat{s}\, \frac{\Delta d\hat{\sigma}}{d\hat{t}} \left[D_u^{\pi^+}(z,Q^2) - D_u^{\pi^-}(z,Q^2)\right] \delta(\hat{s}+\hat{t}+\hat{u}) \qquad (5)$$

with

$$\frac{\Delta d\hat{\sigma}}{d\hat{t}} = \frac{d\hat{\sigma}_{++}}{d\hat{t}} - \frac{d\hat{\sigma}_{+-}}{d\hat{t}}$$

The quantities ΔG_q are not yet well experimentally determined although some polarized leptoproduction experiments have given some first results [3] . They are constrained by the Bjorken sum rule [4] stating

$$\int_0^1 dx \left[\Delta G_u^{val}(x,Q^2) - \Delta G_d^{val}(x,Q^2)\right] = G_A/G_V \qquad (6)$$

assuming as usual SU(2) invariance of the sea. Essentially three

models have been proposed [5-7] with various theoretical inputs. On fig. 3. we show the resulting asymmetries at $s = 200\ GeV^2$ and $p_T = 3\ GeV/c$ for the three models. They yield similar results; this is due to the fact that the polarized structure functions are used in the region where they are well enough constrained by the experimental data, so that the asymmetry is predicted with relatively good accuracy. It is of the order of 0.5 at the peak of the cross section. This is an absolutely non trivial QCD prediction which should be tested.

II - Asymmetries in the Fusion Process

Let us turn now to the fusion graph (fig. 1b) contribution. We have shown in Ref[8] that, among the direct coupling terms, it could be separated from the Compton contribution by studying the following double inclusive cross section difference.

$$F(\vec{p}_1, \vec{p}_2) = \frac{d\sigma}{d\vec{p}_{T1}\, dy_1\, dp_{2x}\, dy_2}(\gamma p \to \pi^+\pi^- X) + \tag{7}$$

$$\frac{d\sigma}{d\vec{p}_{T1}\, dy_1\, dp_{2x}\, dy}(\gamma p \to \pi^-\pi^+ X) - \frac{d\sigma}{d\vec{p}_{T1}\, dy_1\, dp_{2x}\, dy_2}(\gamma p \to \pi^+\pi^+ X) - \frac{d\sigma}{d\vec{p}_{T1}\, dy_1\, dp_{2x}\, dy_2}(\gamma p \to \pi^-\pi^- X)$$

where the observed pions are in opposite hemispheres at large p_T. This difference may be written as

$$F(\vec{p}_1, \vec{p}_2) = \frac{2x}{p_{T1}}\, G_g(x, Q^2)\, \frac{1}{\pi}\, \frac{d\hat{\sigma}^F}{d\hat{t}}\, \frac{5}{9}\, D_u^{\pi^+\pi^-}(z_1, Q^2) \cdot \tag{8}$$

$$\cdot\, D_u^{\pi^+\pi^-}(z_2, Q^2)$$

where y_1 and y_2 denote the rapidities of the observed pions,

$$x = e^{-y_1 - y_2}$$

$$z_1 = p_{T1}\left(e^{y_1} + e^{y_2}\right)/\sqrt{s} \qquad (9)$$

$$z_2 = p_{T2}\, x\left(e^{y_1} + e^{y_2}\right)/\sqrt{s} \,.$$

The fusion cross section is given by

$$\frac{d\hat{\sigma}^F}{d\hat{t}} = \frac{1}{2}\left(\frac{d\hat{\sigma}^F_{++}}{d\hat{t}} + \frac{d\hat{\sigma}^F_{+-}}{d\hat{t}}\right)$$

with

$$\frac{d\hat{\sigma}^F_{++}}{d\hat{t}} = 0 \qquad \frac{d\hat{\sigma}^F_{+-}}{d\hat{t}} = \frac{2\pi\alpha\alpha_s(Q^2)}{\hat{s}^2}\left(\frac{\hat{t}}{\hat{u}} + \frac{\hat{u}}{\hat{t}}\right) \qquad (10)$$

The interesting asymmetry to measure is

$$A^F(\vec{p}_1, \vec{p}_2) = \frac{F_{++}(\vec{p}_1,\vec{p}_2) - F_{+-}(\vec{p}_1,\vec{p}_2)}{F_{++}(\vec{p}_1,\vec{p}_2) + F_{+-}(\vec{p}_1,\vec{p}_2)} \qquad (11)$$

(the second index in $F_{\lambda\mu}$ fixes now the proton polarisation). Since $F(\vec{p}_1\vec{p}_2)$ is just a product of terms (without integration) and using (10), the measure of $A^F(\vec{p}_1,\vec{p}_2)$ gives direct access to the polarized gluon structure function through

$$A^F(\vec{p}_1,\vec{p}_2) = \frac{-\Delta G_g(x,Q^2)}{G_g(x,Q^2)} \qquad (12)$$

This asymmetry of course vanishes in the case of a scalar gluon. For a spin one gluon the measurement of $A^F(\vec{p}_1,\vec{p}_2)$ may well turn out to be the best way to determine how much of the hadron polarization is recalled by the gluons.

III - Conclusion

In conclusion, let us stress that polarized photoproduction experiments[1] give much clearer tests of QCD than hadroproduction at large p_T [5] . This comes basically from the simpler structure of the process (direct coupling of the photon) and from the possibility (due to the electric charge which allows taking differences of cross sections with a non negligible result) of separating the various contributing graphs. Moreover, we have shown that this reaction might well lead to the unique way of determining the polarized gluon structure function.

---

[1] for the polarized beam-unpolarized target case, see ref. [9]

REFERENCES

1. M. Fontannaz, A. Mantrach, B. Pire and D. Schiff, Phys. Lett. 89B, 263 (1980) and Orsay preprint LPTHE 80/12 to appear in Z. Physik C.
2. E. Witten, Nucl. Phys. B120, 189(1977).
   C.H. Llewellyn Smith, Phys. Lett. 79B, 83 (1978)
   R. DeWitt et al, Phys. Rev. D19, 2046 (1979)
   W. Frazer and J. Gunion, Phys. Rev. D20,147(1979)
3. M.J. Algard et al, Phys. Rev. Lett. 37, 1258(1976) ; ibid 37, 1261(1976) ; ibid. 41, 70 (1978).
4. J. Bjorken, Phys. Rev. 148, 1467(1966).
5. J. Babcock, E. Monsay, D. Sivers, Phys. Rev. Lett. 40,1161 (1978) ; Phys. Rev. D19, 1483(1979)
6. R. Field, R. Feynman, Phys. Rev. D15, 2590(1977)
7. R. Carlitz, J. Kaur, Phys. Rev. Lett.38,673(1977);38,1102 (E)(1977)
   J. Kaur, Nucl. Phys. B128, 219(1977)
8. M. Fontannaz, A. Mantrach, B. Pire and D. Schiff, Orsay preprint LPTHE 80/21 to appear in Z. Physik C
9. D. Duke and J. Owens, Phys. Rev. Lett. 44, 1173(1980)
   B. Petersson and B. Pire, Phys. Lett. 95 B, 119 (1980)

FIGURE CAPTIONS

fig. 1 : the direct coupling graphs contributing to large p_T photoproduction a)Compton subprocess ; b)Fusion subprocess.

fig. 2 contribution of the photon structure function to large p_T photoproduction.

fig. 3 : the cross section difference $\Delta^{\pi}(\vec{p})$ at $s = 200$ GeV^2 and $p_T = 3$ GeV/c with the corresponding asymmetry. The full, dashed and dotted curves correspond respectively to the polarized structure function parametrizations of ref [5], [6] and [7].

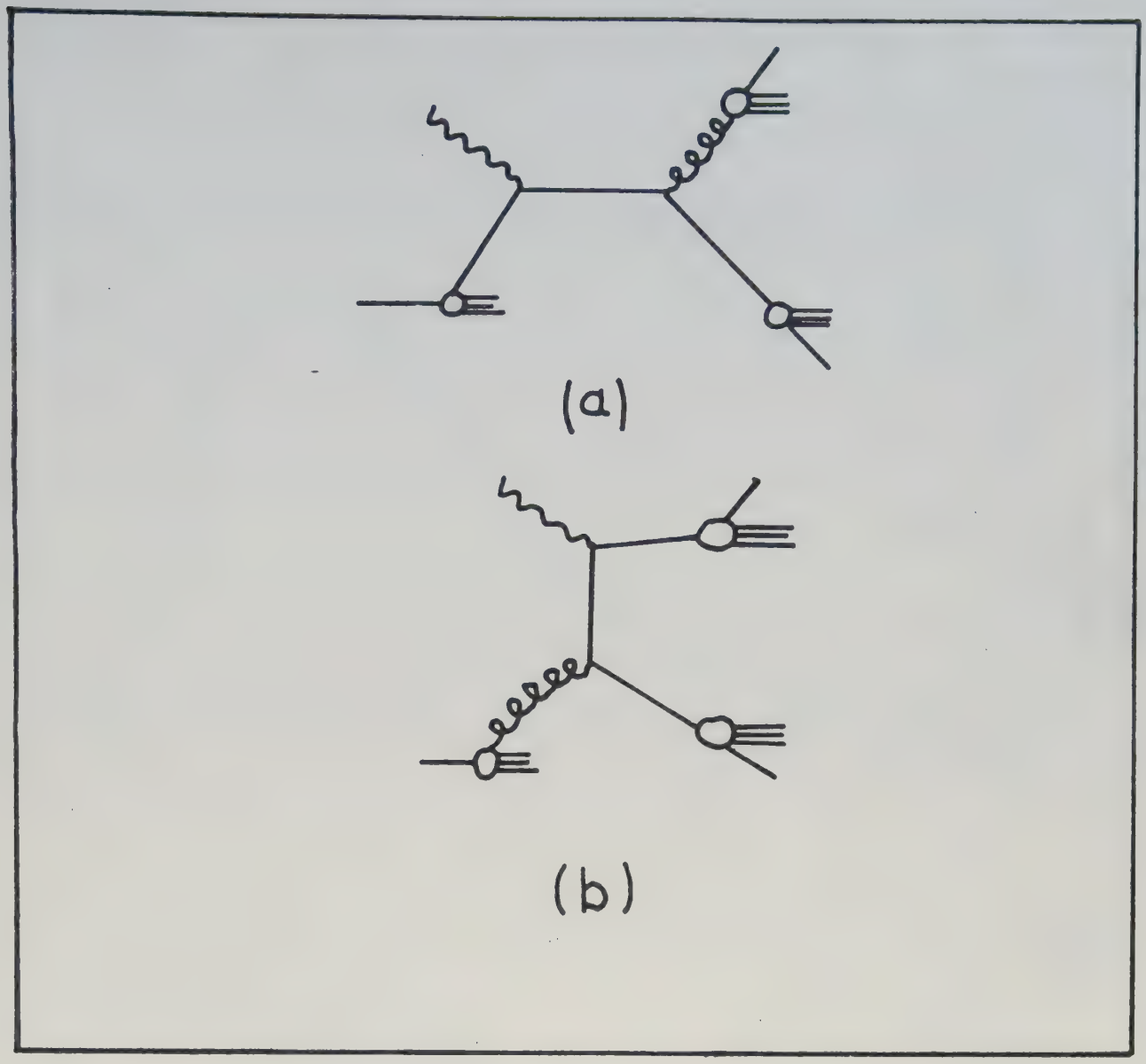

FIG 1

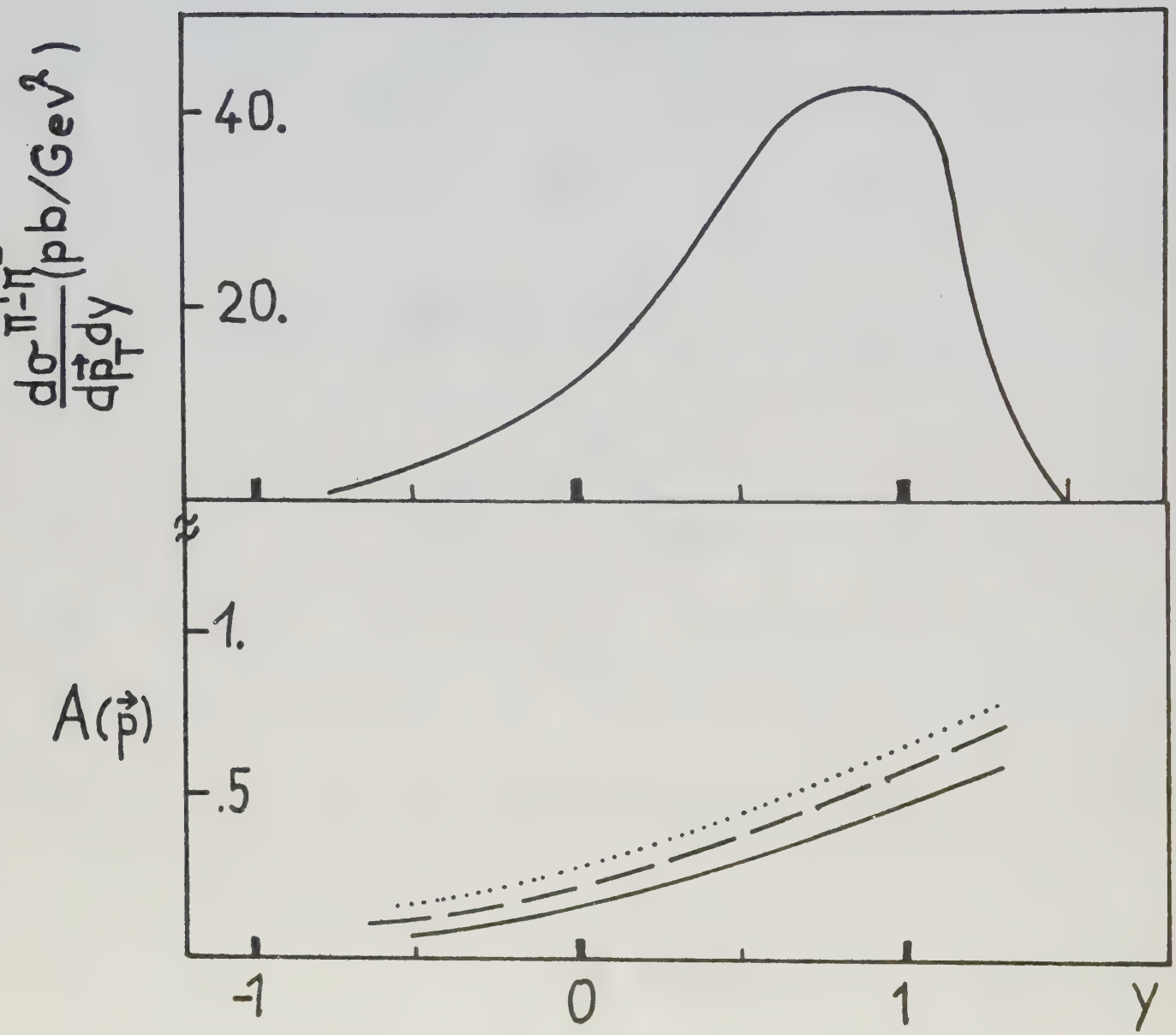

FIG 2

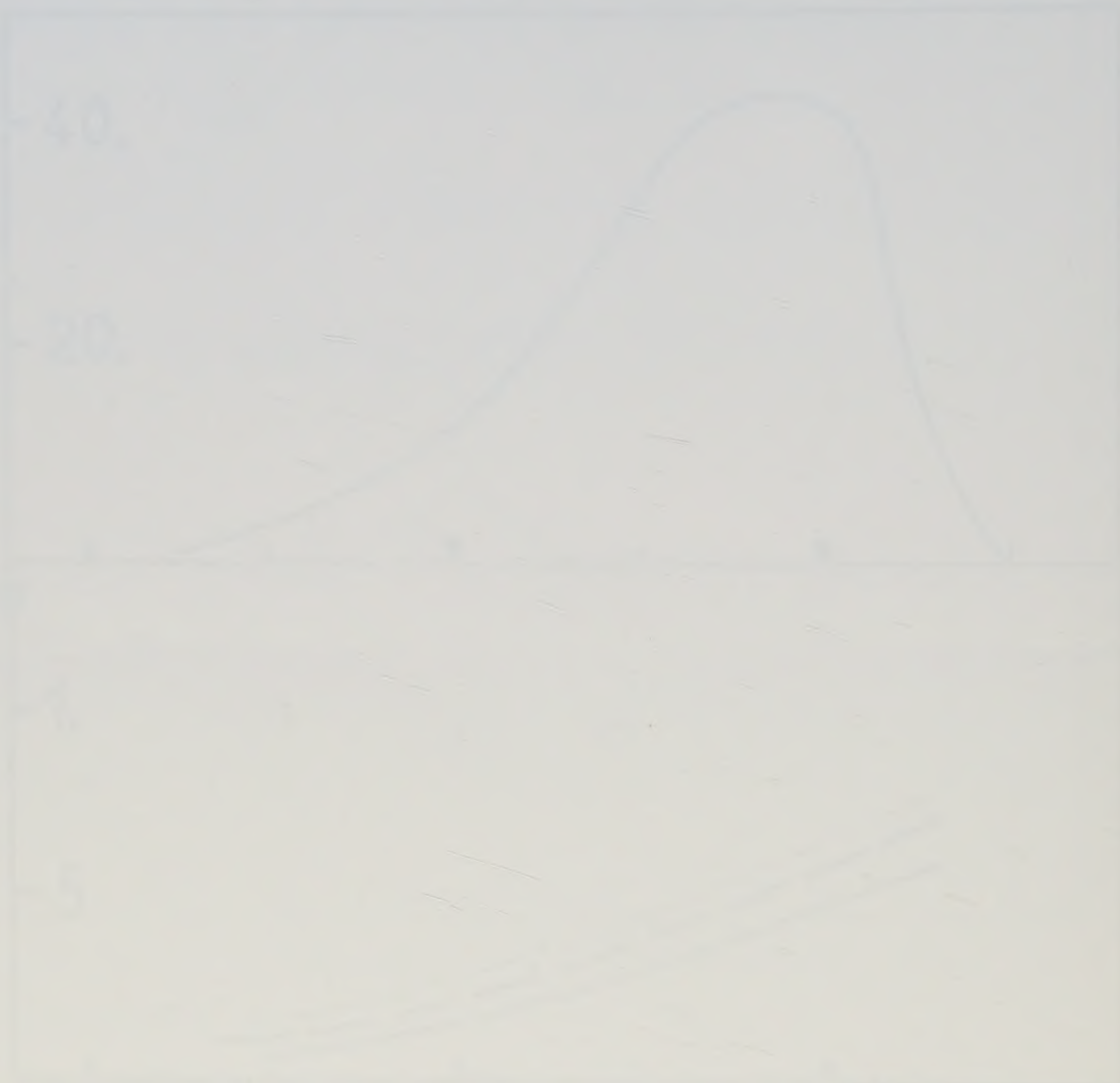
40
20
A(φ)
5